Mechanism of Endocytosis of CD33/Siglec-3: Role of ITIMs, Tyrosine Phosphorylation, and Monoubiquitylation

Roland Bruno Walter

A dissertation submitted in partial fulfillment
of the requirements for the degree of

Doctor of Philosophy

University of Washington
2006

Program Authorized to Offer Degree:
Department of Pathology

INFORMATION TO USERS

The quality of this reproduction is dependent upon the quality of the copy submitted. Broken or indistinct print, colored or poor quality illustrations and photographs, print bleed-through, substandard margins, and improper alignment can adversely affect reproduction.

In the unlikely event that the author did not send a complete manuscript and there are missing pages, these will be noted. Also, if unauthorized copyright material had to be removed, a note will indicate the deletion.

ProQuest Information and Learning Company
300 North Zeeb Road
P.O. Box 1346
Ann Arbor, MI 48106-1346

University of Washington
Graduate School

This is to certify that I have examined this copy of a doctoral dissertation by

Roland Bruno Walter

and have found that it is complete and satisfactory in all respects, and that any and all revisions required by the final examining committee have been made.

Chair of the Supervisory Committee:

Steven J. Collins

Reading Committee:

Jonathan A. Cooper

Bruce E. Clurman

W. Tony Parks

Date: 9/22/06

In presenting this dissertation in partial fulfillment of the requirements for the doctoral degree at the University of Washington, I agree that the Library shall make its copies freely available for inspection. I further agree that extensive copying of the dissertation is allowable only for scholarly purposes, consistent with "fair use" as prescribed in the U.S. Copyright Law. Requests for copying or reproducing of this dissertation may be referred to ProQuest Information and Learning, 300 North Zeeb Road, Ann Arbor, MI 48106-1346, 1-800-521-0600, to whom the author has granted "the right to reproduce and sell (a) copies of the manuscript in microform and/or (b) printed copies of the manuscript made from microform."

Signature 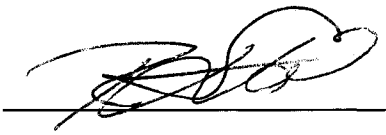

Date 9.25.06

University of Washington

Abstract

Mechanism of Endocytosis of CD33/Siglec-3: Role of ITIMs, Tyrosine Phosphorylation, and Monoubiquitylation

Roland Bruno Walter

Chair of the Supervisory Committee:
Adjunct Professor Steven J. Collins
Department of Pathology

The sialic acid-binding immunoglobulin-like lectin, CD33/Siglec-3, is a founding member of a subgroup of highly related Siglecs with differential expression in the innate immune system. Common structural features include a conserved proximal immunoreceptor tyrosine-based inhibitory motif (ITIM) and a distal ITIM-like motif, which, when phosphorylated, can bind and activate the tyrosine phosphatases, SHP-1 and SHP-2, suggesting an inhibitory function of these Siglecs. Despite its unknown function, CD33 has gained importance as target for immunotherapy as it is expressed on the majority of acute myeloid leukemias. Specifically, some clinical success has been achieved with gemtuzumab ozogamicin (GO; Mylotarg™), an immunoconjugate that utilizes an anti-CD33 antibody to facilitate uptake of a toxic calicheamicin-γ_1 derivative. We have now studied principles underlying endocytosis of CD33, in particular when bound to antibody, in detail. We found that the tyrosine motifs of CD33 control both CD33 internalization and GO-induced cytotoxicity. Pervanadate significantly increased CD33 uptake in an ITIM-dependent manner; this effect was prevented by co-treatment with PP2, suggesting that ITIM phosphorylation is regulated by Src-family kinase activity and critically controls CD33 uptake. We identified several proteins, including SHP-1, SHP-2, and Syk, which differentially bound to phosphorylated wild-type and mutant CD33. Depletion of myeloid cells from SHP-1 and SHP-2 by short interfering RNA resulted in increased CD33

internalization in TF-1 and ML-1 but not in HL-60 or NB4 cells, suggesting significant differences with regard to cellular responses to antibody ligation. Syk was dispensable for CD33 internalization and GO-induced cytotoxicity. Finally, we show that CD33 can undergo ITIM- and Src-family kinase-dependent monoubiquitylation, a process that may include Cbl family proteins as E3 ligases. CD33 internalization was abrogated in HEK293T cells expressing CD33 bearing lysine-to-arginine mutations, a phenotype that was rescued by fusion of ubiquitin to CD33. When lysine-to arginine mutants were expressed in myeloid cells, surface CD33 levels were increased while antibody-internalization was slightly reduced, whereas fusion with ubiquitin reduced surface CD33 display. Together, we demonstrate the role of the ITIMs and tyrosine phosphorylation for endocytosis of CD33, and identify ITIM-dependent monoubiquitylation as a novel post-translational modification involved in receptor downregulation and endocytosis.

TABLE OF CONTENTS

LIST OF FIGURES

Figure Number Page

LIST OF TABLES

ACKNOWLEDGEMENTS

The author wishes to express sincere appreciation to all members of the laboratories of Irwin D. Bernstein, Jonathan A. Cooper, and Steven J. Collins, all committee members, the Department of Pathology, as well as the staff of the core facilities at Fred Hutchinson Cancer Research Center for their outstanding support; without the expertise and support of all these individuals, this thesis would never have been completed. Research presented in this thesis was in part supported by an Interdisciplinary Dual Mentor Fellowship from the Fred Hutchinson Cancer Research Center, an American Society of Hematology Clinical/Translational Research Scholar Award, and a Leukemia & Lymphoma Society Special Fellow Award, as well as a scholarship from the Janggen-Pöhn Foundation that were awarded to the author.

Introduction

One in four deaths is due to cancer in developed countries, rendering cancer a major public health problem. In 2006, a total of 1,399,790 new cancer cases and 564,830 deaths from cancer are expected in the United States.[1] Major advances in anti-cancer therapies and supportive care have fortunately resulted in very high cure rates for some types of cancer; for example, the 5-year relative survival for patients with testicular cancer is 96%.[2] For other types of cancer, however, current treatment modalities fail to achieve cure or long-term disease-free survival in the majority of patients even nowadays. An important example for the latter is acute myeloid leukemia.

Acute myeloid leukemia

Acute myeloid leukemia (AML) is a heterogeneous group of diseases characterized by clonal neoplastic proliferation of myeloid progenitors with aberrant or arrested cellular differentiation and accumulation of abnormal blasts in the bone marrow, frequently resulting in hematopoietic insufficiency (granulocytopenia, thrombocytopenia, or anemia), with or without increased numbers of circulating white blood cells (leukocytosis).[3-5] In 2006, an estimated 11,930 individuals (6,350 men, 5,580 women) in the United States will develop AML, while another 9,040 individuals (5,090 men, 3,950 women) will die from the disease.[1] Importantly, AML is mostly a disease of the elderly: while the average annual incidence of AML is approximately 2.4 per 100,000, it increases progressively with age, to a peak of >20 per 100,000 at age 80. From 1998-2002, the median age at diagnosis was 68 years of age; approximately 6.3% were diagnosed under age 20; 7.2% between age 20 and 34; 7.0% between age 35 and 44; 10.0% between age 45 and 54; 13.9% between age 55 and 64; 22.4% between age 65 and 74; 24.6% between age 75 and 84; and 8.7% above 85 years of age.[2]

30 years ago, the prognosis for patients with AML was grim; for patients diagnosed with AML between 1974 and 1976, the 5-year relative survival was only 6.0%.[2] Due to some improvements in anti-leukemia therapies, but mostly because of substantial improvements in supportive care (e.g. use of more effective broad-spectrum antimicrobial therapies for neutropenic fever, better use of transfusion of platelets and red blood cells), the prognosis has significantly improved over the last decades, yielding a 5-year relative survival of 19.8% for patients diagnosed with AML between 1995 and 2001,[2] but treatment outcome nevertheless remains unsatisfactory. Moreover, the improvement in outcomes is mainly confined to younger adults, whereas the progress in older adults has been much less conspicuous if at all.[6] The biology of AML in the elderly differs considerably from that of younger adults. Older adults frequently have AML that is associated with antecedent blood dyscrasias such as myelodysplastic syndromes and myeloproliferative disorders, and their leukemic cells often have poor-prognosis karyotypes and/or express multidrug resistance proteins such as P-glycoprotein (Pgp, MDR1), rendering them more resistant to chemotherapy.[6] Furthermore, elderly individuals do not tolerate intensive chemotherapy as well as younger patients, particularly if they have preexisting comorbidities.[6] As a consequence, age at diagnosis is an important prognostic factor: while the 5-year relative survival rate for patients <45 years of age is 45.5%, it is 26.0% for patients aged 45-54, 17.4% for patients aged 55-64, and only 5.3% for patients aged 65-74. In other words, the 5-year relative survival is 33.1% for patients under the age of 65, but only 3.7% for patients above the age of 65.[2]

Even though conventional induction chemotherapy with the deoxycytidine analog cytarabine and an anthracycline antibiotic, such as daunorubicin or idarubicin, or the anthracenedione mitoxantrone, induces a complete remission (CR) in 50-75% of adults with *de novo* AML, a significant proportion of responding patients relapses and ultimately dies from treatment-refractory disease.[5,6] The treatment of adults with relapsed or refractory AML is unsatisfactory at best. Intensive

chemotherapy may be effective as a re-induction regimen in some patients who have relapsed, but alone is rarely curative. The highest likelihood of cure may be provided by allogeneic hematopoietic stem cell transplantation,[6] but this approach has significant limitations due to high treatment-related mortality, lack of suitable stem cell donors, and patient characteristics that preclude successful transplantation. Therefore, many of the younger patients with relapsed or refractory AML, as well as elderly patients who have not relapsed but whose disease has poor prognostic features, are candidates for novel investigational approaches.[6] These include farnesyltransferase inhibitors, tyrosine kinase inhibitors, multidrug resistance modulators, histone deacetylase inhibitors, antisense oligonucleotides against pro-apoptotic proteins of the Bcl-2 family, antiangiogenic agents, as well as monoclonal antibodies.[6]

Monoclonal antibodies as biotherapeutics

Monoclonal antibodies targeting tumor cell surface antigens theoretically offer a more specific means to direct therapy towards malignant cells while sparing normal tissues than current chemotherapeutic agents. The potential of antibodies as "magic bullets", a term coined by the 1908 Nobel Prize winner Paul Ehrlich, for cancer therapy has been appreciated for nearly a century.[7,8] For several decades, however, the wide-spread use as biotherapeutics was hindered by the production limitations related to antibody quantity, purity, and reproducibility, and only Hans Köhler and Caesar Milstein's landmark paper in 1975 describing the hybridoma technology finally allowed the production of large antibody quantities with high purity and monospecificity for a single antigen epitope.[7-9] Subsequent studies performed in the 1980s established the safety of antibody administration, defined certain predictable antibody-mediated toxicities, and confirmed that antibodies could reach tumor targets and produce antitumor effects.[7] Nonetheless, the first generation of monoclonal antibodies evaluated in clinical trials demonstrated limited effectiveness, largely due to their immunogenicity and inefficient effector function, yielding inconsistent and often disappointing results.[9]

More recent work has identified a number of important and useful applications for antibody-based cancer therapy.[9] Although the understanding of the critical principles eliciting clinically significant anti-tumor effects is still incomplete, several pivotal mechanisms have been ascribed to currently used onco-therapeutic antibodies.[9,10] Mechanisms carried out by unconjugated antibodies include engagement of the immune system via antibody-dependent cellular cytotoxicity and/or activation of complement pathways leading to complement-mediated cell lysis, alterations of cell signaling pathways central for growth arrest or apoptosis, interference with ligand-receptor interactions by neutralizing circulating ligands or blocking cell membrane receptors, and prevention of enzymatic cleavage of cell surface proteins. A second category encompasses carrier functions exerted by monoclonal antibodies that are armed with conjugated cytotoxic agents to deliver toxic compounds such as radionuclides, microbial or plant toxins, small-molecule chemotherapeutic agents, or cytokines specifically to tumor sites.[7-11]

A number of obstacles to treatment efficacy have been identified in preclinical and clinical studies, including impaired antibody distribution and delivery to tumor sites due to the large size of antibodies, heterogenous tumor blood supply, and epithelial and endothelial barriers; inadequate trafficking of effector cells to the tumor; intratumoral and intertumoral antigenic heterogeneity; shed antigen in the tumor microenvironment that may saturate antibody binding sites and prevent binding to the cell surface; rapid antigen internalization, which, although beneficial in facilitating the uptake of certain toxins and chemotherapy molecules into the cell, may deplete the quantity of cell surface monoclonal antibody capable of initiating antibody-dependent cellular cytotoxicity; insufficient tumor specificity of target antigens, resulting in decreased targeting specificity and unacceptable normal tissue cytotoxicity; pharmacokinetic issues relating to

metabolism and clearance of conjugated antibodies, which may lead to non-specific uptake and toxicity; and human anti-mouse antibody responses.[9]

Some of these obstacles are intrinsic to antibody design and can be addressed by advances in the generation of future antibodies. For example, various immunoglobulin design strategies, including chimerization, hyperchimerization, immunoglobulin resurfacing, deimmunization, humanization, as well as the generation of fully human antibodies without the need for labor-intense *in vitro* manipulations, have been developed to reduce immunoglobulin antigenicity and toxicity.[10] Parallel research aims at improving conjugated antibodies, namely by refining means by which the cytotoxins are linked to the antibody and by which non-specific uptake of these conjugates is decreased, to increase the therapeutic index.[11] Most of the obstacles, however, are intrinsic to the nature of the tumor, such as accessibility of the tumor by the antibody and immune effector cells as well as specificity of targeted antigens. This is much more problematic in the case of solid tumors compared to tumors of hematopoietic cell origin, which are more easily accessible and for which a vast body of knowledge on specific cell surface markers exists.[11] Not surprisingly, therefore, 5 out of 8 antibodies approved for clinical use as anti-cancer biotherapeutics as of April 2006 by the U.S. Food and Drug Administration (FDA), and many additional antibodies in late-stage clinical trials, target hematopoietic malignancies.[9] The FDA-approved antibodies include: Rituximab (Rituxan®), a CD20-targeting unconjugated antibody for treatment of non-Hodgkin's lymphoma; Trastuzumab (Herceptin®), a HER-2/*neu*-targeting unconjugated antibody for treatment of breast cancer; Alemtuzumab (Campath®), a CD52-targeting unconjugated antibody for treatment of chronic lymphocytic leukemia; Ibritumomab tiuxetan (Zevalin®) and Tositumomab (Bexxar®), two CD20-targeting radiolabeled antibodies for treatment of non-Hodgkin's lymphoma; Cetuximab (Erbitux®), an epithelial growth factor receptor (EGFR)-targeting unconjugated antibody for treatment of colorectal as well as head and neck cancers; Bevacizumab (Avastin®), an

unconjugated anti-vascular endothelial growth factor (VEGF) antibody for treatment of colorectal cancer; and Gemtuzumab ozogamicin (Mylotarg®), an immunoconjugate targeting CD33.

CD33 as an AML-associated antigen

Thus far, no truly AML-specific antigen has been identified, but CD33 has proven very valuable as AML-associated antigen. CD33 is normally expressed on early multilineage hematopoietic progenitors and myelomonocytic precursors. As these cells mature, the antigen is down-regulated to low levels on peripheral granulocytes and resident macrophages but retained on circulating monocytes as well as on dendritic cells.[12-14] Some studies have indicated that CD33 may also be found on subsets of B lymphocytes and mitogen- or alloantigen-activated human T and natural killer (NK) cells.[15-22] In addition to its physiological expression, 85 - 90% of adult and pediatric AML cases are considered $CD33^+$, as defined by the presence of CD33 on greater than 20 – 25% of the leukemic blasts.[14,23] Due to its restricted expression in the hematopoietic system, and its presence on tumor cells of the vast majority of patients with AML, CD33 has been used for immunodiagnosis of leukemias[24] and tumor-associated antigen targeted with antibody-based AML therapies,[25,26] despite the fact that the physiological functions of CD33 remain elusive.

Only limited data are available on the density of CD33 on normal and malignant cells. In one study, quantitative flow cytometry using bead standards has been used to calculate the concentration of CD33 antigen on the cell surface in 315 bone marrow samples and 114 corresponding peripheral blood samples from patients with various leukemias, myeloproliferative disorders, myelodysplastic disorders, and control subjects.[27] Using this method, it was estimated that $CD33^+$ bone marrow cells from AML patients had a mean CD33 intensity of 10,380 molecules per cell (range: 709-54,894; n=100), compared to 6,671 (493-53,791; n=135) CD33 molecules per cell on $CD33^+$ bone marrow cells patients with

myelodysplastic syndromes, 4,410 (801-16,108; n=59) CD33 molecules per cell on $CD33^+$ bone marrow cells patients with chronic myelogenous leukemia, and only 2,295 (666-4,279; n=5) as well as 2,997 (859-5,137; n=16) CD33 molecules per cell on $CD33^+$ bone marrow cells from patients with myeloproliferative disorders and control subjects, respectively.[27]

CD33, founding member of the sialic acid-binding immunoglobulin-like lectins (Siglecs) with elusive function

A cDNA encoding CD33 has been isolated and sequenced in 1988.[28] The demonstration that CD33 has properties of a sialic acid-dependent cell adhesion molecule, using human erythrocytes derivatized with N-acetylneuraminic acid in different linkages as a model for sialic acid-dependent binding, has established this 67kD type 1 transmembrane sialoglycoprotein as member of the immunoglobulin (Ig) superfamily subset of sialic acid binding Ig-like lectins (Siglecs; CD33 is also knows as Siglec-3, see Fig 1).[29] There are currently 11 known human *bona fide* Siglecs that can be divided into two subfamilies. A first subgroup encompasses sialoadhesin (Siglec-1), myelin-associated glycoprotein (MAG; Siglec-4), and CD22 (Siglec-2), which share around 25-30% sequence identity but have evolutionary well-conserved orthologs in multiple species and highly conserved binding specificities, cell-type-specific expression patterns, and domain structures. A second subgroup encompasses the CD33/Siglec-3-related Siglecs (CD33/Siglec-3 as well as Siglec-5-11), which share around 50-85% sequence identity, but are rapidly evolving, have poorly conserved binding specificities and domain structures, and show highly variable expression in cells of the immune system.[30-32] With the exception of MAG/Siglec-4, which is found on glial cells, all Siglecs characterized to date are expressed on distinct subsets of hematopoietic cells, such as myeloid progenitors (CD33), a subset of T cells (CD33, Siglec-7, 9), B cells (CD22/Siglec-2, Siglec-5, -6, -9, -10), natural killer (NK) cells (CD33, Siglec-7, -9, -10), monocytes (CD33, Siglec-5, -7, -9, -10), dendritic cells (CD33, Siglec-7), macrophages (CD33, Siglec-1, 5, -11),

neutrophils (Siglecs-5, -9), eosinophils (Siglec-8, -10), and basophils (Siglec-8).[22,32,33]

The CD33-related Siglec gene cluster is among the most rapidly diverging.[34-36] This rapid evolution is due to multiple mechanisms that mainly involve the sialic acid-binding domain. The cause for ongoing evolution is currently under intense study, but host-pathogen interactions are suspected to play a major role. For example, Varki & Angata[32] hypothesize that CD33-related Siglecs have to evolve rapidly to evade pathogens that recognize sialic acids as sign posts for attack, or to evade pathogens that are masquerading as "self" to avoid innate immune cell responses. Although these hypotheses need further experimental confirmation, it is interesting to note that Siglecs have indeed been shown to recognize relevant human pathogens, such as *N. meningitidis* and *C. jejuni*.[37,38]

Structurally, Siglecs are characterized by one (or rarely, two) N-terminal V-set Ig domain mediating sialic acid binding, followed by variable numbers of C2-set Ig domains, ranging from 16 (in the case of sialoadhesin/Siglec-1) to 1 (in the case of CD33; Fig 1).[31,32] Each Siglec exhibits distinct carbohydrate-binding properties with specificity for both the sialic acid linkage and the nature of the sialic acid itself. CD33 has initially been shown to prefer binding to α2-3-linked over α2-6 linked sialic acids by use of a recombinant form of CD33 and resialylated red blood cells.[29] However, in a more recent study, a preferential binding of α2-6 linked sialyllactosamines was found when various sialylated glycans were presented in multivalent form on synthetic polyacrylamide.[39] In addition, the simultaneous presence of fucosylation strongly reduced binding of α2-3 linked sialyllactosamines to CD33.[39] Since specific glycosyltransferases can be induced during myeloid cell maturation,[40,41] the expression of potential ligands with different degrees of affinity for CD33 may depend on the stage of hematopoietic differentiation; indeed, solid-phase binding assays with a purified soluble form of CD33 containing the two extracellular domains fused to the Fc portion of human

IgG_1 and human hematopoietic cell lines showed that early myeloid precursor-like cells (KG1 cell line) and monocyte-like cells (THP-1 cell line) showed weaker binding than intermediate-stage myelomonocytic cells (HL-60 and U937 cell lines), suggesting that molecules able to bind to CD33 might be transiently upregulated during myeloid cell differentiation.[29] Early studies revealed the necessity of treatment with neuraminidase to demonstrate any sialic acid binding property of CD33 when transiently expressed in cells.[29] It has therefore been speculated that CD33 with its two extracellular Ig-like domains does not extend sufficiently far out of the cell membrane glycocalyx to mediate interactions with ligands on adjacent cells, suggesting that a modulation by endogenous sialoglycoproteins is likely.[29] However, subsequent studies have revealed a single *N*-linked glycosylation site located in the first Ig domain of CD33 that is critical for regulating ligand recognition; point mutation of this site unmasks CD33's ligand binding function, as does treatment with neuraminidase. These results suggest that sialylation of a single *N*-linked glycan of CD33 is sufficient to inhibit interaction with ligands, and that the terminal sialylation of CD33 glycans may play a critical role in regulating recognition of ligands.[42]

Signaling of Siglecs

With a few exceptions, Siglecs generally have tyrosine-based signaling motifs in their cytoplasmic tails.[31,32] All CD33-related Siglecs are characterized by the presence of a conserved proximal immunoreceptor tyrosine-based inhibitory motif (ITIM; with its tyrosine at position 340 in the case of CD33) and a distal ITIM-like motif (with its tyrosine at position 358 in the case of CD33; Fig 1).[30] When ITIM-containing receptors are appropriately engaged, they can become tyrosine phosphorylated and then transmit inhibitory signals by binding and activating Src homology-2 domain (SH2)-containing tyrosine phosphatases (SHP-1 and SHP-2) and/or the inositol polyphosphate 5'-phosphatase (SHIP).[43] Indeed, three groups independently confirmed that CD33 could be tyrosine phosphorylated.[44-46] Pervanadate, a tyrosine phosphatase inhibitor and tyrosine

kinase activator, increased phosphorylation of CD33 in human peripheral blood monocytes and various leukemic myeloid cell lines, such as U937, Mo7e, HL-60, KG-1, and THP-1.[44,46] In addition, pervanadate treatment resulted in co-precipitation of tyrosine-phosphorylated SHP-1 and SHP-2, but not SHIP.[44,46] Importantly, the tyrosine phosphatases could only be co-precipitated after pervanadate stimulation but not in unstimulated cells, indicating their strict phosphotyrosine-dependent association.[44,46] The tyrosine motifs of CD33 have been confirmed as target sequences for SHP-1 and SHP-2 binding by use of CD33 constructs bearing point mutations of Y340 and Y358, which resulted in failure to bind SHP-1 and SHP-2. These mutation studies further indicated that the first tyrosine is dominant in binding these tyrosine phosphatases, and the NH2-terminal SH2 domain of SHP-1, which is believed to be essential for activation, showed a much greater binding specificity than the C-SH2 domain for Y340 and was sufficient for CD33 binding.[44-46] The interaction between phosphorylated CD33 and the NH2-terminal SH2 domain is therefore expected to result in enhancement of tyrosine phosphatase activity. Although the NH2-terminal SH2 domain of SHP-2 exhibited the same preference for Y340, the C-SH2 domain bound both tyrosine motifs very poorly. Since some evidence suggested that tandem binding of tyrosine phosphatases was important for optimal signaling, this has been used to argue that CD33 may prefer SHP-1 for signaling.[44] Moreover, although a peptide-capture experiment with a phosphorylated peptide spanning Y358 showed that SHP-2 bound well but SHP-1 was not bound to a significant amount, this residue was only weakly phosphorylated during co-expression studies, again favoring signaling through SHP-1.[46] Since SHP-1 is expressed primarily in hematopoietic cells,[47] the preferential binding of SHP-1 by phosphorylated CD33 would be consistent with the expression pattern of the tyrosine phosphatases. Similar to treatment with pervanadate, cross-linking of CD33 with monoclonal anti-CD33 antibody resulted in tyrosine phosphorylation and recruitment of both SHP-1 and SHP-2.[44] It is important to note that these experiments were performed in the presence of anti-

CD33 antibodies cross-linked with polyclonal anti-mouse IgG, and it is hitherto unknown whether treatment with bivalent antibodies alone also induces tyrosine phosphorylation or whether the more effective receptor aggregation induced by second antibodies is required.

The effect of cross-linking on CD33 phosphorylation could be abrogated by pretreatment with the Src family tyrosine kinase inhibitor PP2, whereas the broad range tyrosine kinase inhibitor genistein and the Syk family-specific tyrosine kinase inhibitor piceatannol were only partially effective, suggesting that Src family kinases are strong candidates for mediating tyrosine phosphorylation of CD33.[44] This finding is corroborated by experiments in which CD33 was co-transfected with various tyrosine kinases. The Src family kinase Lck, but not Syk or Zap70, was capable of mediating CD33 tyrosine phosphorylation with preference for Y340.[46] However, since neither of the two phosphotyrosine motifs of CD33 conforms to the preferred binding sequence of the SH2 domain of Src family kinases, and CD33 lacks any proline-rich region for SH3 domain binding, it has been considered unlikely that CD33 forms a stable association with active Src family kinases, suggesting that CD33 might be phosphorylated by aggregated kinases in close proximity, or during transient, unstable interactions.[44] This is corroborated by the observation that significantly more SHP-1 was associated with CD33 when CD33 was co-ligated with the high affinitity Fcγ receptor I (CD64) compared to cross-linking of CD33 alone, indicating that a tyrosine kinase associated with an activating receptor complex is responsible for tyrosine phosphorylation of CD33.[45] Upon receptor cross-linking, phosphorylation was rapid and became apparent by 1 minute, but was also transient with a decrease of phosphorylation to basal levels within 10 minutes. The protein-tyrosine phosphatases that co-precipitated with CD33 upon receptor cross-linking have been shown to be active and to catalyze CD33 dephosphorylation, thereby potentially resulting in a feedback control of CD33 signaling.[44] The activation of SHP-1 up to 12-fold has been shown to be

dependent on phosphorylated Y340, whereas phosphorylated Y358 did not increase SHP-1 catalytic activity,[45] again pointing to the predominance of Y340 over Y358. In contrast to receptor cross-linking, other myeloid stimuli such as cytokines (CSF-1, GM-CSF), chemotactic peptides (fMLP), or phorbol esters, did not induce CD33 tyrosine phosphorylation.[44]

In addition to tyrosine phosphorylation of the cytoplasmic ITIM and ITIM-like motif, CD33 is also a serine/threonine phosphoprotein and target for protein kinase C.[48] Treatment of human myeloid cell lines (U937, HL-60) in the resting state with [32P]-orthophosphate and subsequent immunoprecipitation revealed CD33 to be phosphorylated. Phorbol esters significantly increased the amount of CD33 phosphorylation in these cell lines and primary human $CD34^+/CD33^+$ progenitor cells, and phosphoamino analyses exclusively identified phosphoserine and trace amounts of phosphothreonine, but no phosphotyrosine in phorbol ester stimulated cells. Besides this pharmacologic stimulus, increased phosphorylation of cytokine-dependent TF1 cells could be achieved in cytokine-deprived cells upon treatment with GM-CSF, EPO, and IL-3. 2 inhibitors of serine/threonine-specific kinases, staurosporine and bisindoylmaleimide (BIM), abrogated the effect of phorbol esters, whereas a stimulator of protein kinase A (dibutryl cAMP) had no effect on CD33 phosphorylation. Interestingly, these studies indicated some level of baseline phosphorylation in resting cells, and this baseline level could be reduced by 80% by treatment with staurosporine, but not by BIM. Protein kinase C dependent phosphorylation of CD33 could also be shown *in vitro* with purified protein kinase C. Phosphopeptide maps identified 2 phosphopeptides, indicating phosphorylation on 2 serine residues, namely S307 and S342.[48]

The cytoplasmic tail of CD33 significantly affects the sialic-acid dependent binding to the extracellular ligand-binding domain. The importance of CD33 tyrosine phosphorylation sites has been demonstrated by use of CD33 constructs

with truncated cytoplasmic tail as well as with constructs that bear mutations of Y340 and/or Y358 when expressed in COS cells.[44,48] Truncation after D335 or T299 resulted in increased formation of red blood cell rosettes to about 150 or 200% of the wild-type level, respectively.[44,48] An increase of 150% was obtained when Y340 or both cytoplasmic tyrosine residues were mutated in full length CD33, whereas mutation of Y358 alone did not affect red blood cell binding.[44] Pre-treatment with the Src family kinase specific inhibitor PP2 in cells expressing wild type CD33 increased red blood cell adhesion to 110-150% of wild-type level, whereas PP2 had no effect in cells expressing CD33 with both tyrosine mutated.[44] Similarly, pre-treatment of cells expressing wild type CD33 with inhibitors of serine/threonine-specific kinases, staurosporine and BIM, increased rosette formation up to 175% of control cells, whereas treatment that increased serine phosphorylation (PMA and okadaic acid) slightly decreased red blood cell adhesion.[48] On the other hand, binding of red blood cells to CD33-transfected COS cells resulted in a decrease of the basal level of CD33 serine phosphorylation by about 70%; by comparison, red blood cell binding did not induce measurable changes in tyrosine phosphorylation of CD33.[44,48] Taken together, these data suggest that there is a cross-talk between the lectin binding site and the intracellular domain, inasmuch as occupancy of the binding site results in a decrease of tyrosine and/or serine phosphorylation, whereas tyrosine and serine phosphorylation result in decreased lectin binding.

There is only scant knowledge about further steps in the CD33 downstream signaling cascade. However, it was recently demonstrated that cross-linking of CD33 induced tyrosine phosphorylation of the proto-oncogenes c-Cbl and Vav in monocytes of normal donors, and these proteins could also be co-precipitated with phosphorylated CD33 upon treatment with pervanadate.[49] Similarly, Syk was found to form a complex with CD33 after it became phosphorylated upon pervanadate treatment.[49] Interestingly, c-Cbl and Vav were constitutively

phosphorylated in a leukemic cell line, indicating that the response to CD33 signaling might be altered in some cells.[49]

Biological functions of Siglecs

With the exception of CD22/Siglec-2, which plays an important role in regulating B-cell activation,[30,32] and MAG/Siglec-4, which has a well defined role in maintenance of myelin organization and inhibition of neurite outgrowth,[32] functions of Siglecs are poorly understood, but mediation of inhibitory signaling, regulation of cell proliferation and apoptosis, as well as adhesive functions have been implicated.[31] The presence of ITIM and ITIM-like motifs in all human CD33-related Siglecs strongly suggests that they have roles in the fine-tuning of cellular functions.[31] In the case of CD33, growing evidence indeed indicates an inhibitory function on several biological responses, including inhibition of Ca^{2+} flux, inhibition of cell growth and/or induction of apoptosis, and release of cytokines.[45,46,49-54] An inhibitory role of CD33 on Ca^{2+} flux has convincingly been shown in experiments in which Fcγ receptor I (CD64) was co-ligated with CD33; this treatment not only resulted in the rapid association of SHP-1 with CD33, but also in decreased intracellular Ca^{2+} mobilization as well as in deceased tyrosine phosphorylation and duration of phosphorylation of many other proteins.[45,46] Expression of a dominant-negative mutation of SHP-1 abolished the inhibitory function of CD33 upon co-ligation with CD64, indicating that the inhibitory function of CD33 is indeed mediated by recruited tyrosine phosphatases.[45,46] However, neither cross-linking Fcγ receptor IIA (CD32) nor CD64 alone resulted in CD33 phosphorylation and subsequent recruitment of SHP1- or SHP-2, and neither of these proteins was detected in the complex with the Fcγ receptor, suggesting that CD33 is not directly activated by immune receptor engagement.[44] Balaian and Ball[49] have reported further evidence for a function as inhibitory receptor. In this study, cross-linking of CD64 increased phagocytic activity of normal human monocytes; both co-ligation of CD64 together with CD33 as well as the treatment with a bispecific anti-CD33/anti-CD64 antibody resulted in less

pronounced enhancement of phagocytic activity.[49] Furthermore, cross-linking of CD33 also decreased baseline phagocytic activity of monocytes, and decreased cell proliferation and colony formation of hematopoietic cell lines.[49] The finding that anti-CD33 antibodies inhibit proliferation has been confirmed in $CD34^+$ progenitor cells isolated from human cord blood, as well as in primary AML and chronic myeloid leukemia (CML) cell samples.[50,52,53] In primary AML cell samples, the effect on cell survival was studied in more detail, and experimental evidence indicated that anti-CD33 antibodies could induce apoptosis, as estimated by increased binding of annexin V and oligonucleosomal DNA fragmentation.[51,52] These inhibitory effects of unconjugated anti-CD33 antibodies have also been explored in clinical trials of patients with AML. In such studies, treatment with unconjugated anti-CD33 antibodies has reproducibly reduced blast cell counts and resulted in a few CRs; in addition, such antibodies have reduced the tumor burden in patients with minimal residual acute promyelocytic leukemia.[25] The mechanisms underlying these inhibitory effects remain elusive. Interestingly, however, one study has suggested that the activity of the unconjugated anti-CD33 antibody is dependent upon the expression level and/or the functional activity of the protein kinase Syk or ZAP-70.[53] It is important to note, however, that all these experiments have relied on the use of antibodies to cross-link CD33, and it is hitherto unclear what physiological processes, if any, are mimicked by artificially cross-linking CD33 with antibodies. In a very recent study, however, specific gene silencing through small interfering RNA (siRNA) and other techniques were used to demonstrate a constitutive repressor activity of CD33 on human monocytes' production of proinflammatory cytokines (IL-1β, TNF-α, and IL-8); this repressor activity was shown to involve phosphoinositide 3-kinase-mediated signaling and required sialic acid recognition.[54] It therefore appears that CD33 might mediate inhibitory functions even in the absence of artificial cross-linking.

Recent studies have provided growing evidence for a role of Siglecs in endocytosis.[31,32] For example, sialoadhesin/Siglec-1, which lacks cytoplasmic tyrosine-based signalling motifs,[31] specifically internalizes a monoclonal anti-sialoadhesin antibody, and is involved in the sialic-acid dependent receptor-mediated entry process of the arterivirus porcine reproductive and respiratory syndrome virus in porcine alveolar macrophages.[55,56] Furthermore, sialoadhesion/Siglec-1 is involved in phagocytic clearance of sialylated *N. meningitidis* in transfected CHO cells and primary murine macrophages.[37] The large isoform of MAG/Siglec-4 has been shown to be endocytosed from the CNS myelin of mice bearing the quaking mutation.[57] On monocytes, Siglec-5 was shown to mediate rapid uptake of anti-Siglec-5 $(Fab)_2$ fragments into early endosomes.[58] Likewise, a very recent report provided evidence that Siglec-9 is internalized when bound to antibody.[59] Another recent example is a novel murine CD33-related Siglec-like molecule, Siglec-H, which is expressed specifically on plasmacytoid dendritic cell precursors in bone marrow, spleen, blood and lymph node, as well as in a subset of marginal zone macrophages in the spleen and in medullary macrophages in lymph nodes. Siglec-H functions as an endocytic receptor and mediates efficient internalization of anti-Siglec-H antibodies. Unlike other CD33-related Siglecs, however, Siglec-H lacks tyrosine based signaling motifs in its cytoplasmic tail.[60] Finally, long before CD33 was recognized as a member of the Siglec family of proteins, multiple studies have shown that binding of bi- and multivalent anti-CD33 antibodies results in CD33 internalization in both $CD33^+$ hematopoietic cell lines and primary AML blast cells (see below).[61-64]

The mechanism underlying these endocytic processes has not been investigated in detail so far, and the exact physiological roles remain elusive. By comparison, much more is known about the endocytosis of CD22/Siglec-2. Initial studies have shown that CD22 undergoes rapid constitutive endocytosis and is able to mediate uptake of anti-CD22 antibodies.[65,66] Subsequently, a polar region of 11 amino acid residues (QRRWKRTQSQQ) proximal to the plasma membrane that

was predicted to form a coil or turn structure, was identified as internalization motif that controls both the unusual rapid constitutive turnover ($t_{1/2}$ at the cell membrane of less than 1h), as well as the uptake of anti-CD22 antibodies.[66,67] Within this motif, the two glutamine residues sandwiching the serine, but not the serine itself, have been shown to be critical to internalization.[67] The exact molecular mechanism underlying CD22 internalization has not been addressed in this early report; however immunoelectron microscopy studies demonstrated clustering of CD22 around coated pits, suggesting a clathrin-dependent mechanism,[67] the predominant mechanism for internalization of cell surface receptors and their cargo.[68] The ITIM and ITIM-like motifs found in Siglecs indeed resemble an YXXØ motif (where X stands for any amino acid and Ø stands for an amino acid residue with a bulky hydrophobic side chain), a major tyrosine-based signal involved in clathrin-mediated protein sorting. This signal has been shown to interact with the μ subunit of the adaptor protein (AP) complex AP-2 and mediate clathrin-dependent endocytosis of, e.g., the transferrin receptor and the asialoglycoprotein receptor.[69] The Y residue is critical as anchor for the interaction with AP-2, whereas the Ø position can accommodate several residues with bulky hydrophobic side chains.[69] In the case of CD22, a later study has demonstrated that the tyrosine motifs around Y843 and Y863 interact in yeast-two hybrid assays with AP50, the medium chain subunit of the AP-2 complex when non-phosphorylated.[70] However, alternate endocytic adaptors have been described whose interactions depend on the presence of (phospho-) tyrosine motifs.[71,72] Furthermore, the fact that both sialoadhesin/Siglec-1 as well as murine Siglec-H show endocytic properties but do not have cytoplasmic tyrosine signaling motifs indicates that more than one mechanism is involved in endocytosis of Siglec family proteins.

Gemtuzumab ozogamicin (Mylotarg®)

The early recognition of the endocytic property of CD33 when engaged with antibody has led to the clinical development of an immunoconjugate,

gemtuzumab ozogamicin (GO; formerly known as CMA-676; Wyeth-Ayerst Laboratories, Philadelphia, PA), consisting of a humanized IgG_4 anti-CD33 monoclonal antibody (hP67.6) joined to a derivative of the cytotoxic drug calicheamicin-γ_1, N-acetyl-γ-calicheamicin dimethyl hydrazide, for treatment of patients with AML.[73] Encouraging clinical results have been reported in Phase II trials revealing that GO monotherapy, administered as two doses 14 days apart, induces a CR in 26% of adults with relapsed $CD33^+$ AML.[74,75] In 2000, GO was approved by the FDA for treatment of $CD33^+$ AML in first relapse in patients 60 years of age or older who are not considered candidates for conventional chemotherapy.[76] However, GO monotherapy fails to induce CR in about three fourths of the patients, and further information on the mechanisms of action of GO is needed to develop novel strategies aimed to improve the therapeutic outcome of patients treated with GO.

hP67.6 itself is largely non-toxic and believed to function primarily as a carrier to facilitate cellular uptake of the calicheamicin-γ_1 derivative, which is then intracellularly cleaved and subsequently induces DNA damage and eventually cell death.[77,78] This putative mechanism implies a critical role for the intracellular accumulation of the calicheamicin-γ_1 derivative as well as the cellular response to the toxin's action for GO-induced cytotoxicity. In support of this notion, previous correlative and *in vitro* studies have shown that drug efflux mediated by members of the adenosine triphosphate (ATP) binding cassette (ABC) superfamily of proteins, predominantly P-glycoprotein (Pgp) and to a lesser degree also multidrug resistance protein (MRP), but not breast cancer resistance protein (BCRP), mediate resistance to GO, and that inhibition of drug efflux effectively increases GO-induced cytotoxicity;[79-82] these studies have also demonstrated that GO-induced cytotoxicity is reduced by anti-apoptotic proteins of the Bcl-2 family.[81] However, only a portion of GO-resistant AML blast cell samples can be rendered sensitive to GO by combining GO with a drug-efflux or Bcl-2 function

inhibitor *in vitro*,[81] and additional therapeutic approaches are needed to optimize GO-based therapy.

Evidently, increased accumulation of the intracellular calicheamicin-γ_1 derivative can not only be achieved by decreased drug efflux, but also by increased cellular CD33-mediated uptake of the immunoconjugate, indicating an important role of the number of CD33 molecules expressed on the cell surface of AML cells and their rate of endocytosis for GO-induced cytotoxicity. So far, experimental evidence supporting this hypothesis is lacking. Furthermore, mechanisms regulating expression and internalization of CD33 remain unknown. However, if the importance of CD33 expression and internalization for GO-induced cytotoxicity could be established and underlying mechanisms elucidated, one could envision novel avenues to enhance clinical efficacy of CD33-targeted chemotherapy of AML, e.g. by increasing CD33 expression or enhancing internalization of antibody-bound CD33. The primary objectives of the studies summarized in this thesis were therefore to investigate the quantitative relationship between CD33 expression and GO-induced cytotoxicity, as well as to elucidate the mechanisms underlying endocytosis and trafficking of CD33 when bound to antibody. The findings are described in the next chapters in detail. Together, they significantly expand the current understanding of CD33 biology, and, more generally, the biology of closely related Siglecs, in particular the subgroup of CD33-related Siglecs. Furthermore, from a clinical perspective, this deepened understanding may provide the rational for novel therapeutic approaches aimed to increase uptake of anti-CD33 antibodies, and eventually to enhance clinical efficacy of anti-CD33 antibody-based therapies.

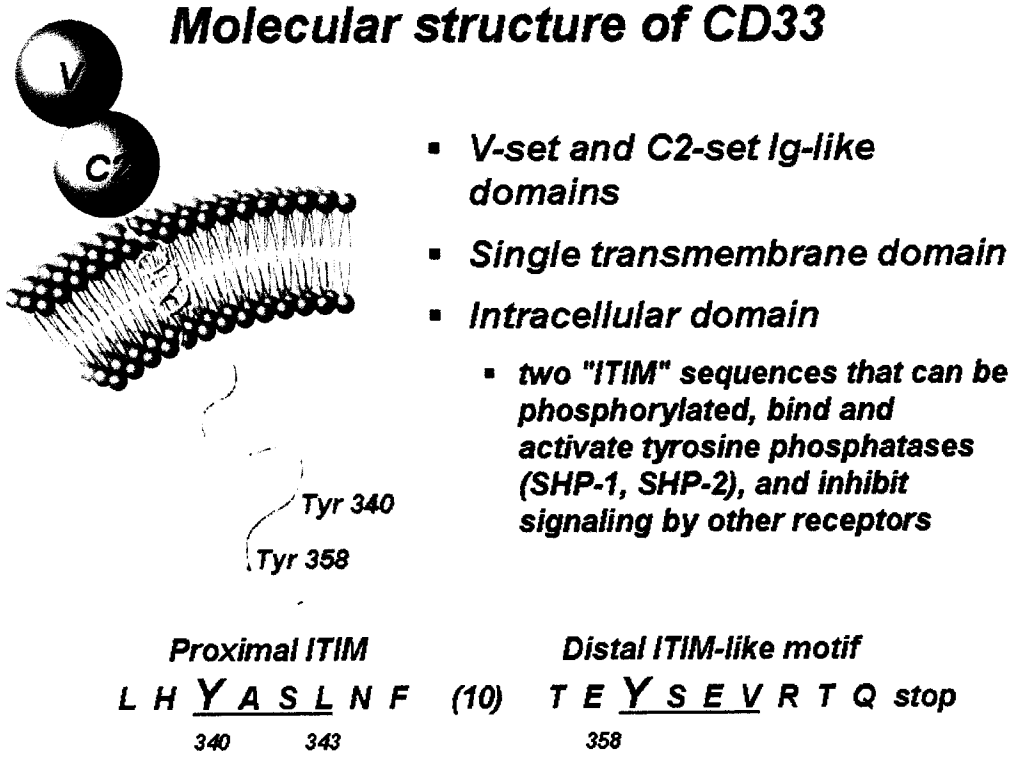

Figure 1. Molecular structure of CD33.

Chapter I: Influence of CD33 expression levels and ITIM-dependent internalization on gemtuzumab ozogamicin-induced cytotoxicity[a]

I.1. Introduction

CD33 is a 67kD type 1 transmembrane sialoglycoprotein and founding member of a rapidly evolving immunoglobulin superfamily subset of sialic acid binding immunoglobulin-related lectins (siglecs; siglec-3).[29,30] CD33 is characterized by the presence of two conserved immunoreceptor tyrosine-based inhibitory motif (ITIM)-like motifs in the cytoplasmic region, a property that is shared with all CD33-related siglecs discovered so far.[30] If phosphorylated upon treatment with pervanadate or anti-CD33 antibody plus cross-linking secondary antibody, these tyrosine motifs recruit and activate Src homology-2 (SH2) domain-containing tyrosine phosphatases (SHP-1 and SHP-2).[44-46]

Physiologically, CD33 expression is restricted to early multilineage hematopoietic progenitors, myelomonocytic precursors, and more mature myeloid cells, but it is absent on normal pluripotent hematopoietic stem cells.[12-14] However, 85 - 90% of adult and pediatric cases of acute myeloid leukemia (AML) express CD33.[14,23] Therefore, CD33 has gained clinical importance as a suitable tumor-associated antigen and target for antibody-based AML therapies.[26]

Promising clinical results have been obtained with gemtuzumab ozogamicin (GO; CMA-676; Mylotarg™), an immunoconjugate consisting of a humanized IgG_4 anti-CD33 monoclonal antibody (hP67.6) joined to a derivative of the cytotoxic

---

[a]This chapter has previously been published: Walter RB, Raden BW, Kamikura DM, Cooper JA, Bernstein ID. Influence of CD33 expression levels and ITIM-dependent internalization on gemtuzumab ozogamicin-induced cytotoxicity. Blood 2005:105:1295-1302.

drug calicheamicin-γ_1, N-acetyl-γ-calicheamicin dimethyl hydrazide.[73] Although some unconjugated anti-CD33 antibodies may have limited cytoreductive activity when used as monotherapy in patients,[83,84] hP67.6 is believed to function primarily as a carrier to facilitate cellular uptake of the calicheamicin-γ_1 derivative, which is then cleaved intracellularly in an acidic compartment, presumably inside lysosomes, and subsequently induces DNA damage and eventually cell death.[78]

This putative mechanism of action of GO still needs firm experimental confirmation, but implies a pivotal role of both the number of CD33 molecules expressed on the cell surface and the rate of internalization of CD33 following GO binding for the cytotoxic effect. However, little is known about the importance of the quantity of CD33 expression for GO-induced cytotoxicity. Although multiple studies have confirmed that binding of bi- and multivalent anti-CD33 antibodies results in CD33 internalization in both $CD33^+$ hematopoietic cell lines and primary AML blast cells,[61-64] some authors have argued that cytotoxic effects of GO are achieved in the absence of CD33 expression.[85] In addition, neither the endocytic process by which CD33 delivers antibody to the cytosol, nor the necessity of CD33 endocytosis for GO-induced cytotoxicity, has been established.

The primary objective of the present study was therefore to investigate the quantitative relationship between CD33 expression and the requirement for CD33 internalization in GO-mediated cytotoxicity. To accomplish this, lentivirus-mediated gene transfer was used to manipulate CD33 expression. We also identified the motif(s) that control internalization of antibody-bound CD33, and determined the requirement of these motifs for GO-induced cytotoxicity.

I.2. Materials and Methods

Cell lines

Human myeloid OCI-AML3 cells (kindly provided by Dr. M.D. Minden, University of Toronto, ON, Canada) and KG-1a cells (kindly provided by Dr. D.E. Banker, Fred Hutchinson Cancer Research Center, Seattle, WA, USA) were maintained in RPMI medium 1640 with 25 mM HEPES (GIBCO Invitrogen, Carlsbad, CA, USA) supplemented with 10% heat-inactivated fetal bovine serum (FBS, HyClone, Logan, UT, USA), 1 mM MEM sodium pyruvate, and 0.1 mM MEM non-essential amino acids (both GIBCO Invitrogen). The interleukin-3 (IL-3)-dependent murine myeloid 32D cell line was maintained in Iscove's Modified Dulbecco Medium (IMDM, GIBCO Invitrogen) with 10% heat-inactivated FBS and 8% conditioned WEHI cell-conditioned medium as a source of IL-3.

Patient AML blast cell samples

Marrow samples were taken from adult patients in untreated first relapse of AML (non-M3 subtypes) who participated in the phase II clinical trials with GO.[74,79] Thawed aliquots of frozen samples of density gradient-isolated mononuclear cells containing leukemic blast cells were used for these studies. All patients signed informed consents, and the institutional review boards of the participating institutions approved all protocols.

Lentiviral vectors and gene transfer

pcDNA3 vectors containing complementary DNA (cDNA) for wild-type CD33, $CD33^{Y340F}$, $CD33^{Y358F}$, and $CD33^{Y340F/Y358F}$ were kindly provided by Dr. D.W. McVicar, National Cancer Institute, Frederick, MD, USA.[46] Site-directed mutagenesis with the primer 5'-ATG AGG AGC TGC ATT ATG CAT CCG CCA ACT TTC ATG GGA TGA ATC-3' was performed to generate $CD33^{L343A}$ (Table I.1). These cDNAs were cloned into the pRRLsin.cPPT.MSCV vector as a CD33-IRES-EGFP cassette using standard PCR cloning procedures. All constructs

were verified by sequencing. The vector pRRLsin.cPPT.MSCV.EGFP was used as control in some experiments. Due to high levels of EGFP expression from this control vector, the maximal MOI used was 10. In a previous study, we found that human AML cell lines (ML-1, NB4, HL-60, U937) that were transduced with the control vector (used at a MOI up to 10) or the vector containing an irrelevant gene (used at a MOI up to 100) were similar to non-transduced cells with regard to cell viability and response to GO or the free calicheamicin-γ_1 derivative.[82] Stocks of VSV-G-pseudotype lentiviral vectors were prepared by calcium phosphate-mediated three-plasmid transfection of HEK293T cells. Briefly, 27 µg of the transfer vector construct, 17.5 µg second generation gag-pol packaging construct pCMVR8.74, and 9.5 µg VSV-G expression construct pMD.G were used for transfection of 1.2 x 10^7 HEK293T cells overnight in 25 mL Dulbecco's Modified Eagle Medium (D-MEM, GIBCO Invitrogen) with 10% heat-inactivated FBS. The cells were treated with 10 mM sodium butyrate during the first of three 12-hour vector supernatant collections. The supernatant was filtered through a 0.22 µm pore-size filter and concentrated 100-fold by ultracentrifugation. All vector stocks were titered by transducing HT1080 cells using limiting dilutions of the stock with analysis for EGFP expression by flow cytometry. Transductions were performed in fibronectin-coated wells in the presence of 8 µg/mL protamine sulfate at a multiplicity of infection (MOI) of 1-100. EGFP-positive cells were sorted by flow cytometry and re-cultured for further analysis.

Flow cytometry assays for determination of CD33 expression and internalization

A cytofluorometric immunofluorescence staining method was used to characterize both the membrane display of CD33 of resting cells as well as the internalization of antibody-bound CD33. Cell surface CD33 expression in untreated cells was detected by staining with phycoerythrin (PE)-conjugated anti-CD33 antibody (clone P67.6; BD Biosciences, San Jose, CA, USA). For a staining negative control, parallel samples were incubated with an irrelevant PE-conjugated isotype control antibody (BD Biosciences) at the same protein

concentration. To measure internalization of antibody-bound CD33 in AML cell lines, cells (typically 1-1.5 x 10^6) were transferred into 5 mL polystyrene round bottom tubes (BD Falcon™, Discovery Labware, Bedford, MA, USA) and incubated for at least 30 minutes with IMDM medium containing 10 µg/mL unconjugated, unlabeled hP67.6 (kindly provided by Wyeth-Ayerst Research, Radnor, PA, USA) in ice-water (to prevent internalization during the staining procedure). Cells were then washed in ice-cold Phosphate Buffered Saline (PBS, GIBCO Invitrogen), resuspended in IMDM medium without antibody, split into several tubes, and incubated at 37°C (in 5% CO_2 and air) for various periods of time. Afterwards, cells were chilled and incubated with biotin-conjugated mouse anti-human IgG_4 monoclonal antibody (used at 5 µg/mL in PBS/2% FBS), followed by incubation with streptavidin-PE conjugate (used at 5 µg/mL in PBS/2% FBS: both from BD Pharmingen™, San Diego, CA, USA) to detect remaining hP67.6 on the cell surface. One sample that was kept in ice-water was used to determine the starting level of antibody bound to the cell surface. The same assay was used to measure internalization of antibody-bound CD33 in primary AML blast cells; however, cells were kept in IMDM supplemented with with 20% FBS and 100 ng/mL of the following recombinant human cytokines: granulocyte-macrophage colony-stimulating factor, stem cell factor, interleukin-3, and granulocyte colony-stimulating factor (all from Amgen, Thousand Oaks, CA) during the assay.[79,80] To identify nonviable cells, all samples were stained with propidium iodide (PI, Sigma, St. Louis, MO). At least 10,000 events were acquired and PI^- cells were analyzed on a FACScan flow cytometer using Cellquest software (BD Biosciences). Linear fluorescence values were used to calculate the percentage of antibody internalization. Using this assay, a time-dependent loss of cell surface hP67.6 was observed in a panel of human $CD33^+$ AML cell lines (ML-1, HL-60, U937, NB4, and TF-1 cells). To verify that the time-dependent loss of cell surface associated hP67.6 reflects antibody internalization, as opposed to shedding or dissociation of hP67.6 from CD33, we repeated these experiments with hP67.6 that had been directly labeled with

Alexa Fluor 488 (Molecular Probes, Eugene, OR, USA). Alexa Fluor 488 is a green small molecular weight dye whose fluorescence properties are relatively independent of changes in surrounding pH. Cell-associated green fluorescence remained unchanged when the internalization assay was performed with Alexa Fluor 488-labeled hP67.6; while cell surface hP67.6 decreased during the assay, as detected by using biotin-conjugated mouse anti-human IgG_4 monoclonal antibody and a streptavidin-PE conjugate. Thus, the loss of cell surface associated hP67.6 measured over time in our assay indeed reflects antibody internalization.

Confocal microscopy

Cells were first incubated for 45 minutes in IMDM medium containing 20 µg/mL hP67.6 that was directly labeled with Alexa Fluor 594 (Molecular Probes) in ice-water. Cells were then washed with ice-cold PBS, resuspended in IMDM medium without antibody, and incubated at 37°C for 30 minutes. Subsequently, cells were fixed with PermiFlow (Inviron, Frankfort, MI, USA) at room temperature for 30 minutes, stained with DAPI, and mounted on polylysine-coated slides with SlowFade antifade solution (Molecular Probes). Slides were visualized at 60x magnification using an Olympus lens (Melville, NY, USA) and a Deltavision SA3.1 wide-field deconvolution microscope. Images were analyzed with SoftWoRX software (both Applied Precision, LLC, Issaquah, WA, USA).

Assays for drug-induced cytotoxicity

Cells were taken during exponential growth and incubated at 37°C (in 5% CO_2 and air) in 96-well round bottom plates (BD Falcon™) at 2 x 10^4 cells/well in 240 µL culture medium containing various concentrations of GO or, in some experiments, N-acetyl gamma calicheamicin dimethyl hydrazine (referred to as calicheamicin-γ_1; both kindly provided by Wyeth-Ayerst Research). In some experiments with KG-1a cells, cyclosporine A (CSA; Sigma) was added at a concentration of 2.5 µg/mL. After three days of culture,[64,80,81] cell numbers and

drug-induced cytotoxicity, using PI to detect non-viable cells, were determined using a FACSCalibur flow cytometer (BD Biosciences) and analyzed with Cellquest Software. In early studies, we used 2-hour exposures to GO, after which cells were washed and then resuspended in GO-free medium and incubated for 3 days before cytotoxicity was assessed, as previously published.[80,81] In this assay, OCI-AML3 cells became more sensitive to GO when CD33 was overexpressed (in one experiment: +7% PI positive cells in parental cells vs. +30% PI positive cells in cells transduced with an MOI of 50 at a dose of GO of 2.5 ng/mL). However, 32D cells remained resistant at the highest GO dose used (40 ng/mL for 2 hours) even when expressing high levels of CD33. KG-1a cells were totally resistant to a pulse of 40 ng/mL GO, even in the continuous presence of CSA (data not shown). We therefore exposed parental and transduced cells to continuous GO for 3 days to measure cytotoxicity. As a control for assaying the toxicity of GO, we first measured the toxicity of free calicheamicin-γ_1. A direct comparison revealed that the sensitivity of the cell lines towards calicheamicin-γ_1 varied greatly and was found to be in the order: OCI-AML3 cells > 32D cells > KG-1a cells. For example, the fraction of PI^+ cells increased by 19.2±5.5% at 0.25 ng/mL calicheamicin-γ_1 and by 60.0±13.1% at 2.5 ng/mL calicheamicin-γ_1, in parental OCI-AML3 cells compared to cells incubated without cytotoxic drug (data given as mean±SEM; n=3), whereas the fraction of PI^+ 32D cells increased to a significant degree only at 5 ng/mL calicheamicin-γ_1 (35.0±11.3%). By comparison, KG-1a cells were completely resistant to 10 ng/mL calicheamicin-γ_1 in the absence of CSA. Therefore, direct comparisons of cytotoxic effects of calicheamicin-γ_1, and by extrapolation of GO, are not possible between different cell lines, but need to be assessed in each cellular background individually.

I.3. Results

Effect of CD33 expression on GO-induced cytotoxicity

We first sought to determine the quantitative relationship between CD33 expression and the cytotoxic effect of GO *in vitro*. Although we have found significantly different levels of endogenous CD33 expression on a panel of human AML cell lines in a previous study,[81] these cell lines also had different susceptibilities to the cytotoxicity induced by free calicheamicin-γ_1 (data not shown), rendering direct comparisons between individual cell lines with regard to GO-induced cytotoxicity impossible. Furthermore, an obvious limitation of comparisons between different cell lines is the fact that they may differ not only with regard to the level of CD33 expression, but also with regard to other parameters that might be important for GO-induced cytotoxicity, such as drug internalization (see below), intracellular trafficking, or the presence of resistance mechanisms. In order to unequivocally assess the importance of CD33 expression, we therefore prepared sublines of a given cell type that were forced to express different levels of CD33 under the murine stem cell virus (MSCV) promoter via lentivirus-mediated gene transfer.

Although nearly all widely used human AML cell lines express endogenous CD33, a previous study found that the OCI-AML3 cell line lacks CD33.[86] However, we found small but detectable levels of endogenous CD33 on parental OCI-AML3 cells, as determined by flow cytometry-based immunostaining (Fig I.1). We also examined the weakly CD33-positive human myeloid KG-1a cell line and the murine 32D myeloid line, which is devoid of CD33.

Lentivirus-mediated transfer of wild-type CD33 at a multiplicity of infection (MOI) of 1-100 in each of these cell lines yielded stable subpopulations of EGFP-positive cells, which were sorted by flow cytometry and expanded. Upon analysis, these cells showed cell surface expression of CD33 with a MOI-dependent increase in expression levels of CD33 (Fig I.1). The range of fluorescence intensities in CD33 transduced cells was very narrow, i.e.

homogeneous populations of CD33 overexpressing cells could be generated (data not shown).

To assess the effect of CD33 expression on GO-induced cytotoxicity in each of the parental and CD33-transduced cell lines that express CD33 at different levels, cells were treated with various concentrations of GO for 3 days and cytotoxicity then determined by flow cytometry with propidium iodide (PI). As shown in Fig I.2, parental 32D, which do not express the CD33 antigen, are resistant to GO at concentrations that effectively kill $CD33^+$ cells. By comparison, parental OCI-AML3 cells, which express low levels of endogenous CD33, are sensitive to GO at a dose-equivalent concentration (DEC) of about 0.01 - 0.025 ng/mL (Fig I.2). Expression of the empty-control vector did not significantly change the response to GO in these cells (data not shown). Parental KG-1a cells were completely resistant to GO (as well as the free toxic calicheamicin-γ_1) at a concentration as high as 10 ng/mL DEC despite endogenous expression of low levels of CD33. Although resistance mechanisms to calicheamicin-γ_1 were not investigated systematically in this study, KG-1a cells were found to express P-glycoprotein (Pgp or MDR1 or ABCB1), as detected by immunostaining with anti-Pgp antibody (clone 4E3.16)[80] and a functional efflux assay with the fluorescent dye 3,3'-diethyloxacarbocyanine iodide ($DiOC_2$) in the presence or absence of the Pgp inhibitor cyclosporine A (CSA)[80] (data not shown). Previous *in vitro* studies have demonstrated that Pgp expressing cell lines and patient AML blast cells are resistant to GO, and that Pgp inhibitors can restore drug sensitivity in Pgp expressing cells.[79-81,87,88] We therefore performed similar cytotoxicity assays with parental KG-1a cells in the presence of CSA to block Pgp-mediated drug efflux. With this co-treatment, these cells became susceptible to GO, as shown in Fig I.2. In all 3 cell lines, however, lentivirus-mediated transfer of wild-type CD33 resulted in significantly enhanced sensitivity to GO. Importantly, GO-sensitivity increased in a MOI-dependent manner, i.e. in a direct correlation with the cell surface expression levels of CD33 (Fig I.2); this MOI-dependency was especially

apparent at lower GO-concentrations. Together, these data demonstrate the importance not only of CD33 expression per se, but also of the level of CD33 expression for GO-induced cytotoxicity.

Measurement of internalization of antibody-bound CD33 in AML cell lines and primary AML blasts

It has previously been established that antibody-bound CD33 is internalized by both $CD33^+$ hematopoietic cell lines and primary AML blast cells.[61-64] To quantify antibody uptake, we modified a flow cytometry-based assay,[64] in which cells labeled with unconjugated hP67.6 were allowed to internalize in antibody-free medium for various periods of time. Second and third step reagents were then used to measure hP67.6 that remained on the cell surface. Control experiments with directly labeled hP67.6 were performed to verify that the time-dependent loss of cell surface associated hP67.6 is reflective of antibody internalization and not indicative of dissociation of the antibody from CD33 or shedding of the antigen (see Materials and Methods). In addition, antibody internalization was visualized with confocal microscopy (data not shown, and Fig I.5). Using this flow cytometry based assay, we could easily detect loss of cell surface associated hP67.6, i.e. internalization of antibody-bound CD33 in a panel of $CD33^+$ human AML cell lines (data not shown) as well as in 32D, OCI-AML3, and KG-1a cells that were transduced with wild-type CD33. As shown in Fig I.3, the loss of cell surface associated hP67.6 ranged from about 10-15% to about 50% after 60 minutes of incubation at 37°C. The percentage of antibody-bound CD33 that was internalized was relatively independent of the levels of cell surface CD33 expression in 32D and KG-1a cells, whereas it was reduced in OCI-AML3 sublines that expressed high levels compared to sublines that expressed low levels of cell surface CD33 (Fig I.3). This suggests that the endocytosis machinery is not saturated by over-expressed CD33, except perhaps in the case of OCI-AML3 sublines expressing high levels of CD33. Accordingly, the total amount of antibody internalization, as estimated by changes in arbitrary

fluorescence units, was greater in sublines expressing higher levels of CD33 (Fig I.3, right panel). We also measured internalization of antibody-bound CD33 in 9 AML blast cell samples. As shown in Fig I.4, the loss of cell surface associated hP67.6 varied about 3-fold between between individual samples; thus, these values were comparable to those determined in AML cell lines expressing endogenous CD33 and AML cell lines transduced with wild-type CD33.

ITIM-dependent internalization of antibody-bound CD33 in transduced cell lines

We next sought to determine the motif(s) that control(s) internalization of antibody-bound CD33. For CD22, a B-cell restricted member of the siglec family, it has recently been shown that antibody-mediated internalization of the antigen is dependent on the integrity of two ITIM motifs.[70] Given the similarity to CD33, we hypothesized that the ITIM motifs on the cytoplasmic tail of CD33 may control antibody-bound internalization of CD33. To test this hypothesis, we expressed a series of CD33 mutants in 32D, OCI-AML3, and KG-1a cells: $CD33^{Y340F}$, in which the tyrosine of the first ITIM motif at position 340 was changed to phenylalanine; $CD33^{L343A}$, in which the leucine contained in the proximal ITIM motif at position 343 was changed to alanine; $CD33^{Y358F}$, in which the tyrosine of the distal ITIM motif at position 358 was changed to phenylalanine; and $CD33^{Y340F/Y358F}$, in which the tyrosines of both ITIM motifs were changed to phenylalanine (Table I.1). Lentivirus-mediated transfer of these CD33 mutants at a multiplicity of infection (MOI) of 10-50 yielded stable subpopulations of EGFP-positive cells, which, after sorting and expansion, showed comparable levels of cell surface expression of CD33 (not shown). As shown in Fig. I.5, disruption of the proximal ITIM motif, either by changing tyrosine to phenylalanine ($CD33^{Y340F}$ mutant) or by changing leucine to alanine ($CD33^{L343A}$ mutant), resulted in an almost complete abrogation of internalization of antibody-bound CD33 in transduced OCI-AML3, KG-1a, and 32D cells. Slightly divergent results were found when the distal ITIM motif was disrupted: in 32D and KG-1a cells, internalization was only partially inhibited, whereas in OCI-AML3 cells, internalization was completely disrupted in

cells expressing $CD33^{Y358F}$. Similar to sublines expressing a mutant proximal ITIM, 32D and KG-1a cells expressing mutated proximal and distal ITIMs ($CD33^{Y340F/Y358F}$ mutant) completely failed to internalize antibody-bound CD33. In contrast, in the OCI-AML3 subline expressing $CD33^{Y340F/Y358F}$ internalization of antibody-bound CD33 was surprisingly only partially inhibited. Internalization of antibody-bound CD33 was also studied visually by use of confocal microscopy, and similar results were obtained, as shown in Fig I.6 for OCI-AML3 cells. Together, these data indicate that the proximal ITIM motif, and, at least to some degree, also the distal ITIM motif, control internalization of antibody-bound CD33 in myeloid cell lines.

Correlation between internalization of CD33 and GO-induced cytotoxicity

Finally, we investigated whether internalization of CD33 correlates with the extent of GO-induced cytotoxicity. For these experiments, we treated 32D, OCI-AML3, and KG-1a cells that were transduced with either wild-type CD33 or CD33 mutants with GO for 3 days, before cytotoxicity was assessed with PI staining. Since our initial experiments have indicated the importance of the expression levels of CD33 for GO-induced cytotoxicity, we used sublines expressing comparable levels of CD33 for these assays.

As shown in Fig I.7, disruption of the proximal ITIM-like motif, or both motifs, resulted in an almost complete abrogation of GO-induced cytotoxicity in 32D cells, whereas disruption of the distal ITIM-like motif only partially abrogated GO-induced cytotoxicity, thus very well correlating to the internalization properties of the CD33 mutants (compare Fig I.7A to Fig I.5A). OCI-AML3 cells transduced with CD33 mutants with disrupted proximal or distal ITIM-like motif were about as sensitive to GO-induced cytotoxicity as parental cells, whereas OCI-AML3 cells transduced with wild-type CD33 (or the $CD33^{Y340F/Y358F}$ mutant) were clearly more sensitive to GO; again, sensitivity to GO very well correlated with the internalization properties of the CD33 mutants (compare Fig I.7B to Fig I.5B).

Similar results were obtained for the KG-1a sublines (in which cells were co-treated with CSA), although the effect of disruption of the ITIM-like motifs was less pronounced than in the 32D or OCI-AML3 sublines (compare Fig I.7C to Fig I.5C). Together, these data indicate that disruption of the proximal ITIM-like motif, and, at least to some degree, also the distal ITIM-like motif, significantly decreases GO-induced cytotoxicity compared to cells expressing wild-type CD33 at comparable levels.

I.4. Discussion

The data presented in this report support three major conclusions. First, we demonstrate the importance not only of CD33 expression per se, but also of the level of CD33 expression for GO-induced cytotoxicity. Second, we identify the ITIMs as the amino acid sequences that largely control internalization of antibody-bound CD33. Finally, we found that disruption of these motifs by introduction of point mutations not only significantly reduced internalization of anti-CD33 antibody, but also significantly reduced GO-induced cytotoxicity. Together, these data show an important role of both the number of CD33 molecules expressed on the cell surface and the amount of internalization of antibody for entry of the immunoconjugate into the cell and GO-induced cytotoxicity.

Previous *in vitro* studies have demonstrated a selective killing of $CD33^+$ AML cells compared to $CD33^-$ lymphoblastic cells with GO.[87,89] In line with these findings, we show in the present study that lentivirus-mediated expression of CD33 in 32D cells renders these cells susceptible to GO-induced cytotoxicity *in vitro* at concentrations that can be achieved after application of GO in patients *in vivo*.[90] Such a comparison of parental $CD33^-$ cells with transduced $CD33^+$ cells offers a major advantage over previous comparisons between different cell

types, as it minimizes the chance of misinterpreting results due to confounding variables, such as cellular differences with regard to behavior of antigen after antibody is bound, trafficking, or drug resistance mechanisms. In addition to demonstrating the importance of CD33 per se, our data show that GO-sensitivity directly correlated with the cell surface expression levels of wild-type CD33 in transduced OCI-AML3, KG-1a, and 32D cells. These data clearly indicate a role of the cell surface expression level of CD33 as a limiting factor for the cytotoxic effect of GO in CD33-transduced myeloid cell lines. Such an effect may be difficult to detect in primary AML blast cells for above mentioned reasons, although quantitative flow cytometry studies have shown that the level of CD33 expression varies widely between individual patients with AML.[27] In fact, a correlation between marrow blast CD33 antigen levels and clinical response was not observed in clinical trials using GO monotherapy for $CD33^+$ relapsed adult AML.[74,75] In these phase II trials, however, only patients with predefined levels of CD33 (i.e. greater than 80% of leukemic blast cells with CD33 immunofluorescence staining four times above background staining was required[74]) were included; in addition, the analysis may be confounded by other factors, such as multidrug resistance, particularly Pgp expression. Together with these findings, our data suggest that manipulation of the expression level of CD33 on AML blasts may be a first novel therapeutic approach to improve clinical efficacy of GO. Unfortunately, the regulation of CD33 expression on both normal and malignant cells is not understood at present. Preliminary *in vitro* studies suggested that granulocyte colony-stimulating factor, granulocyte-monocyte colony-stimulating factor, interferon-α, interleukin (IL)-3, and IL-6 may modestly increase CD33 expression on the surface of $CD34^+/CD33^+$ blasts,[91] but additional more detailed experiments are needed to fully explore ways to manipulate CD33 expression on AML blasts. Furthermore, previous studies have indicated that re-expression of CD33, following internalization of antibody-bound CD33, significantly contributes to the total amount of internalized anti-CD33 antibody.[64] It seems likely that the rate of re-expression of CD33 may be

regulated. If so, variations in the rate of re-expression would impact the total amount of antibody internalization and thus GO toxicity.

Recent studies have shown that drug efflux mediated by members of the adenosine triphosphate-(ATP) binding cassette (ABC) superfamily of proteins, predominantly Pgp but, to a lesser degree, also multidrug resistance protein (MRP), mediate resistance to GO.[74,79-81,87,88] In line with the perceived importance of Pgp for resistance to GO, the Pgp^+ KG-1a cells were completely resistant to GO at clinically useful doses. More importantly, although enforced overexpression of CD33 sensitized KG-1a cells in direct correlation to the level of CD33 expression, this effect on GO-induced cytotoxicity was only readily visible upon co-treatment with CSA, most likely because the capacity of drug efflux exceeded the amount of drug internalization. These findings emphasize the fact that increased accumulation of intracellular calicheamicin-γ_1 can be achieved by either increased uptake of GO, e.g. via increased expression of cell surface CD33, or decreased efflux of calicheamicin-γ_1, e.g. via inhibition of ABC transporters, or both.

In line with previous studies, anti-CD33 antibody was internalized after engagement by cells expressing wild-type CD33.[61-64] Antibody internalization was relatively independent of the expression level of CD33 in 32D and KG-1a cells. By comparison, the percentage of antibody internalization dropped in OCI-AML3 sublines that expressed high levels of CD33. This is not necessarily unexpected, as it has been repeatedly observed that the endocytic machinery can be saturated due to the limited availability of recognition components.[69]

Our experiments with CD33 mutants indicate that the proximal ITIM-like motif, and, at least to some degree, also the distal ITIM-like motif, controls internalization of antibody-bound CD33 in transduced myeloid cell lines. Recent studies have indicated that these motifs are able to bind and activate SHP-1

and SHP-2 and to transmit inhibitory signals, at least under artificial *in vitro* conditions, if the tyrosines become phosphorylated.[44-46] Additional experiments are needed to clarify whether these signaling events can occur *in vivo*, e.g. in patients after treatment with GO, and to test whether outside-in signaling is linked to, or independent from, receptor internalization.

The mechanism(s) underlying internalization of antibody-bound CD33 remain(s) elusive. Mammalian cells have evolved several mechanisms for uptake of extracellular material and membrane components. However, endocytosis via clathrin-coated pits is by far the predominant mechanism for internalization of cell surface receptors and their cargo.[68] Indeed, the ITIM-like motifs of CD33 resemble YXXØ motifs (where X stands for any amino acid and Ø stands for an amino acid residue with a bulky hydrophobic side chain), a major tyrosine-based signal involved in clathrin-mediated protein sorting. This signal has been shown to interact with the μ subunit of the adaptor protein (AP) complex AP-2 and mediate clathrin-dependent endocytosis of, e.g., the transferrin receptor and the asialoglycoprotein receptor.[69] Similarly, it has recently been shown that antibody-mediated internalization of the B cell coreceptor CD22, another ITIM-bearing siglec, is dependent on the integrity of two ITIMs and is mediated by AP-2.[70] The Y residue is critical as anchor for the interaction with AP-2, whereas the Ø position can accommodate several residues with bulky hydrophobic side chains.[69] Our finding that both the $CD33^{Y340F}$ mutant and the $CD33^{L343A}$ mutant did not internalize efficiently when bound with antibody would be consistent with an important role of those two residues, and would fit the recognition pattern of the YXXØ motif with the μ subunit of AP-2, and it is therefore tempting to speculate that AP-2 may be involved in internalization of antibody-bound CD33. However, alternate endocytic adaptors have been described whose interactions depend on the presence of (phospho-) tyrosine motifs,[71,72] and additional studies will be required to dissect out the mechanisms that are involved in internalization of antibody-bound CD33, and to elucidate the role of tyrosine phosphorylation for

effective internalization. The finding that the $CD33^{Y340F/Y358F}$ mutant internalized when expressed in OCI-AML3 cells, but not in KG-1a or 32D cells, cannot be explained satisfactorily at this time. We can speculate, however, that the disrupted tertiary structure of this protein, or a heterodimer formation with endogenous wild-type CD33, enabled the efficient binding of an adaptor protein of the endocytic machinery, and may suggest differences in the posttranslational processing of CD33 or differences in the endocytic machinery in OCI-AML3 cells.

Our findings are limited because primary AML cells were not used. Preliminary studies on internalization of antibody-bound CD33 in 9 primary blast samples from patients with AML showed that between about 25% and 75% of antibody-bound CD33 was internalized over the first 4 hours, a range that is very comparable to what we found in our AML cell lines (data not shown). Although the levels of cell surface CD33 expression were quite different in these samples, meaningful comparisons of GO-cytotoxicity between individual AML blast cell samples were not possible for obvious reasons (e.g. differences in expression patterns of drug resistance proteins). The limited number of primary blast cells that were available per patient sample precluded studying endocytosis and GO toxicity effects of expressing additional wildtype or mutant CD33. We are hoping, however, that, once the mechanism underlying internalization of antibody-bound CD33 has been elucidated in engineered AML cell lines, primary AML cells can be used to study whether such mechanisms are also operative in primary cells.

An important conclusion of this study is that not only the level of CD33 expression but also the rate of endocytosis determines the extent of GO-induced cytotoxicity. Manipulation of the endocytic process therefore appears as a second interesting pharmacological target, as a faster internalization of antibody-bound CD33 may theoretically lead to enhanced GO-induced cytotoxicity, which in turn could lead to improved clinical outcomes of patients treated with GO.

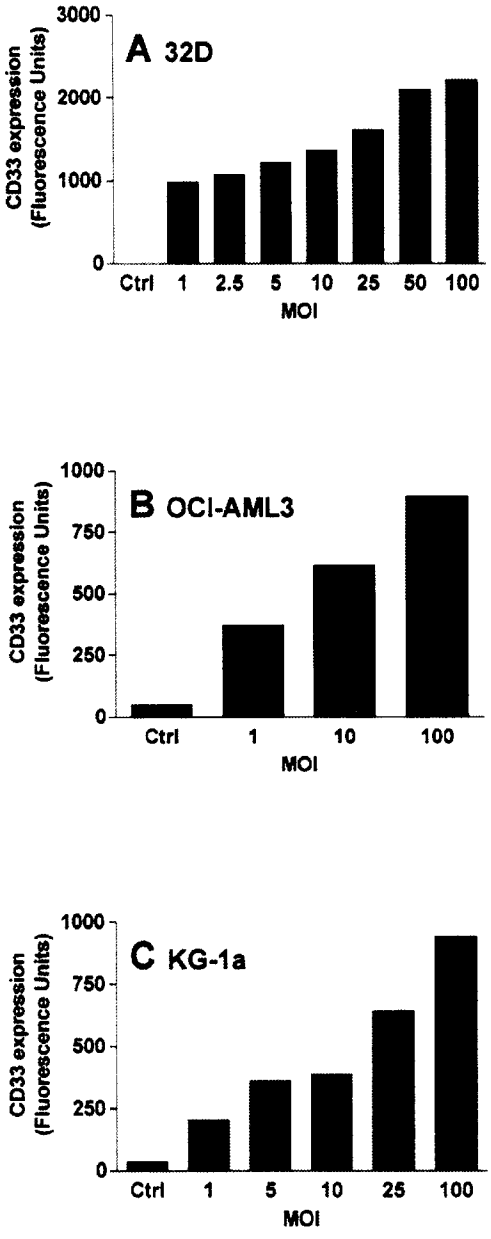

Figure I.1. CD33 wild-type protein expression of parental and transduced cell lines. CD33 cell surface staining intensity, represented by the mean fluorescence intensity of cells stained with monoclonal anti-CD33 antibody (after subtraction of the mean fluorescence intensity of cells stained with isotype control antibody) of (A) murine 32D, (B) human OCI-AML3, and (C) human KG-1a cells. Results from one representative experiment are shown for each cell line. MOI denotes multiplicity of infection. Note that fluorescence intensity values cannot be directly compared between cell lines, as the brightness of the staining of CD33-transduced OCI-AML3 cells required data acquisition with modified voltage parameters.

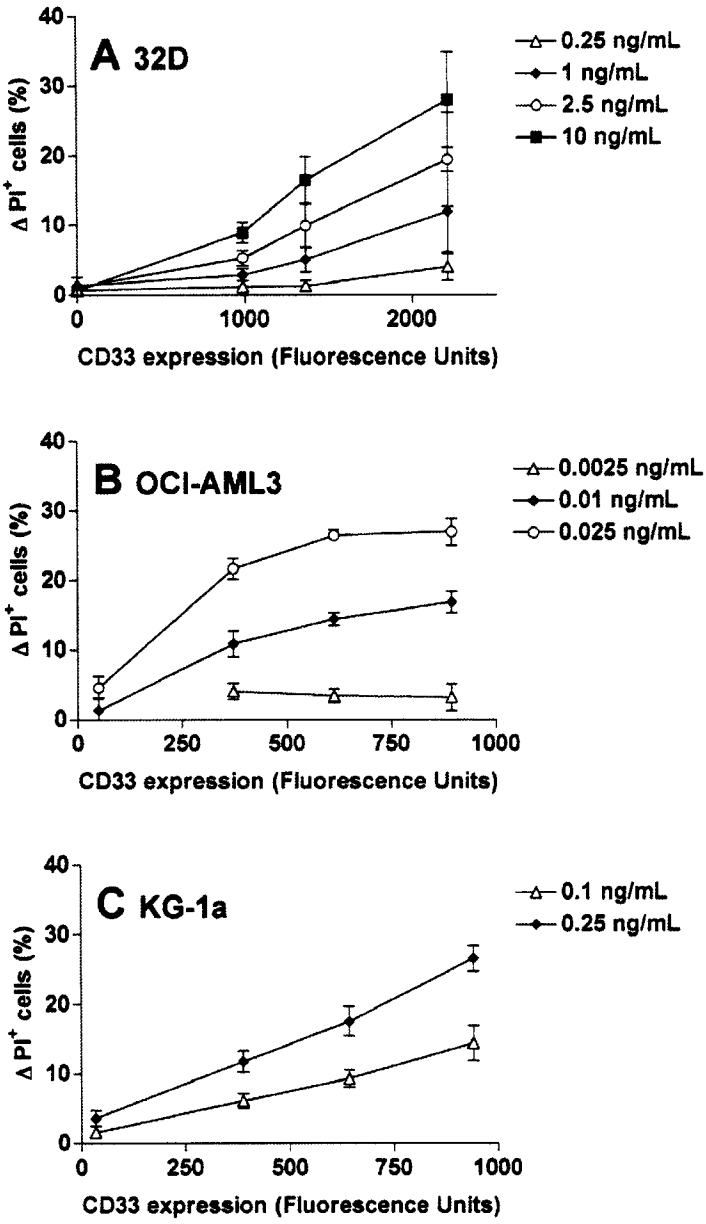

Figure I.2. Effect of CD33 expression on GO-induced cytotoxicity. Parental (A) 32D, (B) OCI-AML3, and (C) KG-1a cells and their sublines that were transduced with wild-type CD33 and expressed CD33 at different levels, as indicated by arbitrary fluorescence units, were incubated with various concentrations of GO for 3 days, before cytotoxicity was assessed with PI staining. In the case of KG-1a sublines, cells were co-treated with CSA. Increases in the percentage of PI^+ cells in GO-treated cells are compared to corresponding cells that were incubated without GO, and results are shown as mean±SEM from 2-4 independent experiments performed in duplicate or quadruplicate wells.

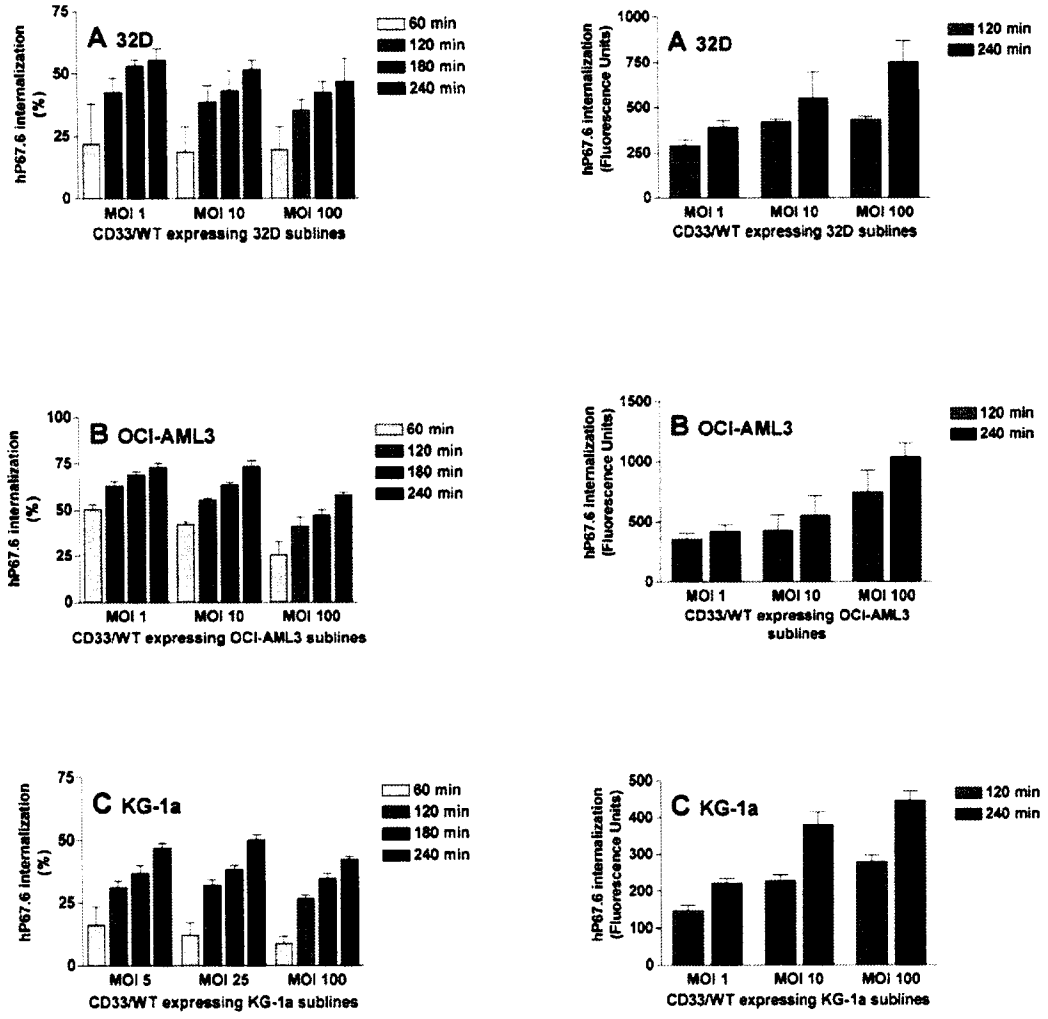

Figure I.3. Internalization of antibody-bound wild-type CD33 in transduced cell lines. (A) OCI-AML3 cell sublines, (B) KG-1a cell sublines, and (C) 32D cell sublines transduced with wild-type CD33 at different MOI were labeled with unconjugated hP67.6 on ice-water before the cells were incubated in 37° C in antibody-free medium to allow internalization of antibody-bound CD33 up to 4 hours as indicated. Subsequently, remaining cell surface associated hP67.6 was detected with biotin-conjugated mouse anti-human IgG_4 monoclonal antibody and a streptavidin-PE conjugate. Right panel shows the percentage of internalized hP67.6 relative to cells kept at 0° C, whereas the right panel depicts total amount of internalized hP67.6, expressed as change in arbitrary fluorescence units. Results are shown as mean±SEM from 2-5 independent experiments.

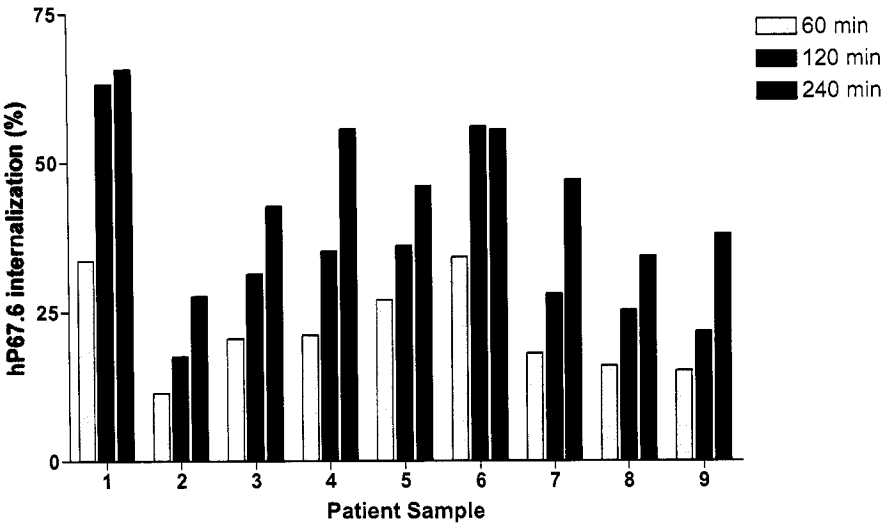

Figure I.4. Internalization of antibody-bound wild-type CD33 in primary AML blast cells. Primary AML blast cells were labeled with unconjugated hP67.6 on ice-water before the cells were incubated in 37° C in antibody-free medium to allow internalization of antibody-bound CD33 up to 4 hours as indicated. Subsequently, remaining cell surface associated hP67.6 was detected with biotin-conjugated mouse anti-human IgG_4 monoclonal antibody and a streptavidin-PE conjugate. Shown is the percentage of internalized hP67.6 relative to cells kept at 0° C.

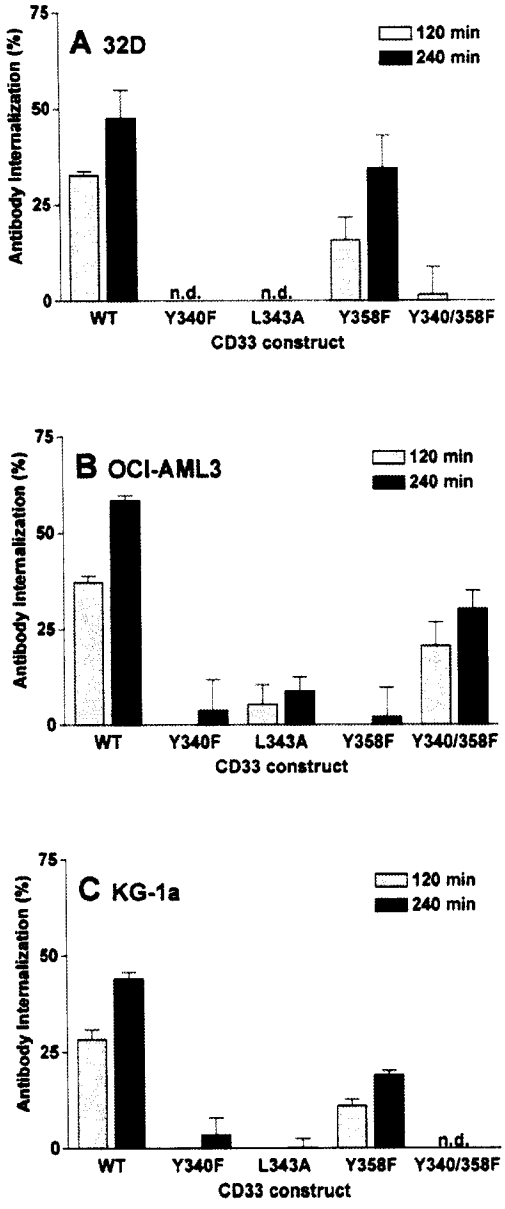

Figure I.5. ITIM-dependent internalization of antibody-bound CD33 in transduced cell lines. (A) 32D sublines, (B) OCI-AML3 sublines, and (C) KG-1a sublines, transduced with either wild-type CD33 or CD33 mutants, were labeled with unconjugated hP67.6 on ice-water before the cells were incubated in 37° C in antibody-free medium to allow internalization of antibody-bound CD33 for 2 (open bars) or 4 hours (filled bars). Subsequently, remaining cell surface associated hP67.6 was detected with biotin-conjugated mouse anti-human IgG_4 monoclonal antibody and a streptavidin-PE conjugate. Results are shown as mean±SEM from 3-4 (for 32D and KG-1a sublines) or 2 (for OCI-AML3 sublines) independent experiments. n.d.: no internalization detected.

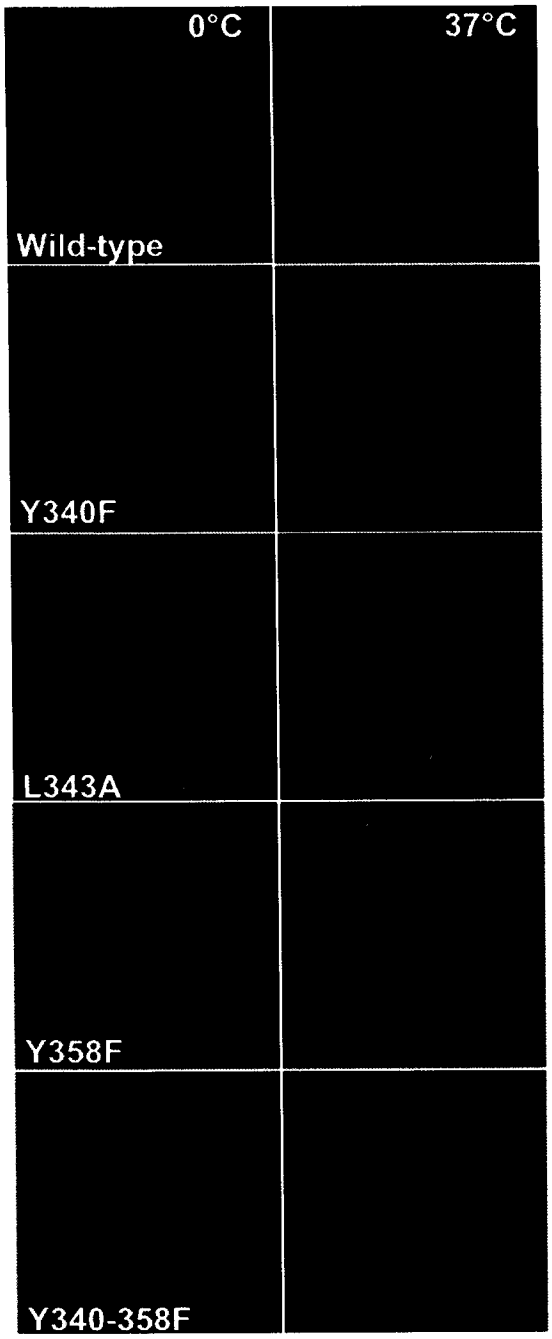

Figure I.6. Confocal microscopy study of ITIM-dependent internalization of antibody-bound CD33 in transduced cell lines. OCI-AML3 cell sublines transduced with either wild-type CD33 or CD33 mutants were incubated with Alexa Fluor 594-labeled hP67.6 on ice-water before the cells were transferred to antibody-free medium and either kept in ice-water (left panel) or incubated in 37° C (right panel) to allow internalization of antibody-bound CD33 for 30 minutes. Cells were then fixed, stained with DAPI, and visualized by confocal microscopy.

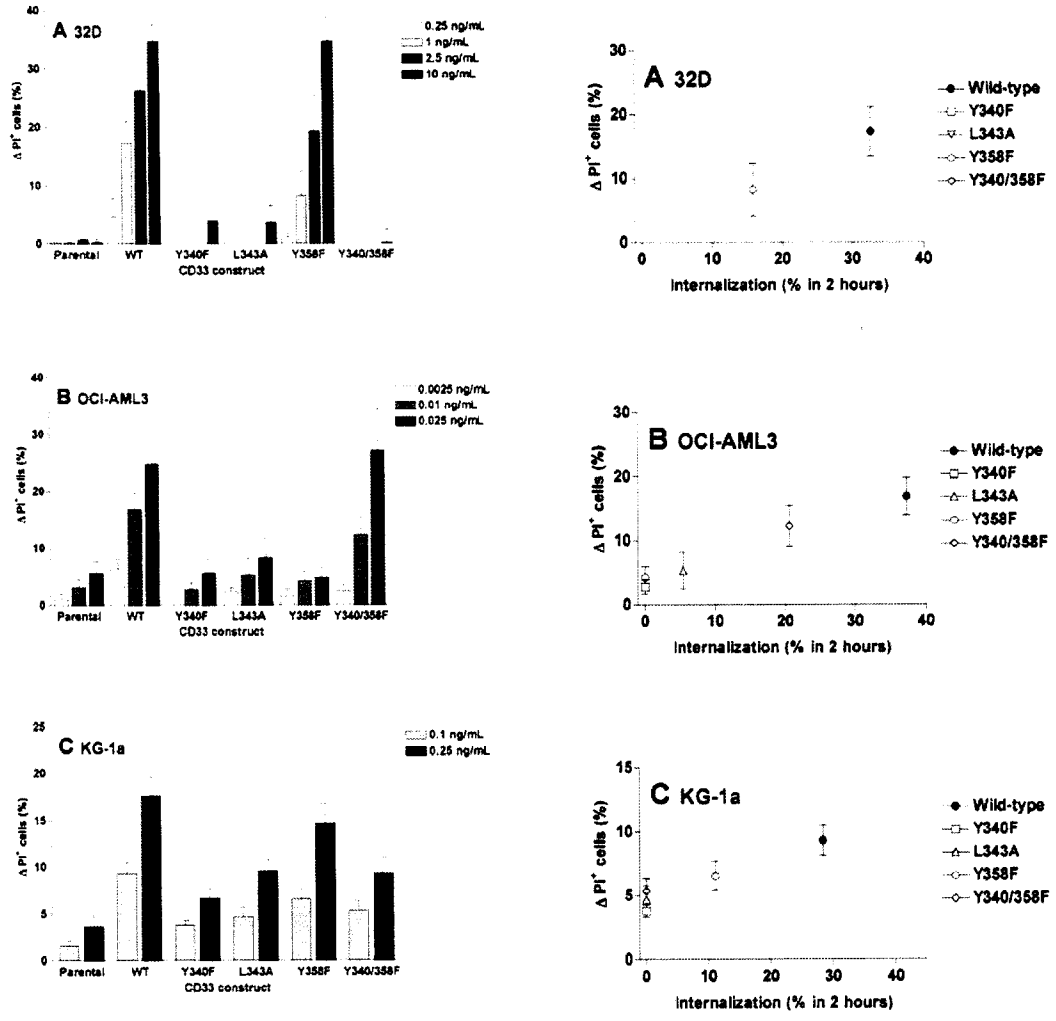

Figure I.7. ITIM-dependent GO-induced cytotoxicity in transduced cell lines. (A) 32D cell sublines, (B) OCI-AML3 cell sublines, and (C) KG-1a cell sublines transduced with either wild-type CD33 or CD33 mutants were incubated with indicated concentrations of GO for 3 days, before cytotoxicity was assessed with PI staining. In the case of KG-1a sublines, cells were co-treated with CSA. Increases in the percentage of PI^+ cells in GO-treated cells are compared to corresponding cells that were incubated without GO, and results are shown as mean±SEM from 2-5 independent experiments performed in duplicate or quadruplicate wells. The left panel shows the data grouped for individual sublines, whereas the right panel shows the effect of GO-induced cytotoxicity in relation to the percentage of internalization of CD33 after 2 hours.

Table I.1. Schematic representation of CD33 mutants used in internalization and cytotoxicity experiments. Single-letter amino acid code is used. Spacing between F and T is shown in brackets.

	Proximal ITIM								Distal ITIM							
$CD33^{WT}$	L	H	**Y**	A	S	**L**	N	F	(10)	T	E	**Y**	S	E	V	R T Q stop
			340			343						358				
$CD33^{Y340F}$	L	H	**F**	A	S	**L**	N	F	(10)	T	E	**Y**	S	E	V	R T Q stop
$CD33^{L343A}$	L	H	**Y**	A	S	**A**	N	F	(10)	T	E	**Y**	S	E	V	R T Q stop
$CD33^{Y358F}$	L	H	**Y**	A	S	**L**	N	F	(10)	T	E	**F**	S	E	V	R T Q stop
$CD33^{Y340F/Y358F}$	L	H	**F**	A	S	**L**	N	F	(10)	T	E	**F**	S	E	V	R T Q stop

Chapter II: Role of antibody and cellular tyrosine phosphorylation on ITIM-dependent internalization of CD33

II.1. Introduction

CD33/Siglec-3 (sialic acid binding immunoglobulin-like lectin), a 67kD type 1 transmembrane sialoglycoprotein, is an I-type lectin and founding member of the CD33/Siglec-3-related subfamily of Siglecs.[29,31,32] This subfamily, which comprises CD33/Siglec-3 as well as Siglec-5-11, is rapidly evolving, has poorly conserved binding specificities and domain structures, and shows highly variable expression on distinct subsets of hematopoietic cells.[30-32] For example, CD33 is normally found on immature and mature myeloid cells[12-14,32,33] and possibly subsets of B and activated T and natural killer (NK) cells,[15-22] but is also expressed on malignant cells of the vast majority of adult and pediatric cases of acute myeloid leukemia (AML).[14,23] Thus, CD33 has gained clinical importance as AML-associated antigen and target for antibody-based therapies.[25,26]

All human CD33-related Siglecs have a conserved proximal immunoreceptor tyrosine-based inhibitory motif (ITIM; with its tyrosine at position 340 in the case of CD33) and a distal ITIM-like motif (with its tyrosine at position 358 in the case of CD33).[30] Generally, when ITIM-containing receptors are appropriately engaged, they can become tyrosine phosphorylated and then transmit inhibitory signals by binding and activating Src homology-2 domain (SH2)-containing tyrosine phosphatases (SHP-1 and SHP-2) and/or the inositol polyphosphate 5'-phosphatase (SHIP).[43] In the case of CD33, several studies have indeed demonstrated that SHP-1 and SHP-2 but not SHIP are recruited and activated once the ITIMs are phosphorylated.[44-46]

Although the presence of ITIMs strongly suggests a role of CD33/Siglec-3-related Siglecs in the fine-tuning of cellular responses in the immune system,[31] their physiological functions remain poorly understood.[31,32] Nevertheless, growing evidence suggests that many Siglecs have endocytic properties.[31,32] Importantly, the early recognition that binding of bi- and multivalent anti-CD33 antibodies results in CD33 internalization in both $CD33^+$ hematopoietic cell lines and primary AML blast cells[61-64] has led to the development and clinical use of gemtuzumab ozogamicin (GO), an immunoconjugate consisting of a humanized IgG_4 anti-CD33 monoclonal antibody (hP67.6) joined to a cytotoxic calicheamicin-γ_1 derivative.[73-75,77] hP67.6 is believed to facilitate uptake of the toxic moiety, which is then intracellularly cleaved and subsequently induces DNA damage;[77,78] thus, the therapeutic success of GO largely depends on its CD33-dependent uptake.

In addition to CD33, other Siglecs also undergo endocytosis.[37,55-60,65,66] The mechanism of endocytosis has however only been investigated in detail for CD22. Initial studies have identified a polar region of 11 amino acid residues in close proximity to the transmembrane domain as internalization motif that controls both the unusually rapid constitutive turnover and the uptake of anti-CD22 antibodies.[67] Subsequent studies demonstrated that the tyrosine motifs around Y843 and Y863 interact with AP50, the medium chain subunit of the AP-2 complex.[70] These two tyrosine motifs are examples of the ITIM and ITIM-like motifs found in Siglecs, and resemble YXXØ motifs (where X denotes any amino acid and Ø denotes an amino acid residue with a bulky hydrophobic side chain), such motifs represent major tyrosine-based signals that bind to AP-2 in the absence of tyrosine phosphorylation, and thereby mediate clathrin-based endocytosis and protein sorting.[68,69]

Our results summarized in chapter I provided evidence that the proximal ITIM of CD33 and, to some degree, the distal ITIM-like motif control internalization of antibody-bound CD33 as well as GO-induced cytotoxicity,[92] but the underlying

mechanism has not been addressed. Another recent study demonstrated that the proximal ITIM is involved in uptake of Siglec-9 when bound to antibody.[59] Even though AP-2 appears as a likely candidate adaptor protein, alternate endocytic adaptors have been described whose interactions depend on either phosphorylated or non-phosphorylated tyrosine motifs.[69,71,72] For example, the YXXØ motif is also found in Fc receptors, in which it mediates the internalization process in a largely AP-2-independent manner when the tyrosine is phosphorylated.[93] Furthermore, the fact that both sialoadhesin/Siglec-1 as well as murine Siglec-H show endocytic properties but are both devoid of cytoplasmic tyrosine signaling motifs indicates that more than one mechanism is involved in endocytosis of Siglec family proteins. The primary objective of the present study was therefore to investigate the mechanisms underlying ITIM-dependent internalization of CD33, in particular when bound to anti-CD33 antibody. To address this question, we studied which phosphorylation state favors uptake of antibody-bound CD33, identified proteins that bind to CD33 in an ITIM-dependent manner, and assessed their importance for CD33 internalization and GO-induced cytotoxicity in human myeloid cells by specific silencing of target genes through expression of small interfering RNA (siRNA). Since previous studies have indicated that the internalization of ligated cell surface receptors and toxicity of immunoconjugates may significantly depend on the monoclonal antibody or antibody fragment used for cross-linking, as shown for example for uptake of anti-CD19 antibodies,[94,95] we also investigated the role of the anti-CD33 antibody on the cellular uptake of ligated CD33.

II.2. Materials and Methods

Cell cultures

Human myeloid HL-60, NB4, and U937 cells were maintained in RPMI medium 1640 with 25 mM HEPES ([*N*-2-hydroxyethylpiperazine-*N'*-2-ethanesulfonic acid],

GIBCO-Invitrogen, Carlsbad, CA) supplemented with 5% heat-inactivated bovine calf serum (BCS; HyClone, Logan, UT). Human myeloid ML-1 cells were maintained in Iscove's Modified Dulbecco's Medium (IMDM; GIBCO-Invitrogen) with 10% heat-inactivated fetal bovine serum (FBS; HyClone). The human erythroblastic TF-1 cell line was maintained in RPMI medium 1640 with 25 mM HEPES buffer supplemented with 10% heat-inactivated BCS, 1 mM MEM sodium pyruvate (GIBCO-Invitrogen), and 4 ng/mL granulocyte-macrophage colony-stimulating factor (GM-CSF; Amgen, Thousand Oaks, CA). The human Jurkat T cell line was maintained in RPMI medium 1640 with 25 mM HEPES supplemented with 10% heat-inactivated FBS, 1 mM MEM sodium pyruvate, and 0.1 mM MEM non-essential amino acids (GIBCO-Invitrogen). HEK293T and COS-7 cells were maintained in Dulbecco's Modified Eagle medium (D-MEM, GIBCO-Invitrogen) supplemented with 10% heat-inactivated FBS. All media also contained penicillin and streptomycin (GIBCO-Invitrogen).

Antibodies

The following primary antibodies were used: anti-CD32 (clone AT10: Serotec, Kidlington, Oxford, United Kingdom), anti-CD33 (hP67.6: kindly provided by Wyeth-Ayerst Research, Radnor, PA; clone mP67.6), anti-HA (clone 3F10: Roche Diagnostics, Indianapolis, IN; clone 16B12: Covance, Berkeley, CA), anti-phosphotyrosine (clone 4G10, Upstate Biotechnology, Charlottesville, VA), anti-T7 (Novagen, Madison, WI), anti-MAPK (clone 1913.3[96]), anti-SHP-1 (clone 52: BD Biosciences Pharmingen, San Diego, CA; clone D-11: Santa Cruz Biotechnology, Santa Cruz, CA), anti-SHP-2 (clone B-1: Santa Cruz Biotechnology), anti-Syk (clone 4D10: Santa Cruz Biotechnology), anti-Crk-L (clone C-20, Santa Cruz Biotechnology), anti-phospholipase C (PLC) γ1 (Upstate Biotechnology), anti-GST (clone 38.3), and anti-murine Thy 1.1 (used as murine IgG_1 isotype control antibody; clone 31.A[97]). $F(ab)_2$ fragments of the murine IgG_1 anti-CD33 antibody (mP67.6) were prepared by digestion with pepsin (Sigma, St. Louis, MO) and purification with a protein A column using standard procedures.

Gel electrophoresis was used to verify purity of the $mF(ab)_2$ fragment preparation. Secondary antibodies used were: horseradish peroxidase (HRP)-conjugated sheep anti-mouse Ig, goat-anti rat IgG, and donkey anti-rabbit Ig (GE Healthcare, Amersham Biosciences, Buckinghamshire, England), as well as biotin-conjugated mouse anti-human IgG_4 and rat anti-mouse Ig kappa light chain (both BD Biosciences).

Cellular transfection with cDNA constructs

A T7-tag was introduced into pcDNA3 vectors containing complementary DNA (cDNA) for $CD33^{WT}$, $CD33^{Y340F}$, $CD33^{Y358F}$, and $CD33^{Y340F/Y358F}$ (kindly provided by Dr. D.W. McVicar, National Cancer Institute, Frederick, MD[46]) by site-directed mutagenesis using standard polymerase chain reaction (PCR) cloning procedures with the following primers: forward 5'-ACAGGTGGCCAACAGATGGGTTGATCTAGAGGGCCCTATTCTATAGTG-3'; and reverse 5'-TTGGCCACCTGTCATCGATGCCATCTGGGTCCTGACCTCTGAG-3'; all constructs were verified by sequencing. HEK293T and COS-7 cells, grown in 6-well plates (Costar, Corning, NY), were transiently transfected with polyethylenimine (Polysciences, Warrington, PA) or lipofectamine 2000 (Invitrogen, Carlsbad, CA), respectively, using 2 µg per cDNA. Cells were harvested 48 hours after transfection. In some experiments, cells were treated with 100 µM pervanadate for 15 min at 37°C prior to harvest.

Lentivirus-mediated gene transfer and gene silencing by siRNA

Generation of bicistronic lentiviral vectors pRRLsin.cPPT.MSCV.$CD33^{WT/MUT}$.IRES.EGFP encoding cDNA for $CD33^{WT}$, $CD33^{Y340F}$, $CD33^{L343A}$, $CD33^{Y358F}$, or $CD33^{Y340F/Y358F}$ were previously described.[92] A wild-type CD33 construct bearing an HA-tag on the C-terminus was generated by PCR amplification of wild-type CD33 with the following primers: forward 5'-GGAATTCGCCACCATGCCGCTGCTGCTACTG-3', and reverse 5'-

TCCCCCCGGGTCATGCGTAATCGGGGACATCGTAGGGGTACTGGGTCCTG ACCTCTGAG-3', and verified by sequencing. The PCR product was then subloned into the pRRLsin.cPPT.MSCV.IRES.EGFP lentivirus backbone using the EcoRI and XmaI restriction sites. A lentivirus vector, LentiLox 3.7 (pLL3.7),[98] was used for inducing RNA interference: this vector contains an U6 promoter for expression of small hairpin RNA, as well as a CMV promoter for expression of EGFP. An YFP-expressing pLL3.7 construct was generated as follows: a two-step site-directed mutagenesis PCR (primer set 1: forward 5'-CTTCGGCTACGGCCTGCAGTGCTTCGCCCGCTACCCCGACCACATG-3', reverse 5'-GCGAAGCACTGCAGGCCGTAGCCGAAGGTGGTCACGAGGGTGGGC-3'; primer set 2: forward 5'-CCCGACAACCACTACCTGAGCTACCAGTCCGCCCTGAGCAAAG-3', reverse 5'-CTTTGCTCAGGGCGGACTGGTAGCTCAGGTAGTGGTTGTCGGG-3') was used to change amino acids at position 65 (from EGFP to YFP: L->F; amino acid single letter code), 66 (T->G), 69 (V->L), 73 (S->A), and 204 (T->Y). The construct was verified by sequencing. Target sequences were selected by rational design using si*DESIGN*™ Center (Dharmacon, Lafayette, CO; http://www.dharmacon.com/sidesign/default.aspx) and/or Block-iT™ RNAi Designer (Invitrogen; https://rnaidesigner.invitrogen.com/rnaiexpress) against the following genes (target sites are referred to by sense strand with the base position being indicated relative to the start nucleotide): SHP-1 (NM_002831), GCAAGAACCGCTACAAGAA, bp 989 (construct A), and TGACACAACCGAATACAAA, bp 1329 (construct B); SHP-2 (NM_002834), GCAATGACGGCAAGTCTAA, bp 859 (construct A), ATATGGCGGTCCAGCATTA, bp 1924 (construct B), and ACACTGGTGATTACTATGA, bp 553 (construct C); and Syk, GCACTATCGCATCGAACAAA (NM_003177, bp 789). Stocks of vesicular stomatitis virus G glycoprotein (VSV-G)–pseudotype lentiviral vectors were prepared by the Gene Marking and Tracking Facility (Core Center of Excellence

in Molecular Hematology, Fred Hutchinson Cancer Research Center, Seattle, WA) with calcium phosphate–mediated 3-plasmid transfection of HEK293T cells.[92] 27 μg of the transfer vector construct, 17.5 μg second generation gag-pol packaging construct pCMVR8.74, and 9.5 μg VSV-G expression construct pMD.G were used for transfection of 1.2 x 10^7 HEK293T cells overnight in 25 mL D-MEM with 10% heat-inactivated FBS. Cells were treated with 10 mM sodium butyrate during the first of 3 12-hour vector supernatant collections. The supernatant was filtered through a 0.22 μm pore-size filter and concentrated 100-fold by ultracentrifugation. All vector stocks were titered by infecting HT1080 cells using limiting dilutions of the stock with analysis for EGFP/YFP expression by flow cytometry. Infections of hematopoietic cell lines were performed in fibronectin-coated wells in the presence of 8 μg/mL protamine sulfate at a multiplicity of infection (MOI) of 2.5 – 25 for gene transfer experiments and a MOI of 5-10 for expression of siRNA, respectively. EGFP and/or YFP-positive cells were sorted by flow cytometry and re-cultured for further analysis.

Immunoprecipitation and Western blotting

Cells were washed twice in ice-cold Dulbecco's Phosphate Buffered Saline (PBS, GIBCO-Invitrogen) and then lysed in lysis buffer containing 25 mM HEPES (pH 7.4), 100 mM NaCl, 50 mM NaF, 1% NP-40 (Igepal CA-630, Sigma), 10% glycerol, 1 mM phenylmethylsulphonyl fluoride (PMSF), and protease inhibitors (Roche Diagnostics, Mannheim, Germany); in some experiments, 1 mM sodium orthovanadate was added. After incubation on ice for 45 min, lysates were precleared by centrifugation. For immunoprecipitations, precleared lysates were incubated with 1 μg of antibody overnight at 4°C, and then either Protein A Sepharose CL-4B or Protein G Sepharose 4 Fast Flow beads (both GE Healthcare, Amersham Biosciences) added for 2 hours. Beads were then washed 4 times in ice-cold lysis buffer and boiled in 1x reducing sample buffer (2% SDS, 10% glycerol, 20% β-mercaptoethanol, 105 mM Tris [tris(hydroxymethyl)aminomethane]/HCl, 0.03% bromophenol blue). In a subset

of experiments, washed beads were treated with N-glycosidase F (PNGase F; New England Biolabs, Ipswich, MA) according to the manufacturer's instructions before boiling in reducing sample buffer. For Western blotting, samples were separated on either 7.5% or 10% sodium dodecyl sulfate-polyacrylamide gel electrophoresis (SDS-PAGE), transblotted to nitrocellulose, blocked with 5% non-fat dry milk in Tris-buffered saline (TBS; 50 mM Tris [pH 7.5], 150 mM NaCl) containing 0.1% Tween 20 (TBST) for 30 minutes at room temperature, and then incubated with primary antibodies overnight at 4°C. For assessment of tyrosine phosphorylation, blots were blocked with TBS containing 6% bovine serum albumin (BSA; Sigma), 0.05% Tween 20, 5 mM NaF, and 0.005% NaN_3 for 24 – 48 hours prior to incubation with primary antibody. After washing, blots were incubated for 60 minutes with horseradish peroxidase-conjugated secondary antibody in TBST/BSA, washed, and immunoreactive signals visualized with enhanced chemiluminescence (PerkinElmer, Boston, MA) and exposed to CL-XPosure film (Pierce, Rockford, IL).

Glutathione-S-transferase (GST) fusion proteins and pull-down assays

To generate glutathione-S-transferase (GST) fusion protein constructs with wild-type and mutant CD33, the cytoplasmic tails of wild-type or mutant CD33 starting at amino acid 289 were subcloned into the pGEX2T vector by standard PCR cloning procedures using the following primers: forward 5'-CGCGGATCCGCAGCCAGGACAGCAGTG-3', reverse 5'-CCGGAATTCTCACTGGGTCCTGACCTCTG-3'; constructs were verified by sequencing. Fusion proteins were expressed after isopropyl-beta-D-thiogalactoside (IPTG) induction in *E. coli* BL-21 or *E. coli* TKB1 (Stratagene, La Jolla, CA) as non-tyrosine-phosphorylated or tyrosine-phosphorylated proteins, respectively. The TKB1 strain contains an elk1 tyrosine kinase that can be induced with indoleacrylic acid to phosphorylate bacterial fusion proteins expressed after IPTG-induction in the same cells. Bacteria were lysed in ice-cold PBS containing 1% Triton X-100 (Sigma), 1 mM phenylarsine oxide (PAO), 0.1%

β-mercaptoethanol, 1 mM PMSF, and 1 mM ethylene diaminetetraacetic acid (EDTA). After sonication, lysates were cleared by centrifugation and stored at -20°C. An aliquot of the lysate was checked for purity and concentration of the isolated proteins by incubation with a 50% slurry of Glutathione Sepharose 4B beads (GE Healthcare, Amersham Biosciences) in lysis buffer, rotating for 1 hour at 4°C, washing with ice-cold lysis buffer, and analysis by SDS-PAGE and Coomassie staining. For pull-down assays, GST fusion proteins were incubated with a 50% slurry of Glutathione Sepharose 4B beads in lysis buffer and rotated for 1 hour at 4°C. Beads were isolated by centrifugation, washed 4 times with ice-cold lysis buffer, and then incubated with cell lysates from human myeloid cell lines that were or were not stimulated with pervanadate prior to lysis to promote tyrosine phosphorylation. After rotating for 2 hours at 4°C, beads were again isolated by centrifugation, washed 4 times with ice-cold lysis buffer, boiled in 1x reducing sample buffer, and analyzed by Western blotting.

Flow cytometry assays for determination of CD33 expression and internalization

Internalization of antibody-bound CD33 in AML cell lines was measured as described previously.[92] 1-1.5 x 10^6 cells were transferred into 5 mL polystyrene round bottom tubes (BD Biosciences Discovery Labware, Bedford, MA) and incubated for 30 minutes with IMDM medium containing 2.5 - 10 μg/mL unconjugated, unlabeled hP67.6 or, in some experiments, mP67.6 or mF(ab)$_2$ fragments, in ice-water (to prevent internalization during the staining procedure). Cells were then washed in ice-cold PBS, resuspended in IMDM medium without antibody, split into several tubes, and incubated at 37°C (in 5% CO_2 and air) for various periods of time in the presence or absence of pervanadate (100 μM) and/or the Src family kinase inhibitor, PP2 (10 μM; Calbiochem, EMD Biosciences, La Jolla, CA). In some experiments, cells were resuspended in PBS supplemented with either 2%FBS or 20% human AB serum during incubation at 37°C. Afterwards, cells were chilled and incubated with biotin-conjugated secondary antibodies (used at 5 μg/mL in PBS/2% FBS), followed by incubation

with streptavidin-phycoerythrin (PE) conjugate (used at 5 µg/mL in PBS/2% FBS; BD Biosciences Pharmingen, San Diego, CA) to detect remaining antibody or antibody fragment on the cell surface. One sample kept in ice-water was used to determine the starting level of antibody bound to the cell surface. To identify nonviable cells, samples were stained with propidium iodide (PI; Sigma). At least 10,000 events were acquired and PI^- cells were analyzed on a FACScan Flow Cytometer using Cellquest software (both BD Biosciences Immunocytometry Systems, San Jose, CA). Linear fluorescence values were used to calculate the level of cell surface CD33 expression and the percentage of antibody internalization.

Assays for drug-induced cytotoxicity

Assays for drug-induced cytotoxicity in AML cell lines were performed as described previously.[92] 0.5 - 2 x 10^4 cells were taken during exponential growth and incubated at 37°C (in 5% CO_2 and air) in 96-well round bottom plates (BD Biosciences Discovery Labware) in 240 µL culture medium containing various concentrations of GO or N-acetyl gamma calicheamicin dimethyl hydrazine (referred to as calicheamicin-γ_1; both kindly provided by Wyeth-Ayerst Research). After three days of culture,[64,80,81,92] cell numbers and drug-induced cytotoxicity, using PI to detect non-viable cells, were determined using a FACSCalibur Flow Cytometer and analyzed with Cellquest Software.

Statistical analysis

Results from CD33 expression and internalization studies are presented as means±SEM from at least 3 independent experiments. Parametric statistical analysis was performed using repeated measures ANOVA with Tukey-Kramer Multiple Comparisons Test (InStat 3.05; GraphPad, San Diego, CA, USA); $p<0.05$ was considered significant.

II.3. Results

Fc receptor interactions enhance internalization of antibody-bound CD33

It has been a long-standing observation that bi- and multivalent anti-CD33 antibodies are internalized by $CD33^+$ hematopoietic cell lines and primary AML blast cells,[61-64] but the underlying mechanism(s) have not been investigated. Previous studies indicated a pivotal role of the Fc-part of antibodies on both internalization and cytotoxic effects of immunoconjugates targeting other antigens.[94,95] Even though the exact mechanisms remain elusive, interactions with Fcγ receptor II (CD32) have been implicated.[94,95] We therefore tested internalization of three anti-CD33 antibodies and antibody fragments: mP67.6 (murine IgG_1 antibody), its $F(ab)_2$ fragment ($mF(ab)_2$), and hP67.6, a humanized version of mP67.6 that was constructed to contain the complementarity-determining regions of mP67.6 but human IgG_4 kappa sequences in the remainder.[89] As shown in Fig II.1, mP67.6, $mF(ab)_2$, and hP67.6 were internalized by human $CD33^+$ myeloid cell lines (NB4, HL-60, and ML-1); importantly, however, internalization of $mF(ab)_2$ was significantly slower compared to mP67.6 and hP67.6, Similar results were obtained with two additional human myeloid cell lines (U937, TF-1; data not shown), and indicated that the Fc-part contributes to uptake of anti-CD33 antibodies. This notion is supported by the observation that the uptake of mP67.6, but not $mF(ab)_2$, was significantly slowed down in the presence of 20% human AB serum to block Fc receptor interactions, compared to cells kept in 2% FBS (Fig II.2; Panel A). Immunophenotyping indicated that none of the three cell lines express Fcγ receptor III (CD16). Fcγ receptor I (CD64) was expressed at low level by NB4 and HL-60 cells and at high level by ML-1 cells, while CD32 was expressed at high level by all cell lines (all data not shown). We thus assessed a possible interaction of anti-CD33 antibodies with CD32 by immunoprecipitation of resting ML-1 cells or ML-1 cells stimulated with mP67.6, $mF(ab)_2$, and hP67.6 with anti-CD32 antibody, and found that incubation with mP67.6, and minimally also

hP67.6, but not mF(ab)$_2$, resulted in tyrosine phosphorylation of CD32. Together, these data provide evidence that the Fc-part of anti-CD33 antibodies significantly interacts with CD32 and stimulates antibody uptake. Furthermore, the Fc-part of anti-CD33 antibodies is able to activate CD32 and may thus result in activation of signaling pathways that are independent of CD33.

Tyrosine phosphorylation of CD33 favors uptake of anti-CD33 antibodies

Since sequences that resemble ITIMs can function as endocytosis signals either when not phosphorylated or when phosphorylated,[71,72] we sought to determine which phosphorylation state of CD33 favors endocytosis. We used pervanadate, a non-specific tyrosine phosphatase inhibitor and tyrosine kinase activator to stimulate tyrosine phosphorylation of CD33. In line with previous studies,[44-46] treatment of myeloid cells with pervanadate resulted in increased tyrosine phosphorylation of a protein that was immunoprecipitated with anti-HA antibodies from cell lines expressing HA-tagged CD33 (Fig II.1, panel A). To ascertain that this signal represents tyrosine phosphorylated CD33, we took advantage of the fact that CD33 is a glycoprotein and treated parallel immunoprecipitates with the N-glycosidase PNGase F, which resulted in a significant size shift of both the HA as well as the phosphotyrosine band, indicating that the phosphotyrosine signal indeed originates from CD33 rather than a co-immunoprecipitated unidentified protein (Fig II.3, right side of panel A). As expected, the pervanadate-induced increase in tyrosine phosphorylation was strictly ITIM-dependent, as shown in HEK293T cells expressing either wild-type or mutant CD33 (Fig II.3, panel B), with the proximal ITIM contributing more to the total tyrosine phosphorylation than the distal ITIM-like motif. As shown in Fig II.4 (Panel A), manipulation of cellular tyrosine phosphorylation with pervanadate (100 µM) significantly enhanced uptake of hP67.6 in a panel of human CD33$^+$ AML cell lines (NB4, HL-60, ML-1, U937, and TF-1 cells). Given our findings indicating an interactions of hP67.6 with CD32, we also determined uptake of F(ab)$_2$ fragments generated from the murine parental anti-CD33 antibody, mP67.6. As shown in Fig II.4

(Panel B), pervanadate (100 μM) similarly increased uptake of these bivalent antibody fragments in HL-60, NB4, and ML-1 cells.

To study the mechanism involved in pervanadate-stimulated increase of uptake of antibody-bound CD33 in more detail, we transduced a human T-cell line that is endogenously devoid of CD33 (Jurkat cell line) with wild-type and mutant CD33. As shown in Fig II.5 (Panel A), pervanadate (100 μM) significantly increased uptake of hP67.6 in cells expressing $CD33^{WT}$, similar to its effect in myeloid cells. In contrast, pervanadate was unable to increase uptake of hP67.6 in Jurkat sublines expressing $CD33^{Y340F}$, $CD33^{L343A}$, or $CD33^{Y340F/Y358F}$, and was only minimally effective in sublines expressing $CD33^{Y358F}$ (Fig II.5, Panel A). Previous studies using co-transfection experiments have indicated that the Src family kinase, Lck, is able to phosphorylate CD33.[46] Consistent with the notion that Src family kinases phosphorylate CD33, we found that another member of the Src family of kinases, Fyn, phosphorylated CD33 in a strictly ITIM-dependent manner (see chapter III). Importantly, the Src family kinase inhibitor, PP2 (10 μM), almost completely abrogated the stimulatory effect of pervanadate in $CD33^{WT}$-expressing Jurkat cells (Fig II.5, Panel B). Together, this series of experiments demonstrates enhanced uptake of antibody-bound CD33 by pervanadate-mediated increase of tyrosine phosphorylation; this effect is dependent upon the integrity of the ITIMs and is prevented by co-treatment with the Src tyrosine kinase inhibitor PP2, suggesting that phosphorylation of the ITIMs by a Src family kinase favors uptake of antibody-bound CD33, probably because (adaptor-) proteins involved in this endocytic process favor binding to tyrosine phosphorylated CD33.

Several SH2 domain containing proteins interact with phosphorylated CD33

We next attempted to identify proteins that interact with CD33 and could be involved in the internalization process of antibody-bound CD33. Since our data suggested that tyrosine phosphorylation favors internalization of antibody-bound

CD33, we focused on the identification of proteins that bind to tyrosine phosphorylated CD33. To screen for such proteins, we generated CD33/glutathione-S-transferase (GST) fusion constructs and expressed them in bacteria that concomitantly expressed a tyrosine kinase to yield tyrosine phosphorylated fusion proteins, and used these proteins in pull-down experiments with cell lysates from human myeloid cell lines (HL-60, NB4, and ML-1). Interacting proteins were eluted and separated by gel electrophoresis. Only one band of interest, i.e. strong interaction with $CD33^{WT}$ but only weak or absent interaction with mutant CD33 was identified by Coomassie and Silver staining. Mass spectroscopy identified this band to contain SHP-1 (all data not shown), and subsequent pull-down experiments followed by Western blotting with a specific anti-SHP-1 antibody indeed verified that SHP-1 interacted with the phosphorylated GST/$CD33^{WT}$ fusion protein. In contrast, SHP-1 only weakly interacted with phosphorylated GST/$CD33^{Y358F}$ whereas it failed to significantly interact with GST/$CD33^{Y340F}$ or $CD33^{Y340F/Y358F}$ (Fig II.6, Panel A), consistent with previous publications reporting an ITIM-dependent interaction between SHP-1 and phosphorylated CD33.[44-46] Similarly, and again consistent with previous reports,[44-46] parallel studies showed that SHP-2 was able to interact with phosphorylated GST/CD33 fusion proteins in an ITIM-dependent manner (Fig II.6, Panel A). Both SHP-1 and SHP-2 contain SH2 domains that have previously been shown to be responsible for the interaction with the tyrosine motifs of CD33.[44-46] To test whether other SH2 domain-containing proteins are also able to interact with phosphorylated CD33, we performed additional experiments probing for spleen tyrosine kinase (Syk), a non-receptor tyrosine kinase that has been reported to form a complex with CD33 in some circumstances,[49,53] as well as for CrkL and PLC-γ1, two randomly chosen SH2 domain proteins for which an interaction with CD33 has not been assessed so far. Importantly, however, most of these proteins have been implicated in endocytic processes. For example, SHP-1, a cytoplasmic protein tyrosine phosphatase that contains 2 SH2 domains, a single catalytic domain, and a C-terminal tail containing tyrosine

residues, can undergo phosphorylation of the C-terminal tyrosine residues upon mitogenic stimuli,[99-102] and then serve an adaptor function by recruitment of the SH3-SH2-SH3 growth factor receptor–bound protein 2 (Grb2).[103] Similarly, SHP-2 can bind Grb2 via phosphorylated C-terminal tyrosine residues.[104] In turn, Grb2 can bind to dynamin, an interaction mediated through association of its proline-rich domain of dynamin with the SH3 domains of Grb2,[105,106] offering a link to clathrin-mediated endocytosis pathways; in addition, Grb2 can recruit Cbl family proteins, an interaction that was shown to be essential and sufficient to support endocytosis of the transmembrane tyrosine kinase, epithelial growth factor receptor (EGFR).[107] Alternatively, given the importance of tyrosine phosphorylation for internalization of antibody-bound CD33, we reasoned that SHP-1 and SHP-2 might have an alternative role in this process by altering the phosphorylation status of CD33, as tyrosine phosphatases associated with phosphorylated CD33 have previously been shown to be active and able to catalyze CD33 dephosphorylation.[44] Syk is a proximal and central non-receptor tyrosine kinase involved in the internalization process that follows engagement of the ITAM-containing Fcγ receptors.[93,108,109] And finally, PLC-γ1 can act as a guanine nucleotide exchange factor (GEF) of dynamin-1 via interaction of its SH3 domain with dynamin-1, establishing a role in the regulation of endocytosis.[110] As shown in Fig II.6 (Panel A), Syk was found to interact with phosphorylated GST/CD33 proteins, but not with GST alone. Similarly, both CrkL and PLC-γ1 bound to GST/CD33 proteins but not to GST alone (data not shown). Together, these studies identify several SH2 domain proteins to interact with phosphorylated CD33 in co-immunoprecipitation or GST fusion protein pulldown experiments in an ITIM-dependent manner. Interestingly, some of these proteins (i.e., SHP-1, SHP-2, and Syk), albeit not all (i.e., CrkL and PLC-γ1; data not shown), showed a pattern of binding to cytoplasmic tails of CD33 that closely resembled the endocytic properties of the corresponding CD33 protein, i.e. strong binding/internalization of wild-type CD33, attenuated binding/internalization of $CD33^{Y358F}$, and very weak or absent

binding/internalization of $CD33^{Y340F}$, revealing SHP-1, SHP-2, and Syk as the most appealing candidates for mediating endocytosis of CD33. Co-immunoprecipitation experiments were therefore performed to further study the interaction between wild-type CD33 and those SH2 domain containing proteins in more detail. Because of the poor performance of anti-CD33 antibodies, myeloid cells expressing HA-tagged $CD33^{WT}$ were again used for these experiments, and lysates were pretreated with pervanadate to promote tyrosine phosphorylation of CD33. Both SHP-1 and SHP-2 were found to bind to CD33 in pervanadate pretreated, but not in pervanadate untreated cell lysates in bi-directionally performed co-immunoprecipitation experiments (Fig II.6; Panel B and C), while Syk failed to bind to CD33 in these experiments.

Effect of siRNA targeting SHP-1, SHP-2, and Syk on endocytosis of antibody-bound CD33

Finally, we aimed to investigate the role of SHP-1, SHP-2, and Syk on the uptake of antibody-bound CD33. To accomplish this, we generated lentivirus constructs encoding siRNAs for these proteins and transduced NB4 cells at a MOI of 5-10. After several days of culture, GFP^+ or YFP^+ cells were sorted by FACS, sorted cells expanded, and then Western blot experiments performed to assess efficiency of protein knock-down. Two of three constructs targeting SHP-1 (SHP-1A and SHP-1B) and all three constructs targeting SHP-2 (SHP-2A, SHP-2B, SHP-2C) yielded almost complete protein knock-down (data not shown). We also generated cells doubly infected with siRNAs targeting SHP-1 (using GFP) and SHP-2 (using YFP), sorted double-positive cells, and expanded them for further analysis. Upon completion of CD33 expression, CD33 internalization, as well as drug-induced cytotoxicity experiments, cell lysates were obtained to assess the degree of protein depletion. As shown in Fig II.7 (Panel A), in sublines infected with either SHP-1 (constructs A and B) or SHP-2 (constructs A, B, and C), an almost complete depletion of either SHP-1 or SHP-2, respectively, persisted. Similarly, sublines infected with both siRNA targeting SHP-1 (construct A) and

SHP-2 (construct A, B, or C) had greatly diminished SHP-1 and SHP-2 protein levels, albeit the degree of protein reduction was less compared to singly infected sublines. As shown in Fig II.7 (Panel B-D), expression of siRNA constructs only slightly affected the abundance of CD33 on the cell surface compared to parental cells, and internalization of antibody-bound CD33 was relatively unchanged in sublines expressing siRNA constructs targeting SHP-1 and/or SHP-2 compared to parental cells. Likewise, there was no difference in GO-induced or calicheamicin-γ_1-induced cytotoxicity, as assessed by increase in PI^+ cells and reduction in cell number, in cells expressing SHP-1A, SHP-2B, or SHP-2C siRNA alone or SHP-1A siRNA in combination with SHP-2B or SHP-2C siRNA, compared to parental cells (Fig II.8, Panel A-B). Surprisingly, however, GO-induced cytotoxicity was significantly reduced, and calicheamicin-γ_1-induced cytotoxicity tended to be reduced, in cells expressing SHP-2A siRNA either alone or in combination with SHP-1A (Fig II.8, Panel A-B). Since this reduction of drug-induced cytotoxicity was only observed in one construct targeting SHP-2, this most likely represents an off target effect of this particular siRNA construct.

We then generated HL-60 sublines transduced with either siRNA targeting SHP-1 and/or SHP-2, and assessed cell surface expression of CD33 and internalization of antibody-bound CD33, as shown in Fig II.9 (Panel A-C). Similar to the findings obtained in NB4 cells, HL-60 sublines had relatively similar amounts of CD33 expressed on the cell surface compared to parental cells, and internalization of antibody-bound CD33 was not statistically significantly different in sublines expressing siRNA constructs targeting SHP-1 and/or SHP-2 compared to parental cells. Furthermore, GO- and calicheamicin-γ_1-induced cytotoxicity was not affected in HL-60 sublines expressing these siRNAs (data not shown).

While the data thus far indicated that both SHP-1 and SHP-2 are dispensable for internalization of antibody-bound CD33 and GO-induced or calicheamicin-γ_1-

induced cytotoxicity in NB4 and HL-60 cells, we obtained a different result in two additional cell lines, ML-1 and TF-1 cells. Similar to NB4 and HL-60 cells, siRNA constructs targeting either SHP-1 or SHP-2 failed to affect internalization of antibody-bound CD33 in ML-1 cells when compared to parental cells (Fig II.10, Panel A and B). By comparison, uptake of antibody-bound CD33 was significantly enhanced in cells simultaneously expressing both SHP-1 and SHP-2 siRNA constructs (Figure II.10, Panel C). Likewise, uptake of antibody-bound CD33 was significantly enhanced in TF-1 sublines simultaneously expressing SHP-1 and SHP-2 siRNA constructs compared to non-infected, parental TF-1 cells (Figure II.11), while preliminary experiments indicated that expression of either SHP-1 or SHP-2 siRNA alone did not significantly affect antibody internalization (n=1; data not shown). We also attempted to investigate the effect of SHP-1 and SHP-2 siRNA on drug-induced cytotoxicity in these two cell lines. Consistent with previous experiments,[81] ML-1 cells were found to be exquisitely sensitive to both GO and calicheamicin-γ_1, and expression of SHP-1 and/or SHP-2 siRNA failed to affect drug-induced cytotoxicity to a measurable degree (data not shown). By comparison, and also consistent with previous experiments,[81] TF-1 cells are highly resistant to both GO and calicheamicin-γ_1, at least in part due to expression of P-glycoprotein (Pgp). Despite the use of the drug efflux reversal agent, PK11195 (75 μM),[81] we only observed a minimal effect of both drug on the percentage of propidium iodide (PI)-positive cells (at 10 ng/mL: +14% with GO and +17% with calicheamicin-γ_1, respectively) or the total cell number (at 10 ng/mL: -7% with GO and -22% with calicheamicin-γ_1, respectively), and expression of SHP-1 and SHP-2 siRNA was unable to increase drug-induced cytotoxicity to a significant degree (data not shown).

In both NB4 and HL-60 cells, infections with a siRNA construct targeting Syk resulted in very efficient Syk protein knockdown but unaltered levels of SHP-1 and SHP-2, as verified by Western blotting (Fig II.12, Panel A). As shown in Fig II.12 (Panel B and C), NB4 cells infected with Syk siRNA showed similar cell

surface expression of CD33 and exhibited unchanged internalization of hP67.6 compared to parental cells. By comparison, the Syk siRNA infected HL-60 subline had slightly increased cell surface abundance of CD33 and a slightly increased rate of hP67.6 internalization compared to parental HL-60 cells (Fig II.12, Panel B and C). In both cell lines, however, Syk siRNA-infected sublines showed similar sensitivity to GO-induced cytotoxicity, as assessed by increase in PI^+ cells and reduction in cell number (Fig II.13, Panel A and B) compared to their parental counterparts. Likewise, free calicheamicin-γ_1 was equally cytotoxic in parental and Syk siRNA infected cells (data not shown). Similar to NB4 and HL-60 cells, Syk siRNA did not affect internalization of antibody-bound CD33 in ML-1 and TF-1 cells, as shown in Fig II.14. A second pLL3.7 construct encoding a siRNA targeting Syk (target sequence: GCAGCTAGTCGAGCATTAT) failed to reduce Syk protein levels to a noticeable degree (data not shown) and was used for control experiments. In both NB4 and HL-60 cells, cells infected with this construct had unchanged cell surface expression and hP67.6 internalization compared to uninfected parental cells (data not shown). Together, this data indicate that Syk is dispensable for internalization of antibody-bound CD33, and GO-induced or calicheamicin-γ_1-induced cytotoxicity.

II.4. Discussion

There are currently 8 antibodies approved by the FDA as anti-cancer agents, and many additional antibodies are in late-stage clinical trials; this rapidly evolving field of antibody-based therapeutics thus represents an important novel approach aiming at directing selective antitumor responses that spare normal tissues.[9] The CD33-targeting immunoconjugate, GO, is unique among the FDA-approved antibodies as the anti-CD33 antibody mainly serves as a carrier to facilitate uptake of the cytotoxic calicheamicin-γ_1 moiety.[77] This putative mechanism of action suggests the importance of intracellular levels of calicheamicin-γ_1 for the

drug's cytotoxic effects; indeed, we were able to provide experimental evidence for this notion very recently by demonstrating the critical dependence of GO-induced cytotoxicity on the amount of CD33 expressed on the cell surface, as well as on the rate of ITIM-dependent internalization of antibody-bound CD33 (chapter I and ref[92]). Unraveling important principles that govern the uptake of anti-CD33 antibodies may thus not only deepen our understanding of the biology of CD33, but equally important, may provide novel avenues to enhance clinical efficacy of CD33-targeted chemotherapy of AML. These principles could also serve as important paradigm for other similar immunoconjugate drugs. The data presented in this chapter now support four major conclusions. First, the Fc-part of anti-CD33 antibodies significantly enhances internalization of antibody-bound CD33, and is able to activate Fcγ receptor II (CD32), potentially resulting in signaling effects in addition to CD33 signaling. Second, tyrosine phosphorylation increases internalization of anti-CD33 antibody and bivalent anti-CD33 antibody fragments. Third, once phosphorylated, CD33 binds several SH2 domain-containing proteins in an ITIM-dependent manner, some of which have not previously been shown to bind to CD33. And finally, several CD33-interacting proteins, namely the tyrosine phosphatases, SHP1 and SHP-2, and the non-receptor tyrosine kinase, Syk, are dispensable for the process of internalization of anti-CD33 antibody and GO-induced cytotoxicity.

Cell surface proteins that enter the receptor-mediated endocytosis pathway can be cleared very rapidly from the cell surface if they are efficiently concentrated in clathrin-coated pits (10-50%/min).[68] By comparison and consistent with previous results (chapter I and ref[92]), internalization of antibody-bound CD33 proceeds at a much slower rate. Interestingly, the $mF(ab)_2$ antibody fragment was internalized even more slowly than either the mP67.6 of hP67.6 antibody in all cell lines assessed. This finding implies an effect of the Fc-part of the antibody on its uptake when bound to CD33, and, indeed, we found evidence for an interaction of the Fc-part of anti-CD33 antibodies with CD32 (the only Fcγ receptor that was

consistently expressed by all myeloid cell lines tested in our studies), which resulted in tyrosine phosphorylation and, by extrapolation, activation of the latter. Conversely, blocking Fc interactions with human AB serum decreased mP67.6 internalization to the rate of its $mF(ab)_2$ fragment. An importance of the Fc-part on antibody internalization has previously been reported for anti-CD19 antibodies.[94,95] In those studies, the IgG_1 isotype of an anti-CD19 monoclonal antibody resulted in faster antibody uptake compared to its switch variant IgG_{2a}. This enhanced modulation and intracellular uptake of the monoclonal anti-CD19-IgG_1 antibody also appeared to be mediated by CD32, and could be abrogated by co-treatment with a blocking anti-CD32 antibody, whereas uptake of the switch variant IgG_{2a} antibody was not significantly affected by the anti-CD32 antibody.[94,95] The exact mechanism by which the Fc-part of CD33 antibodies affects internalization of antibody-bound CD33 is, however, unclear, and additional experiments will be required to address this issue. In particular, it is unclear whether signaling through CD32 is required for this effect of the Fc-part, or whether passive interaction is sufficient, e.g. by changing geometry of the complexes formed on the cell surface. Since competitive binding assays indicated a lower relative affinity of hP67.6 compared to mP67.6,[89] a direct comparison between those two antibodies may not be possible. However, it was interesting to note that in 4 out of 5 human myeloid cell lines assessed (ML-1, HL-60, U937, TF-1, but not NB4), the rate of internalization of mP67.6 was enhanced compared to hP67.6. Current experiments are investigating whether this discrepancy between individual cell lines is due to the expression of different CD32 isoforms on these cells, or whether interactions with other Fcγ receptors are also of importance.

The relatively slow rate of internalization of antibody-bound CD33 and the recognition gained from the study of many cell surface receptor systems that there is a high background level of signal-independent internalization,[68] raises the question whether CD33-related signaling events are involved and critically

required for uptake of anti-CD33 antibodies. However, our previous findings demonstrating abrogation of the internalization of antibody-bound CD33 by mutating the ITIM or ITIM-like sequence of CD33 (chapter I and ref[92]) suggests that signal-dependent events are involved in this process, although alternative explanations, such as alterations in the localization of CD33 in membrane domains induced by the ITIM mutation, are possible. Endocytic properties have been previously demonstrated for several Siglecs,[37,55-58,60,65,66] but have only been studied in some detail in the case of CD22, for which a polar membrane-proximal internalization motif was identified initially, and subsequent studies then demonstrated that AP-2 binds to the two most distal ITIMs when non-phosphorylated and mediates clathrin-dependent internalization.[67,70] In the current studies, we were unable to detect binding of AP-2 to non-phosphorylated wild-type and mutant CD33, both by GST-fusion protein pull-down experiments and co-immunoprecipitations, using an antibody that recognizes the α-adaptin subunit of AP-2 (data not shown). By comparison, however, we found that forced tyrosine phosphorylation by pervanadate increases uptake of antibody-bound CD33 in both a Src family kinase dependent and ITIM-dependent manner, indicating that, first, this uptake process is amenable to manipulation, and, second, that the adaptor protein(s) involved in this process favor(s) binding to tyrosine phosphorylated rather than non-phosphorylated CD33. Thus, the mechanism underlying endocyosis of ligated CD33 appears distinct from the mechanisms underlying CD22 endocytosis.

To further characterize proteins that are involved in the endocytic process of CD33, we attempted to identify proteins that are able to bind well to the tyrosine phosphorylated form of wild-type CD33 but not CD33 bearing mutations on the ITIM sequences in GST-fusion protein pull-down assays. In addition to SHP-1 and SHP-2, which have been previously recognized as binding partners of tyrosine phosphorylated ITIM-containing receptors including CD33,[44-46] as well as Syk that one research group has found to find to CD33,[49,53] we also found that

two randomly chosen additional SH2-domain containing proteins, namely CrkL and PLC-γ1, bind to CD33. Whereas binding and activation of PLC-γ1 to another ITIM-containing receptor, the bradykinin B2 receptor, has been described previously,[111] an interaction between CrkL and a receptor with an ITIM sequence has not been reported so far. Given the random selection of the SH2 domain proteins we tested for interaction with CD33, it thus appears that the spectrum of proteins that are able to bind to CD33, and by extrapolation to other receptors with highly conserved ITIM sequences, is larger than previously recognized, and may in particular include additional proteins that contain SH2-domains.

In the present studies, we have assessed the role of three CD33 interacting proteins for internalization of antibody-bound CD33 in more detail. These proteins, SHP-1, SHP-2, and Syk, were selected because they have been implicated in endocytic processes of other proteins, and because their pattern of binding to cytoplasmic tails of CD33 closely resembled the endocytic properties of the corresponding CD33 protein. The pivotal importance of SHP-1 and SHP-2 for the inhibition of signaling cascades following the activation of ITIM-bearing receptors has long been appreciated.[112] In the case of CD33, some data have suggested that CD33 not only recruits tyrosine phosphatases upon tyrosine phosphorylation, but results in their activation and may in turn become a target for dephosphorylation.[44] We therefore hypothesized that SHP-1 and/or SHP-2 might have a role in the internalization of antibody-bound CD33, either by affecting the phosphorylation state of CD33, and/or by having an adaptor protein function. Indeed, in ML-1 and TF-1 cell lines, simultaneous depletion of SHP-1 and SHP-2 by lentivirus-mediated siRNA significantly increased internalization of antibody-bound CD33 and GO-induced cytotoxicity. This finding is consistent with a role of these phosphatases in regulating the phosphorylation status of CD33, by which SHP-1 and SHP-2-catalyzed CD33 dephosphorylation results in decreased CD33 tyrosine phosphorylation and reduced internalization. By comparison, this finding is not consistent with a prominent role of SHP-1 and

SHP-2 as adaptor mediating endocytosis; however, a minor role as adaptor protein cannot be completely excluded by our studies. Interestingly, depletion of SHP-1 and SHP-2 failed to affect internalization of antibody-bound CD33 in HL-60 and NB4 cells, indicating that there are important cell-type specific factors that influence this internalization process. Several possible explanations might account for this finding: first, the baseline tyrosine phosphorylation state of CD33 may be different in NB4 and HL-60 relative to ML-1 and TF-1 cells. Second, the response of ML-1 and TF-1 cells might differ with regard to tyrosine phosphorylation as a consequence of CD33 ligation induced by primary antibody. We have only inconsistently been able to detect antibody-induced tyrosine phosphorylation in myeloid cell lines (data not shown), indicating that the level of phosphorylation induced by primary anti-CD33 antibody in the absence of cross-linking with a secondary antibody is relatively low and not well sustained. It is noteworthy that TF-1 and ML-1 cells have higher cell surface levels of CD33 compared to NB4 and HL-60 cells, and ligation by antibody may thus provoke different levels of responses. Third, additional yet unrecognized tyrosine phosphatases may exist in NB4 and HL-60 cells that keep CD33 in its dephosphorylated state despite the functional absence of SHP-1 and SHP-2. Such a redundancy would be missed by our experimental setting. And forth, ligation of CD33 with primary antibody in the absence of secondary antibody is insufficient to recruit and activate those tyrosine phosphatases in NB4 and HL-60 cells, while they become activated in ML-1 and TF-1 cells.

Syk is implicated in a variety of diverse cellular processes. Most notably, it is known as non receptor tyrosine kinase pivotal for signaling through a number of immunoreceptors, thereby mediating cellular responses such as proliferation, differentiation, and phagocytosis in B and T cells, platelets, mast cells, neutrophils, and macrophages; furthermore, Syk is expressed in non-hematopoietic tissues, and plays a role in signaling from receptors not thought to belong to the immunoreceptor family.[113,114] Two previous reports have provided

evidence that Syk forms a complex with CD33 upon pervanadate stimulation or ligation by anti-CD33 antibody.[49,53] The present GST-fusion protein pulldown assays are consistent with these previous reports and confirm that phosphorylated CD33 interacts with Syk. A functional role for Syk in CD33 signaling has not been established so far; however, using a set of 25 primary AML samples, it was suggested that the anti-proliferative response of AML cells to CD33 ligation correlated with Syk expression.[53] Herein, we have used siRNA to deplete human myeloid cells of Syk to directly test a potential role of Syk in the response of these cells to conjugated and naked anti-CD33 antibodies. In contrast to the studies by Balaian *et al.*,[53] however, our experiments fail to reveal any significant role of Syk in either the uptake of antibody-bound CD33 or the cytotoxic effect inflicted by GO or free calicheamicin-γ_1. While these studies suggest that Syk has no essential role in these processes, they do not exclude the possibility that Syk may have some role that is redundant with the function of another protein and can be compensated by that protein when Syk is depleted in an isolated manner. The identification of proteins important for uptake of anti-CD33 antibodies and a deepened understanding of involved signaling pathways will help addressing this issue.

In summary, studies presented in this chapter indicate the importance of the Fc-part of anti-CD33 antibodies and tyrosine phosphorylation for the uptake of antibody-bound CD33. Thus, these studies identify the manipulation of the tyrosine phosphorylation status of CD33, for example by activating pivotal tyrosine kinases or interfering with tyrosine phosphatases, as a novel pharmacological means that could be exploited with the aim to enhance internalization of anti-CD33 antibodies, and possibly effectiveness of CD33-targeting therapies.

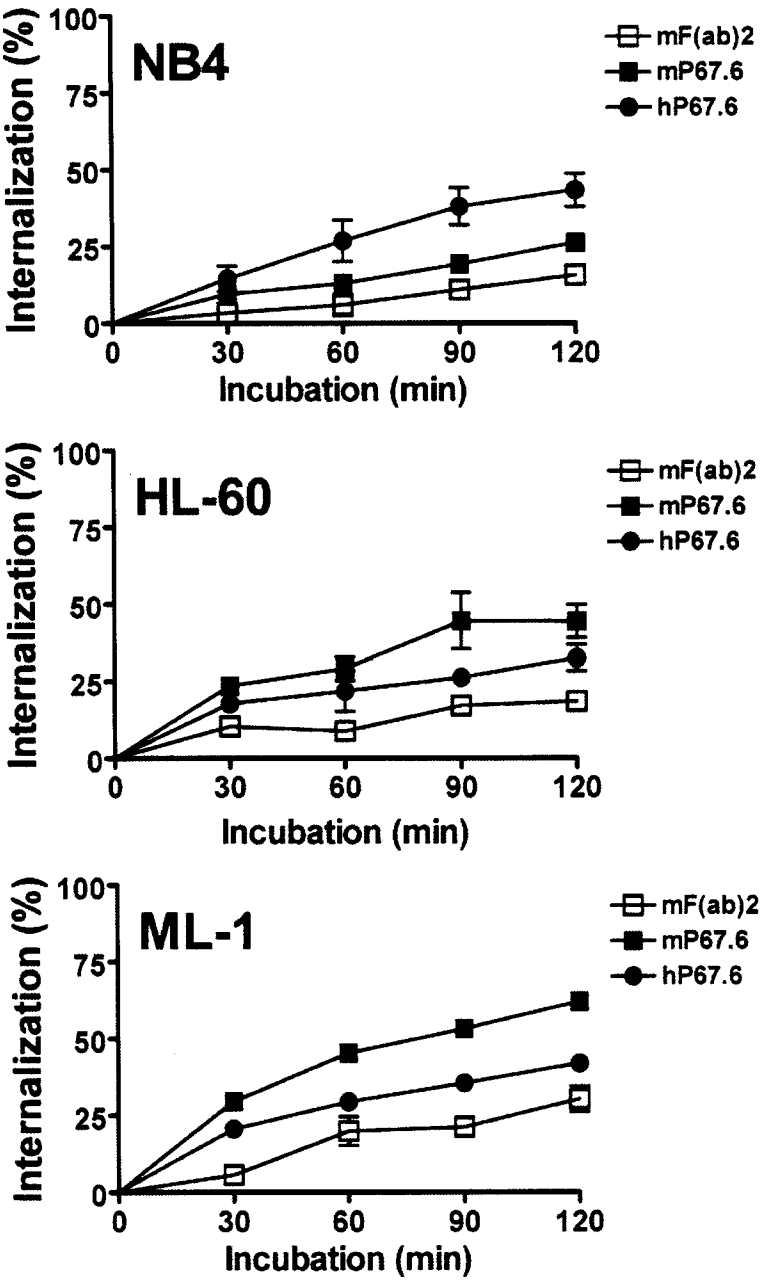

Figure II.1: Internalization of anti-CD33 antibodies and antibody fragments in human myeloid cells. NB4, HL-60, and ML-1 cells were labeled with the murine IgG_1 anti-CD33 antibody (mP67.6), its $F(ab)_2$ fragment ($mF(ab)_2$), or the humanized version of the murine antibody (hP67.6) as indicated. Internalization of the antibody or antibody fragment was then assessed over 2 hours, and expressed as percentage of internalized antibody relative to cells kept at 0° C. Results are shown as mean±SEM from 2-7 independent experiments.

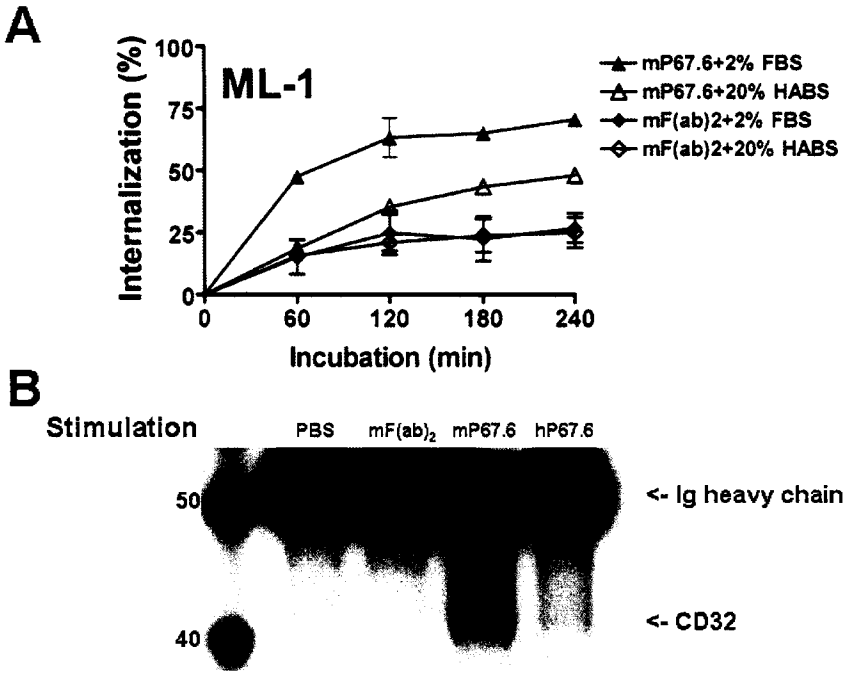

Figure II.2: Interaction of anti-CD33 antibodies with Fcγ receptor II. (A) ML-1 cells were labeled with mP67.6 or its $F(ab)_2$ fragment ($mF(ab)_2$), and internalization then assessed over 4 hours in the presence of either 2% FBS or 20% human AB serum to block interactions with Fc receptors; data are expressed as as percentage of internalized antibody relative to cells kept at 0° C. Shown are mean±SEM values from 2-3 independent experiments. (B) ML-1 cells were either left untreated or stimulated with either mP67.6, $mF(ab)_2$, or hP67.6 (10 µg/mL) for 15 min at 37 ° C prior to lysis and immunoprecipitation with anti-CD32 antibody. The blot was then probed with anti-phosphotyrosine antibodies. Shown is one representative experiment.

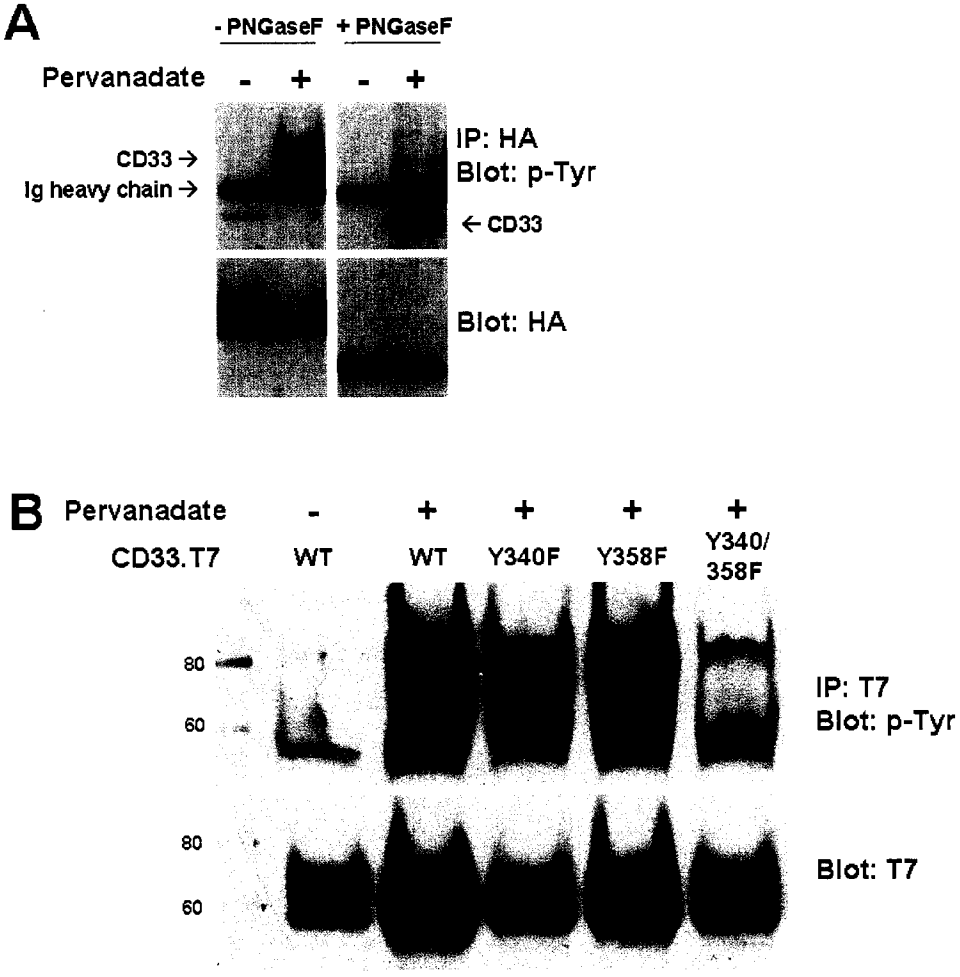

Figure II.3: Enhancement of CD33 tyrosine phosphorylation by pervanadate. (A) HL-60 cells infected with HA-tagged wild-type CD33 were either left untreated or stimulated with pervanadate (100 μM) for 30 min at 37° C prior to lysis and immunoprecipitation with anti-HA antibody; parallel samples were then either treated with PNGase F to remove saccharide side chains, or left untreated. The blot was subsequently probed for phosphotyrosine (top panel), stripped, and reprobed for HA to visualize CD33 (bottom panel). (B) HEK293T cells were transfected with T7-tagged wild-type or mutant CD33 as indicated. After two days, cell were either left untreated or stimulated with pervanadate (100 μM) for 15 min at 37° C prior to lysis and immunoprecipitation with anti-T7 antibody; the blot was then probed for phosphotyrosine (top panel), stripped, and reprobed for T7 to visualize CD33 (bottom panel). Presented is one representative experiment; similar findings were obtained with COS-7 cells.

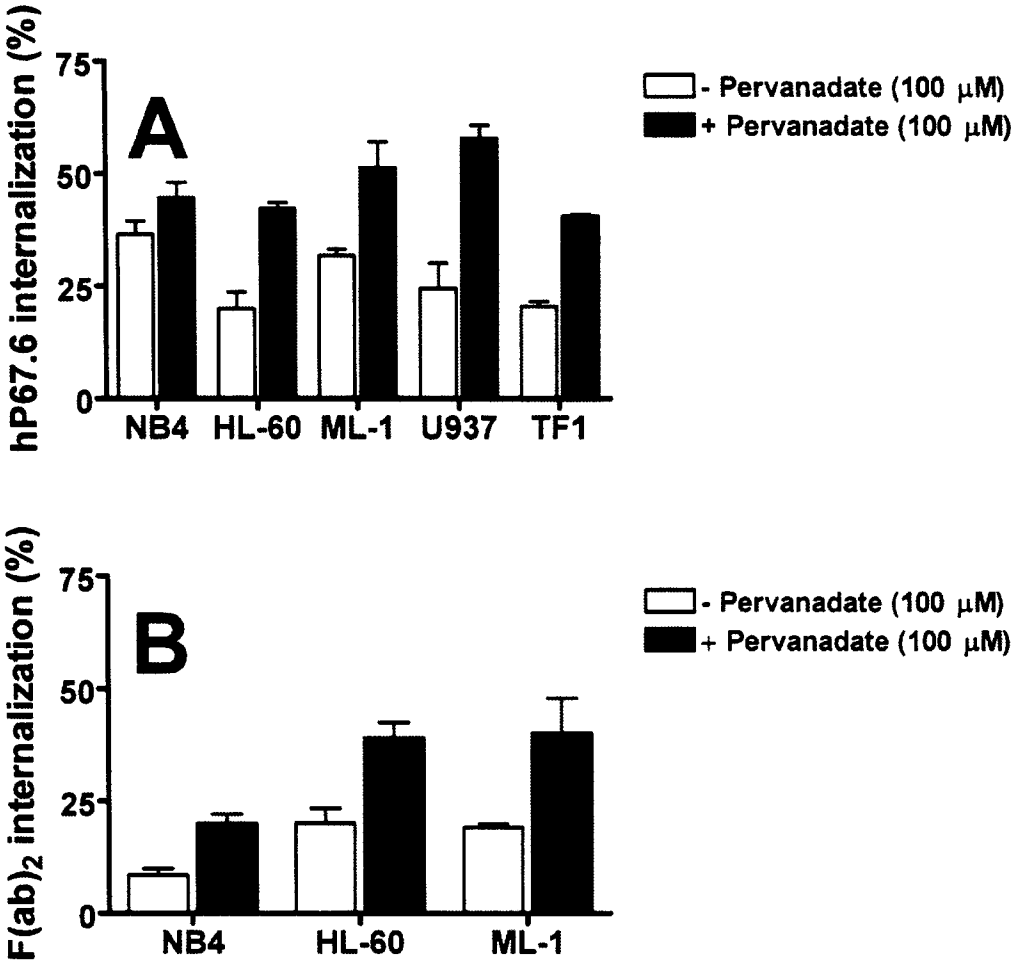

Figure II.4: Enhancement of uptake of antibody-bound CD33 by pervanadate. The indicated human $CD33^+$ AML cell lines were labeled with either (A) the unconjugated human anti-CD33 antibody, hP67.6, or (B) the unconjugated $F(ab)_2$ fragment of the murine anti-CD33 antibody, mP67.6, on ice-water before the cells were incubated in 37° C in antibody-free medium in the presence or absence of pervanadate (100 μM) to allow internalization for up to 1 hour as indicated. Subsequently, remaining cell surface associated hP67.6 or mP67.6 $F(ab)_2$ was detected with biotin-conjugated mouse anti-human IgG_4 monoclonal antibody or biotin-conjugated rat anti-mouse Ig kappa light chain monoclonal antibody and a streptavidin-PE conjugate. The percentage of internalized antibody/antibody fragment is expressed relative to cells kept at 0° C. Results are shown as mean±SEM from 3-7 independent experiments with the exception of TF1 cells (n=2). Treatment with pervanadate increases uptake of antibody-bound CD33 in all cell lines assessed, indicating that phosphorylation favors uptake of CD33 when bound to antibody.

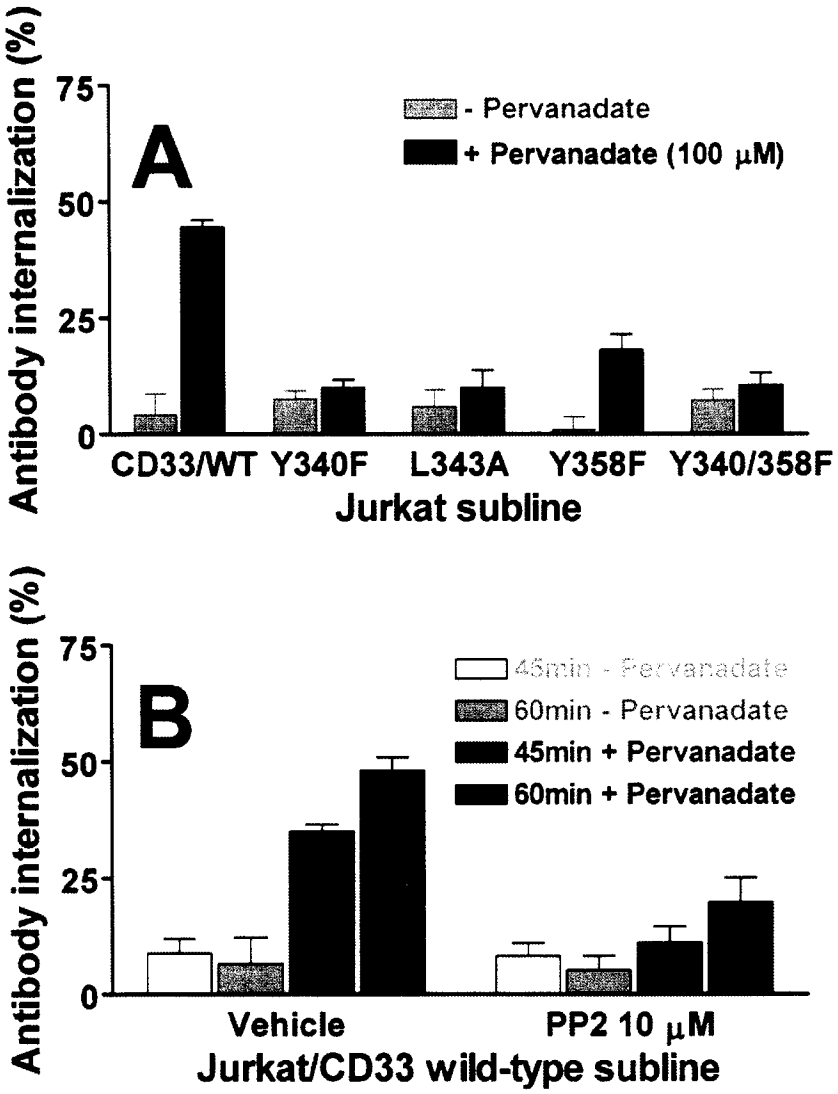

Figure II.5: Effect of pervanadate and/or PP2 on uptake of antibody-bound CD33 in transduced Jurkat cells. The human CD33$^-$ Jurkat T cell line was virally transduced with wild-type or mutant CD33 constructs as indicated, and internalization of the human anti-CD33 antibody hP67.6 assessed for up to 1 hour in the presence or absence of pervanadate (100 μM; Panel A) and/or either the Src family tyrosine kinase inhibitor, PP2 (10 μM), or DMSO vehicle (Panel B). The percentage of internalized antibody/antibody fragment is expressed relative to cells kept at 0° C. Results are shown as mean±SEM from 3-4 independent experiments. Pervanadate stimulation increases endocytosis of antibody-bound CD33; this effect is dependent on the integrity of the ITIMs of CD33 and was prevented by PP2, suggesting that both the ITIMs per se as well as the phosphorylation status of the ITIMs, critically control uptake of antibody-bound CD33. These data further suggest that a Src-family tyrosine kinase is involved in the critical phosphorylation step.

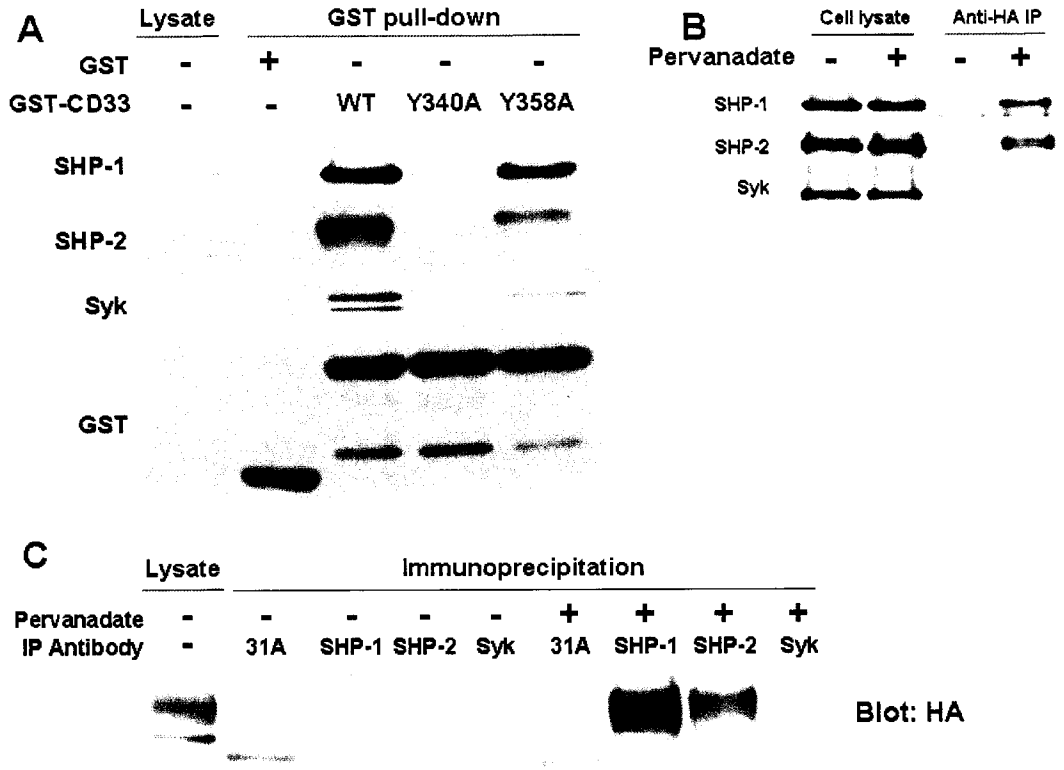

Figure II.6: ITIM- and phosphotyrosine-dependent interactions between CD33 and SH2-domain proteins. (A) GST proteins fused to cytoplasmic tails of wild-type and mutant CD33 were expressed in E.coli, and used in pull-down assays with cell lysates from human myeloid U937 cells that were stimulated with pervanadate (100 μM) for 30 min at 37° C prior to lysis. After beads were washed, proteins were separated by SDS-PAGE, and blots probed for SHP-1, SHP-2, and Syk as indicated. Blots were then stripped and reprobed with anti-GST antibody to ascertain equal amounts of fusion proteins. Similar results were obtained with cell lysates from HL-60, NB4, and ML-1 cells. (B) NB4 cells transduced with HA-tagged $CD33^{WT}$ were incubated in the presence or absence of pervanadate (100 μM) for 15 min at 37° C, lysed, and immunoprecipitated with anti-HA antibody. Blots were then probed with anti-SHP-1, anti-SHP-2, and anti-Syk antibodies as indicated. Similar results were obtained with HL-60 and ML-1 cells. (C) NB4 cells transduced with HA-tagged $CD33^{WT}$ were incubated in the presence or absence of pervanadate (100 μM) for 15 min at 37° C, lysed, and immunoprecipitated with isotype control antibody (31.A), anti-SHP-1, anti-SHP-2, or anti-Syk as indicated. Blots were then probed with anti-HA antibody. Similar findings were obtained with transduced HL-60 and ML-1 cells.

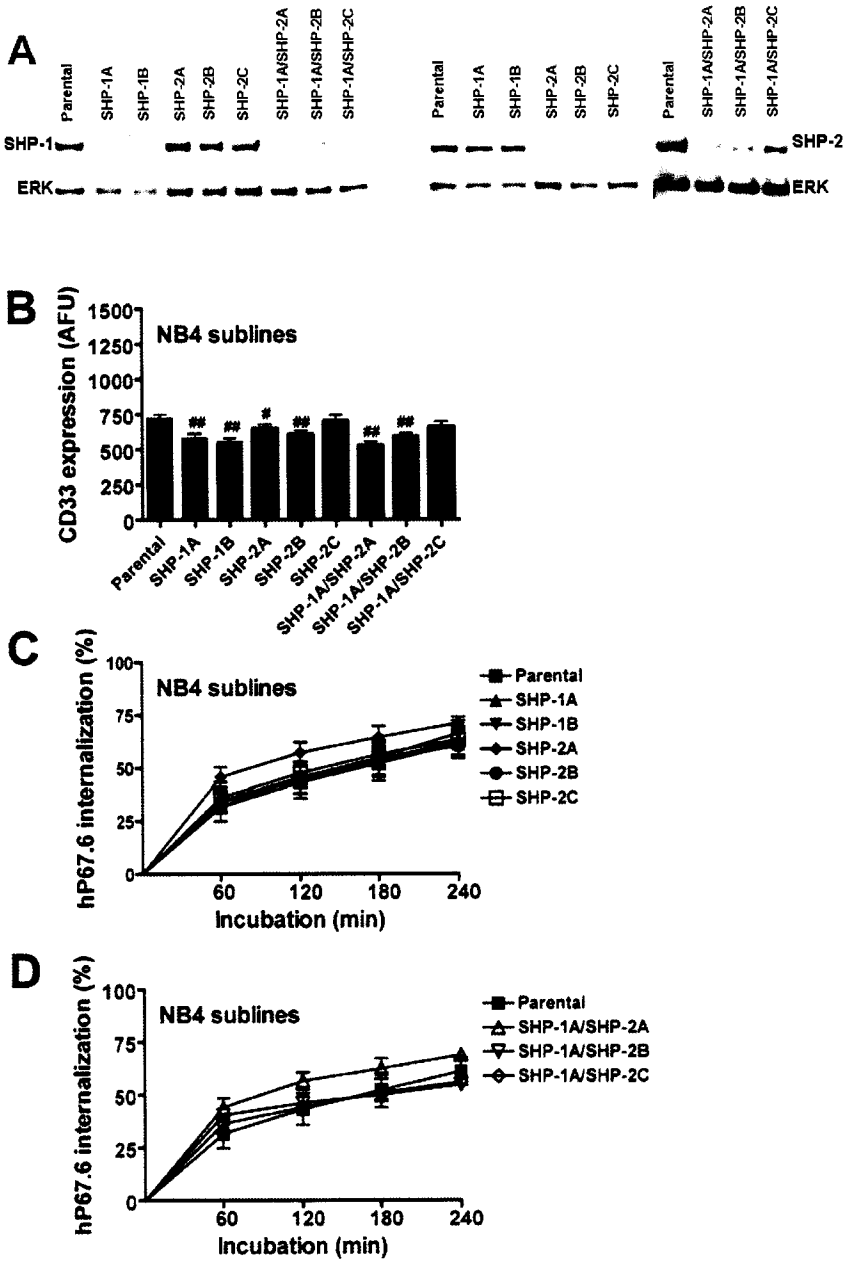

Figure II.7: Effect of SHP-1 and/or SHP-2 siRNA on CD33 expression and internalization in NB4 cells. (A) NB4 cells were virally transduced with siRNAs targeting SHP-1 and/or SHP-2 as indicated. Cell lysates were prepared, and Western blots performed to assess protein knock-down. (B) Cell surface CD33 expression was determined by staining with the human anti-CD33 antibody hP67.6, and expressed as arbitrary fluorescence units (AFU). (C) and (D) Internalization of hP67.6 was assessed over 4 hours, and expressed as percentage of internalized antibody relative to cells kept at 0° C. Results are shown as mean±SEM from 3 independent experiments. $^{\#}p<0.05$, $^{\#}p<0.01$ compared to parental cells.

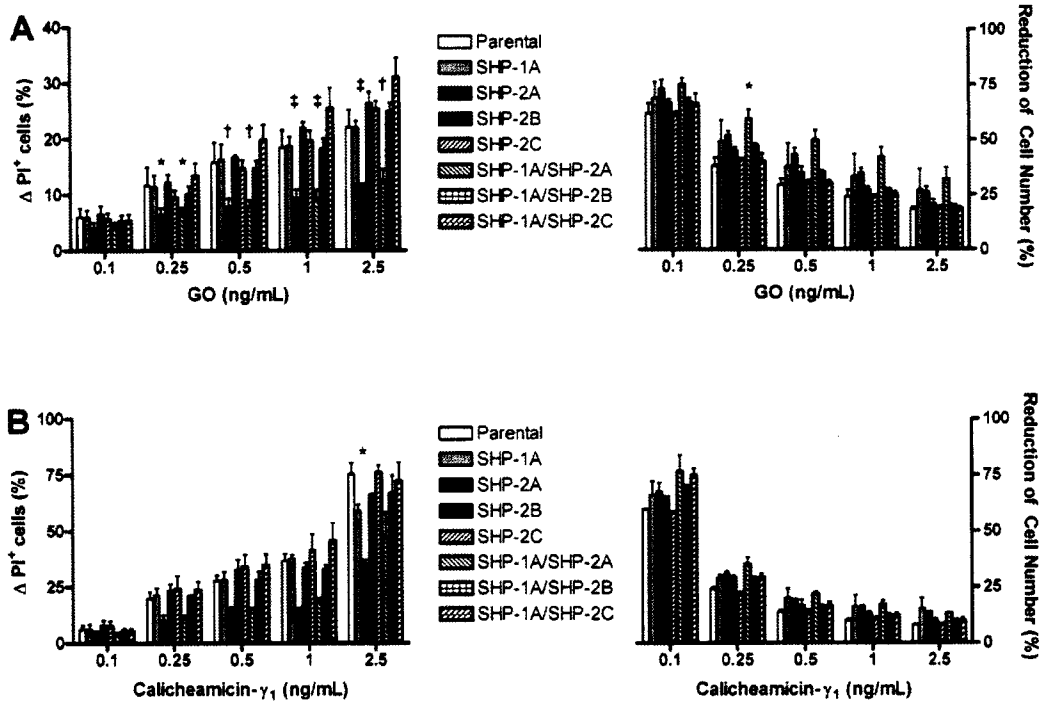

Figure II.8: Effect of SHP-1 and/or SHP-2 siRNA on drug-induced cytotoxicity in NB4 cells. NB4 cells were virally transduced with siRNAs targeting SHP-1 and/or SHP-2 as indicated. (A) and (B) Cells were incubated with various concentrations of GO or calicheamicin-γ_1 for 3 days, before cytotoxicity was assessed with PI staining and cell numbers were determined. Results are shown as mean±SEM from 3 independent experiments assessing GO-induced cytotoxicity and 2 independent experiments assessing calicheamicin-γ_1-induced cytotoxicity.*$p<0.05$, $^{\dagger}p>0.01$, $^{\ddagger}p<0.001$ compared to parental cells.

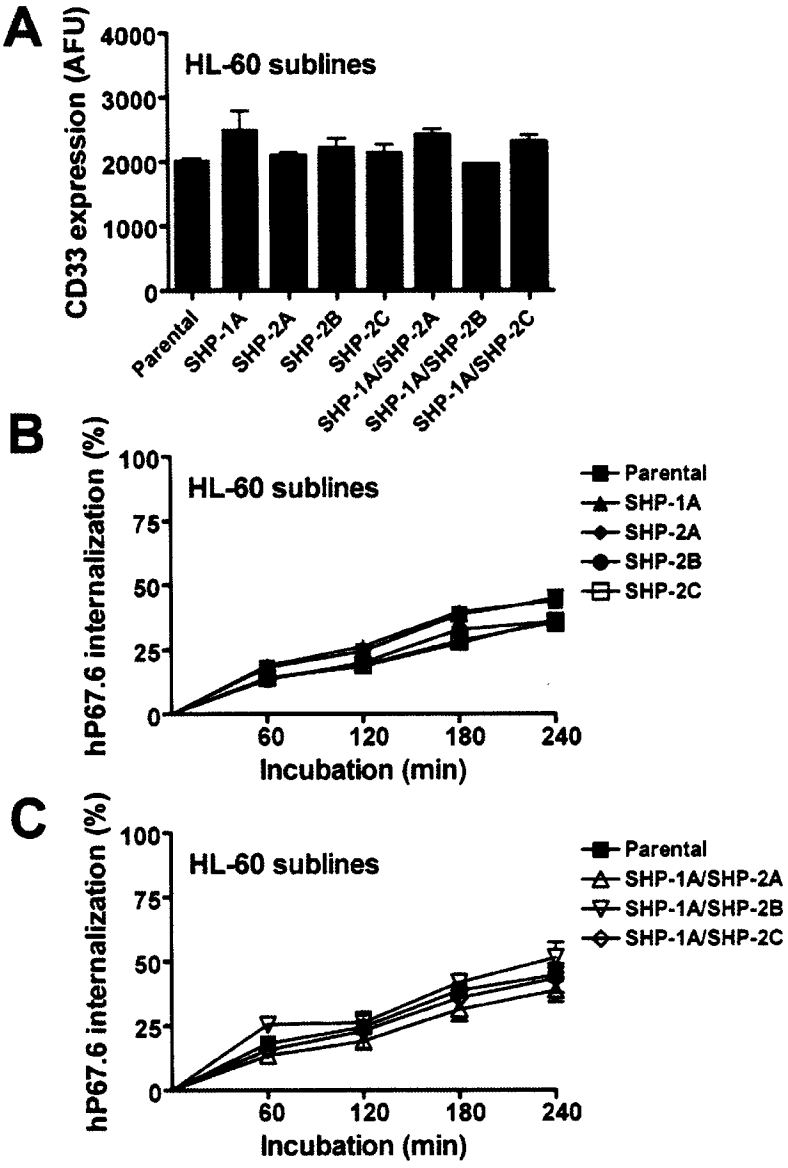

Figure II.9: Effect of SHP-1 and/or SHP-2 siRNA on CD33 expression and internalization in HL-60 cells. HL-60 cells were virally transduced with siRNAs targeting SHP-1 and/or SHP-2 as indicated. (A) Cell surface CD33 expression was determined by staining with the human anti-CD33 antibody hP67.6, and expressed as arbitrary fluorescence units (AFU). (B) and (C) Internalization of hP67.6 was assessed over 4 hours, and expressed as percentage of internalized antibody relative to cells kept at 0° C. Results are shown as mean±SEM from 3 independent experiments.

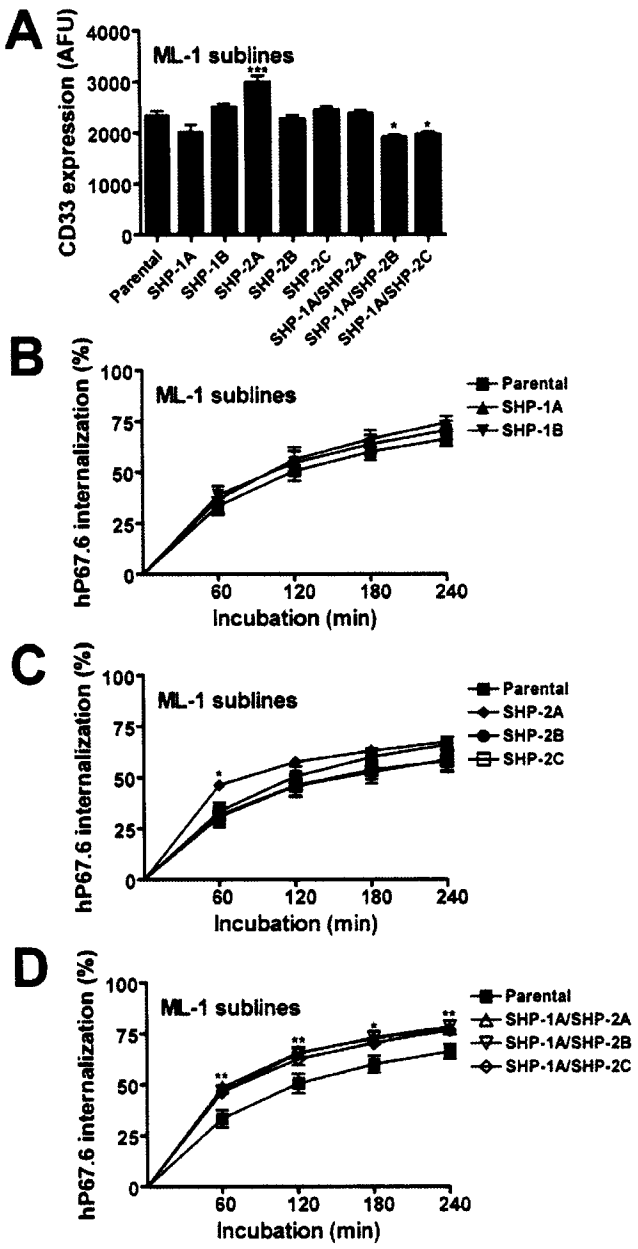

Figure II.10: Effect of SHP-1 and/or SHP-2 siRNA on CD33 expression and internalization in ML-1 cells. ML-1 cells were virally transduced with siRNAs targeting SHP-1 and/or SHP-2 as indicated. (A) Cell surface CD33 expression was determined by staining with the human anti-CD33 antibody hP67.6, and expressed as arbitrary fluorescence units (AFU). (B), (C), (D) Internalization of hP67.6 was assessed over 4 hours, and expressed as percentage of internalized antibody relative to cells kept at 0° C. Results are shown as mean±SEM from 4 independent experiments. *p<0.05, **p<0.01, ***p<0.001 compared to parental cells

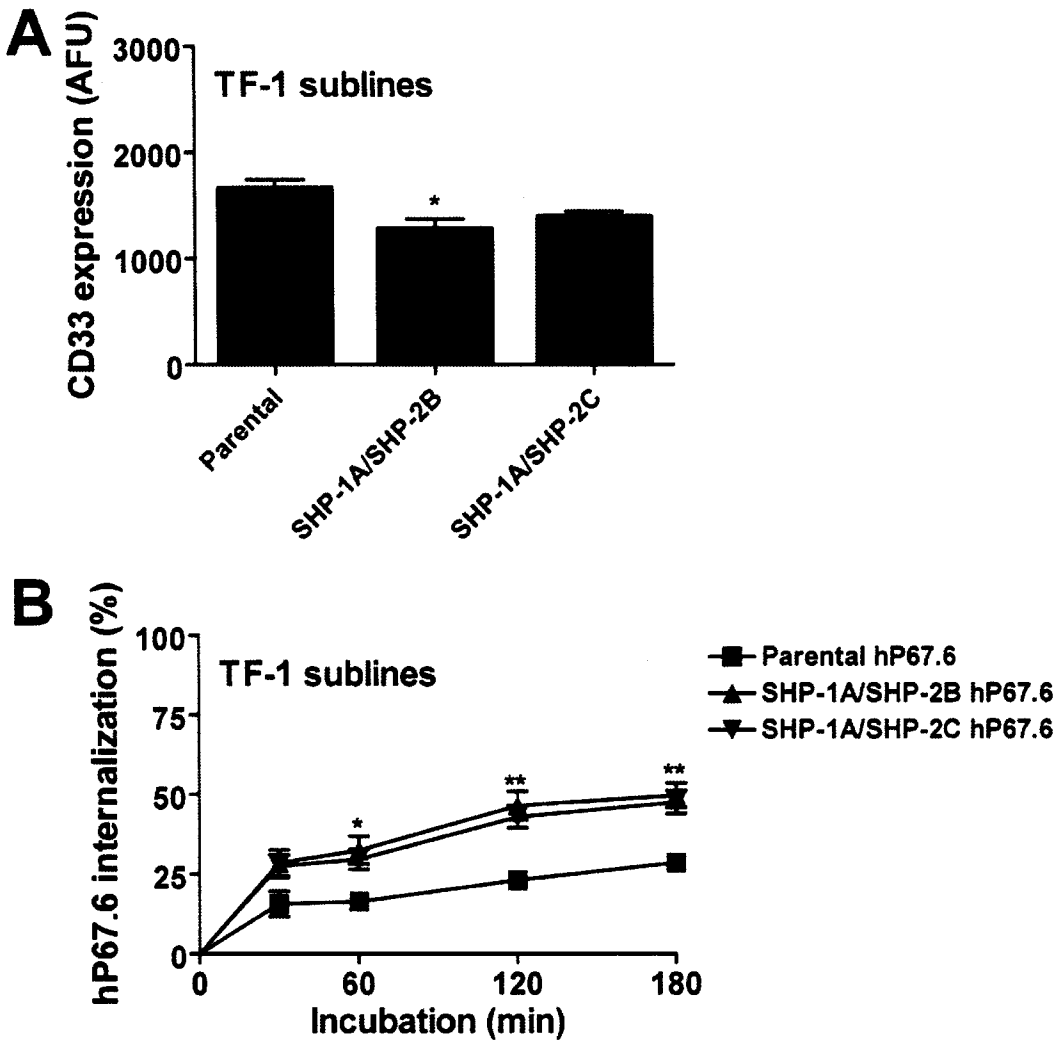

Figure II.11: Effect of SHP-1 and SHP-2 siRNA on CD33 expression and internalization in TF-1 cells. TF-1 cells were virally transduced with siRNAs targeting SHP-1 and/or SHP-2 as indicated. (A) Cell surface CD33 expression was determined by staining with the human anti-CD33 antibody hP67.6, and expressed as arbitrary fluorescence units (AFU). (B) Internalization of hP67.6 was assessed over 4 hours, and expressed as percentage of internalized antibody relative to cells kept at 0° C. Results are shown as mean±SEM from 4 independent experiments. *$p<0.05$, **$p<0.01$ compared to parental cells.

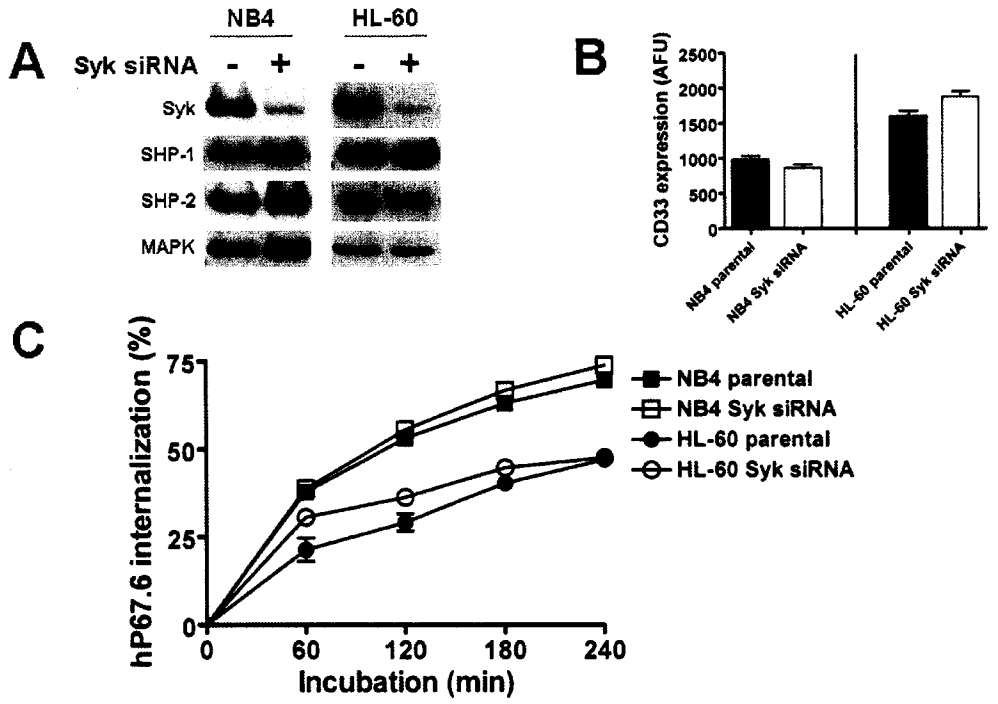

Figure II.12: Effect of Syk siRNA on CD33 expression and internalization in NB4 and HL-60 cells. (A) NB4 and HL-60 cells were virally transduced with siRNAs targeting Syk at a MOI of 5 or left untreated as indicated. Cell lysates were prepared, and Western blots performed to verify efficient Syk protein knock-down and unaffected SHP-1 and SHP-2 protein levels. (B) Cell surface CD33 expression was determined by staining with hP67.6, biotin-conjugated mouse anti-human IgG_4, and streptavidin-PE, and expressed as arbitrary fluorescence units (AFU). (C) Internalization of hP67.6 was assessed over 4 hours, and expressed as percentage of internalized antibody relative to cells kept at 0° C.

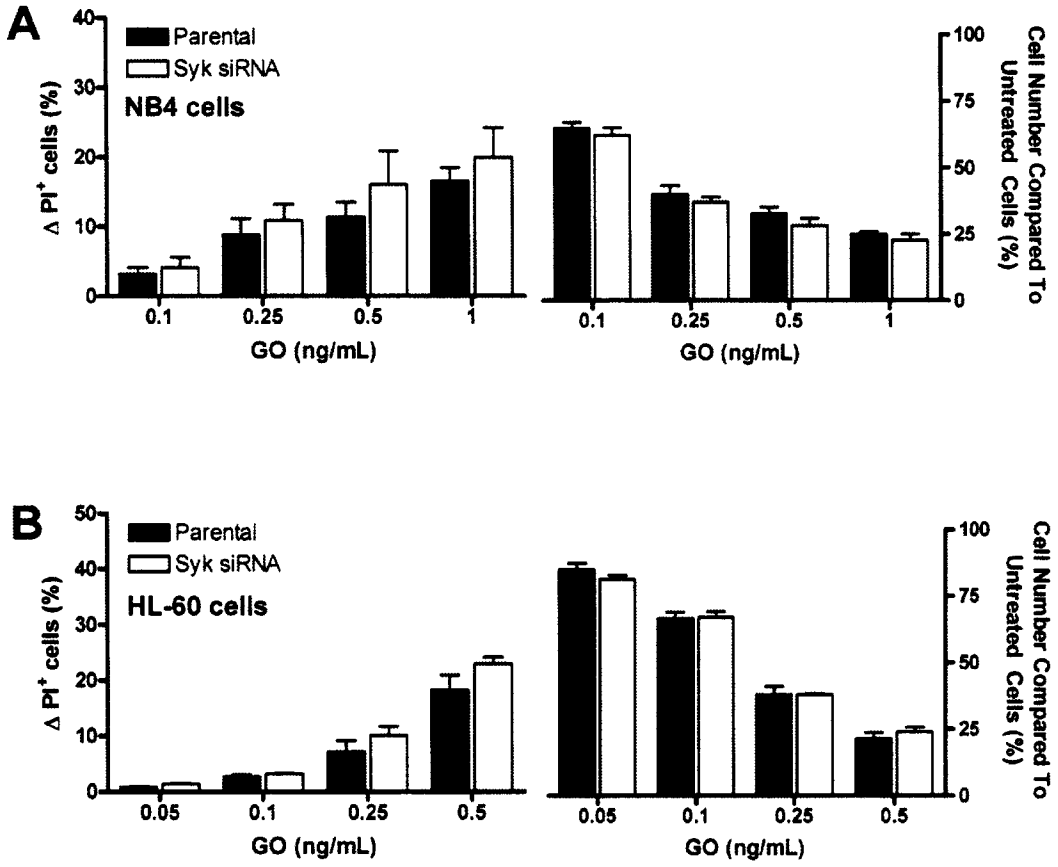

Figure II.13: Effect of Syk siRNA on GO-induced cytotoxicity in NB4 and HL-60 cells. (A) Parental and Syk siRNA-infected NB4 (A) and HL-60 (B) cells were incubated with various concentrations of GO for 3 days, before cytotoxicity was assessed with PI staining and the cell numbers were determined. Results are shown as mean±SEM from 3 independent experiments.

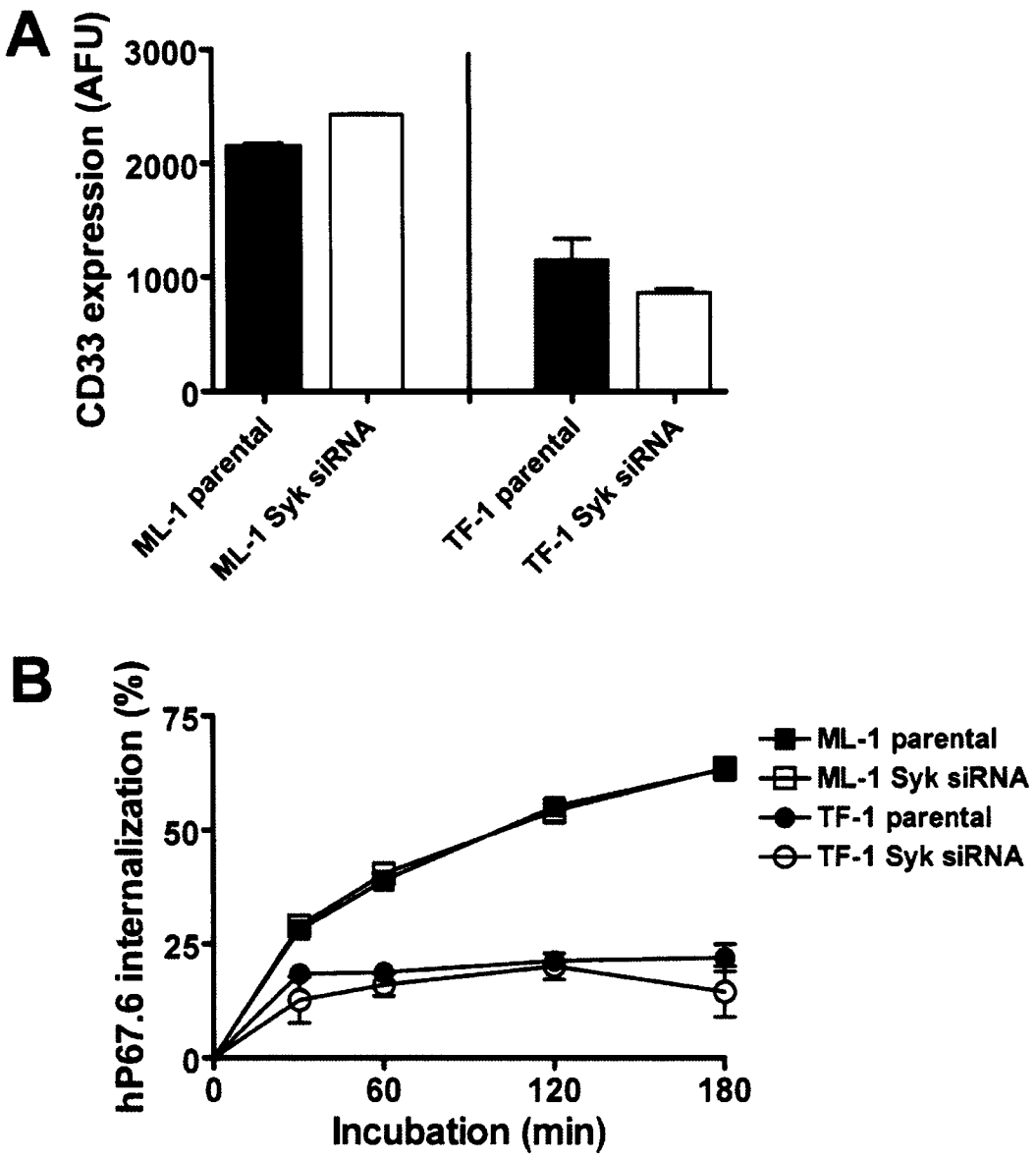

Figure II.14: Effect of Syk siRNA on CD33 expression and internalization in ML-1 and TF-1 cells. ML-1 and TF-1 cells were virally transduced with siRNAs targeting Syk at a MOI of 5 or left untreated as indicated. (A) Cell surface CD33 expression was determined by staining with hP67.6, biotin-conjugated mouse anti-human IgG_4, and streptavidin-PE, and expressed as arbitrary fluorescence units (AFU). (B) Internalization of hP67.6 was assessed over 4 hours, and expressed as percentage of internalized antibody relative to cells kept at 0° C.

Chapter III: Regulation of CD33 cell surface expression and internalization by ITIM-dependent monoubiquitylation

III.1. Introduction

Cells of the immune system are activated by cell-surface receptors transducing positive signals through a short tyrosine-based cytoplasmic motif, the immunoreceptor tyrosine-based activation motif (ITAM).[115,116] Activating receptors are in turn paired with inhibitory counterparts to restrict the duration and/or intensity of positive signals, thereby allowing proper modulation of immune responses.[115,117,118] These inhibitory receptors are characterized by the immunoreceptor tyrosine-based inhibitory motif (ITIM), a highly conserved cytoplasmic stretch of amino acids with the consensus sequence (I/V/L/S)-X-Y-X-X-(L/V).[115,118] Tyrosine phosphorylation, often by a Src family kinase, provides a docking site for the recruitment and activation of various Src homology 2 (SH2) domain-containing proteins, including the tyrosine phosphatases SHP-1 and SHP-2 and/or the inositol phosphatase SHIP, which subsequently transmit inhibitory signals.[118] The importance of negative signaling is unequivocally demonstrated by the development of fatal autoimmune disorders in animals with targeted disruption of single inhibitory immunoreceptors.[118] Evidently, the delicate balance between transmission of activating and inhibitory signals requires tight cellular control over both the signal transduction machinery as well as the cell surface display of ITAM and ITIM-containing receptors.

Recent evidence indicates an important role of ubiquitin in the regulation of immunoreceptor signaling.[119] For example, activated protein tyrosine kinases of the Src and spleen tyrosine kinase (Syk)/ZAP-70 families are target for polyubiquitylation, leading to their proteosomal degradation.[119,120] Likewise, monoubiquitylation and subsequent lysosomal degradation has been shown to

be involved in the activation-dependent downmodulation of the ζ chain of the T cell receptor and the FcγRIIA receptor, both ITAM-containing molecules.[121,122] By comparison, principles that govern cell surface display, internalization, and degradation of inhibitory receptors are largely unexplored.

An example of an inhibitory immunoreceptor is CD33, which contains a proximal ITIM (with its tyrosine at position 340) and a distal ITIM-like motif (with its tyrosine at position 358).[29,31,44-46] Previous studies summarized in chapter I[92] have provided evidence that CD33 is internalized in an ITIM-dependent manner when ligated with anti-CD33 antibody. While some of the molecular mechanisms involved were addressed in chapter II, the primary objective of the studies presented in this chapter was to investigate whether ubiquitylation is involved in the regulation of cell surface display of CD33, and/or in the process of internalization and intracellular trafficking of ligated CD33.

III.2. Materials and Methods

Cells

Human myeloid HL-60 and NB4 cells were maintained in RPMI medium 1640 with 25 mM HEPES ([*N*-2-hydroxyethylpiperazine-*N'*-2-ethanesulfonic acid], GIBCO-Invitrogen, Carlsbad, CA) supplemented with 5% heat-inactivated bovine calf serum (BCS; HyClone, Logan, UT). The interleukin-3 (IL-3)-dependent murine myeloid 32D cell line was maintained in Iscove's Modified Dulbecco's Medium (IMDM, GIBCO-Invitrogen) with 10% heat-inactivated fetal bovine serum (FBS, HyClone) and 8% WEHI cell-conditioned medium as a source of IL-3. The human Jurkat T cell line was maintained in RPMI medium 1640 with 25 mM HEPES supplemented with 10% heat-inactivated FBS, 1 mM MEM sodium pyruvate, and 0.1 mM MEM non-essential amino acids (GIBCO-Invitrogen). HEK293T and COS-7 cells were maintained in Dulbecco's Modified Eagle

medium (D-MEM, GIBCO-Invitrogen) supplemented with 10% heat-inactivated FBS. All media also contained penicillin and streptomycin (GIBCO-Invitrogen).

Antibodies

The following antibodies were used: anti-CD33 (clone hP67.6; kindly provided by Wyeth-Ayerst Research, Radnor, PA), anti-HA (clone 3F10, Roche Diagnostics, Indianapolis, IN), anti-phosphotyrosine (clone 4G10, Upstate Biotechnology, Charlottesville, VA), anti-T7 (Novagen, Madison, WI), anti-MAPK (clone 1913.3[96]), and anti-GST (clone 38.3). Secondary antibodies used were: horseradish peroxidase (HRP)-conjugated sheep anti-mouse Ig, goat-anti rat IgG, and donkey anti-rabbit Ig (GE Healthcare, Amersham Biosciences, Buckinghamshire, England), as well as biotin-conjugated mouse anti-human IgG_4 (BD Biosciences Pharmingen, San Diego, CA).

Cellular transfection with cDNA constructs

An expression vector encoding an octameric ubiquitin precursor protein under the CMV enhancer-promoter was kindly provided by Dr. Robert N. Eisenman (Fred Hutchinson Cancer Research Institute, Seattle, WA). The precursor is efficiently processed by cellular ubiquitin-COOH-terminal hydrolases into single units that contain an HA tag at their NH2-terminus.[123] A pME-vector based expression construct encoding wild-type human Fyn (kindly provided by Dr. Tohru Tezuka, University of Tokyo, Tokyo, Japan) has been described previously.[124] pCEFL plasmids encoding human Cbl and Cbl-b (kindly provided by Dr. Stanley Lipkowitz, National Cancer Institute, Bethesda, MD) have been described previously.[125] Expression constructs encoding wild-type and catalytically inactive SHP-1 ($SHP\text{-}1^{WT}$ and $SHP\text{-}1^{C453S}$, respectively) were kindly provided by Dr. Benjamin G. Neel, Beth Israel Deaconess Medical Center, Boston, MA. A T7-tag was introduced into pcDNA3 vectors containing complementary DNA (cDNA) for $CD33^{WT}$, $CD33^{Y340F}$, $CD33^{Y358F}$, and $CD33^{Y340F/Y358F}$ (kindly provided by Dr. Daniel W. McVicar, National Cancer

Institute, Frederick, MD[46]) by site-directed mutagenesis using standard polymerase chain reaction (PCR) cloning procedures with the following primers: forward 5'-ACAGGTGGCCAACAGATGGGTTGATCTAGAGGGCCCTATTCTATAGTG-3'; and reverse 5'-TTGGCCACCTGTCATCGATGCCATCTGGGTCCTGACCTCTGAG-3'. PCR-based site-directed mutagenesis was used to generate the lysine to arginine mutants $CD33^{K283/288R}$ (referred to as $CD33^{K2R}$; forward 5'-CCCACAGGAGGAGGGCAGCCAGGACAGCAGTG-3', reverse 5'-CTCCTGTGGGTCCTCACTATGAAGAAGATGAGGCAGAG-3'), $CD33^{K309/312/313/315R}$ (referred to as $CD33^{K4R}$; forward 5'-CACCAGAGGAGGTCCAGGTTACATGGCCCCACTGAAACC-3', reverse 5'-GGACCTCCTCTGGTGTCTCGGGGAGGCTGACCCTG-3'), $CD33^{K352R}$ (referred to as $CD33^{K1R}$; forward 5'-CCTTCCAGGGACACCTCCACCGAATAC-3', reverse 5'-GGTGTCCCTGGAAGGATTCATCCCATG-3'), $CD33^{K309/312/313/315/352R}$ (referred to as $CD33^{K5R}$), and $CD33^{K283/288/309/312/313/315/352R}$ (referred to as $CD33^{K7R}$), as shown in Table III.1. Fusion proteins between wild-type and mutant CD33 and human ubiquitin were generated by amplifying the CD33-ubiquitin cassette from pRRLsin.cPPT.MSCV.CD33-ubiquitin.IRES.EGFP with flanking Eco RI and Acc65 I restriction sites and subcloning this fragment into the pcDNA3.1(-) backbone. All constructs were verified by sequencing. HEK293T and COS-7 cells, grown in 6-well plates (Costar, Corning, NY), were transiently transfected with polyethylenimine (Polysciences, Warrington, PA) or lipofectamine 2000 (Invitrogen, Carlsbad, CA), respectively, using 2 µg per cDNA. Cells were harvested 24 - 48 hours after transfection. In some experiments, cells were treated with 100 µM pervanadate for 15 min at 37°C prior to harvest.

Lentivirus-mediated gene transfer

Bicistronic lentiviral vectors pRRLsin.cPPT.MSCV.$CD33^{WT/MUT}$.IRES.EGFP encoding cDNA for $CD33^{WT}$, $CD33^{Y340F}$, $CD33^{Y358F}$, or $CD33^{Y340F/Y358F}$ were

previously described.[92] Additional lysine-to-arginine mutants were generated by site-directed mutagenesis using standard PCR cloning procedures as described above, and verified by sequencing. Fusion proteins between wild-type or mutant CD33 and human ubiquitin were generated by standard PCR cloning procedures as follows: in a first step, an Xho I-Xma I cassette was introduced after the C-terminal amino acid of CD33 into the pRRLsin.cPPT.MSCV.CD33.IRES.EGFP construct (forward 5'-CGAGCCGCCCGGGATCCGCCCCTCTC-3', reverse 5'-CCGGGCGGCTCGAGCTGGGTCCTGACCTCTGAGTATTCG-3'). In a second step, human ubiquitin was amplified with appropriate flanking restriction sites (forward 5'-CCGCTCGAGATGCAGATCTTCGTGAAAACCCTTAC-3', reverse 5'-TCCCCCCGGGTTAACCACCTCTCAGACGCAGGACC-3'), and ligated into the Xho I and Xma I sites. All constructs were verified by sequencing. Stocks of vesicular stomatitis virus G glycoprotein (VSV-G)–pseudotype lentiviral vectors were prepared by the Gene Marking and Tracking Facility (Core Center of Excellence in Molecular Hematology, Fred Hutchinson Cancer Research Center, Seattle, WA) with calcium phosphate–mediated 3-plasmid transfection of HEK293T cells.[92] 27 µg of the transfer vector construct, 17.5 µg second generation gag-pol packaging construct pCMVR8.74, and 9.5 µg VSV-G expression construct pMD.G were used for transfection of 1.2×10^7 HEK293T cells overnight in 25 mL D-MEM with 10% heat-inactivated FBS. Cells were treated with 10 mM sodium butyrate during the first of 3 12-hour vector supernatant collections. The supernatant was filtered through a 0.22 µm pore-size filter and concentrated 100-fold by ultracentrifugation. All vector stocks were titered by infecting HT1080 cells using limiting dilutions of the stock with analysis for EGFP expression by flow cytometry. Infections of hematopoietic cell lines were performed in fibronectin-coated wells in the presence of 8 µg/mL protamine sulfate at a multiplicity of infection (MOI) of 5 – 25. EGFP-positive cells were sorted by flow cytometry and re-cultured for further analysis.

Immunoprecipitation and Western blotting

Cells were washed twice in ice-cold Dulbecco's Phosphate Buffered Saline (PBS, GIBCO-Invitrogen) and then lysed in lysis buffer containing 25 mM HEPES (pH 7.4), 100 mM NaCl, 50 mM NaF, 1% NP-40 (Igepal CA-630, Sigma, St. Louis, MO), 10% glycerol, 1 mM phenylmethylsulphonyl fluoride (PMSF), and protease inhibitors (Roche Diagnostics, Mannheim, Germany); in some experiments, 1 mM sodium orthovanadate was added. After incubation on ice for 45 min, lysates were precleared by centrifugation. For immunoprecipitations, precleared lysates were incubated with 1 µg of antibody overnight at 4°C, and then Protein G Sepharose 4 Fast Flow beads (GE Healthcare, Amersham Biosciences) added for 2 hours. Beads were then washed 4 times in ice-cold lysis buffer and boiled in 1x reducing sample buffer (2% SDS, 10% glycerol, 20% β-mercaptoethanol, 105 mM Tris [tris(hydroxymethyl)aminomethane]/HCl, 0.03% bromophenol blue). In a subset of experiments, washed beads were treated with N-glycosidase F (PNGase F; New England Biolabs, Ipswich, MA) according to the manufacturer's instructions before boiling in reducing sample buffer. For Western blotting, samples were separated on either 7.5% or 10% sodium dodecyl sulfate-polyacrylamide gel electrophoresis (SDS-PAGE), transblotted to nitrocellulose, blocked with 5% non-fat dry milk in Tris-buffered saline (TBS; 50 mM Tris [pH 7.5], 150 mM NaCl) containing 0.1% Tween 20 (TBST) for 30 minutes at room temperature, and then incubated with primary antibodies overnight at 4°C. For assessment of tyrosine phosphorylation, blots were blocked with TBS containing 6% bovine serum albumin (BSA; Sigma), 0.05% Tween 20, 5 mM NaF, and 0.005% NaN_3 for 24-48 hours prior to incubation with primary antibody. After washing, blots were incubated for 60 minutes with horseradish peroxidase-conjugated secondary antibody in TBST/BSA, washed, and immunoreactive signals visualized with enhanced chemiluminescence (PerkinElmer, Boston, MA) and exposed to CL-XPosure film (Pierce, Rockford, IL).

Glutathione-S-transferase (GST) fusion proteins and pull-down assays

GST-Cbl TKB domain and GST-Cbl-b TKB domain fusion proteins were kindly provided by Dr. Hamid Band (Evanston Northwestern Healthcare Research Institute, Feinberg School of Medicine, Northwestern University, Evanston, IL) and Dr. Stanley Lipkowitz, and have been described previously.[126] To generate glutathione-S-transferase (GST) fusion protein constructs with wild-type and mutant CD33, the cytoplasmic tails of wild-type or mutant CD33 starting at amino acid 289 were subcloned into the pGEX2T vector by standard PCR cloning procedures using the following primers: forward 5'-CGCGGATCCGCAGCCAGGACAGCAGTG-3', reverse 5'-CCGGAATTCTCACTGGGTCCTGACCTCTG-3'; constructs were verified by sequencing. Fusion proteins were expressed after isopropyl-beta-D-thiogalactoside (IPTG) induction in *E. coli* BL-21 or *E. coli* TKB1 (Stratagene, La Jolla, CA) as non-tyrosine-phosphorylated or tyrosine-phosphorylated proteins, respectively. The TKB1 strain contains an elk1 tyrosine kinase that can be induced with indoleacrylic acid to phosphorylate bacterial fusion proteins expressed after IPTG-induction in the same cells. Bacteria were lysed in ice-cold PBS containing 1% Triton X-100 (Sigma), 1 mM phenylarsine oxide (PAO), 0.1% β-mercaptoethanol, 1 mM PMSF, and 1 mM ethylene diaminetetraacetic acid (EDTA). After sonication, lysates were cleared by centrifugation and stored at -20°C. An aliquot of the lysate was checked for purity and concentration of the isolated proteins by incubation with a 50% slurry of Glutathione Sepharose 4B beads (GE Healthcare, Amersham Biosciences) in lysis buffer, rotating for 1 hour at 4°C, washing with ice-cold lysis buffer, and analysis by SDS-PAGE and Coomassie staining. For pull-down assays, GST fusion proteins were incubated with a 50% slurry of Glutathione Sepharose 4B beads in lysis buffer and rotated for 1 hour at 4°C. Beads were isolated by centrifugation, washed 4 times with ice-cold lysis buffer, and then incubated with cell lysates from human myeloid cell lines that were or were not stimulated with pervanadate prior to lysis to promote tyrosine phosphorylation. After rotating for 2 hours at 4°C, beads were again

isolated by centrifugation, washed 4 times with ice-cold lysis buffer, boiled in 1x reducing sample buffer, and analyzed by Western blotting.

Flow cytometry assays for determination of CD33 expression and internalization
Internalization of antibody-bound CD33 in AML cell lines was measured as described previously.[92] 1-1.5 x 10^6 cells were transferred into 5 mL polystyrene round bottom tubes (BD Biosciences Discovery Labware, Bedford, MA) and incubated for 30 minutes with IMDM medium containing 2.5 - 10 µg/mL unconjugated, unlabeled hP67.6 in ice-water (to prevent internalization during the staining procedure). Cells were then washed in ice-cold PBS, resuspended in IMDM medium without antibody, split into several tubes, and incubated at 37°C (in 5% CO_2 and air) for various periods of time. Afterwards, cells were chilled and incubated with biotin-conjugated mouse anti-human IgG_4 monoclonal antibody, followed by incubation with streptavidin-PE conjugate (BD Biosciences Pharmingen) to detect remaining hP67.6 on the cell surface. One sample kept in ice-water was used to determine the starting level of antibody bound to the cell surface. To identify nonviable cells, samples were stained with propidium iodide (PI; Sigma). At least 10,000 events were acquired and PI^- cells were analyzed on a FACScan Flow Cytometer using Cellquest software (both BD Biosciences Immunocytometry Systems, San Jose, CA). Linear fluorescence values were used to calculate the level of cell surface CD33 expression and the percentage of antibody internalization.

Confocal microscopy
Cells were first incubated for at least 30 minutes in ice-water in IMDM containing 20 µg/mL hP67.6 that was directly labeled with either Alexa Fluor 488 or Alexa Fluor 594 (Molecular Probes-Invitrogen, Carlsbad, CA). Cells were then washed with ice-cold PBS, resuspended in IMDM without antibody, and incubated at 37°C for various periods of time. 30 minutes prior to the end of the incubation, Hoechst 33342 (Sigma), and, in some experiments, LysoTracker Red DND-99

(Molecular Probes-Invitrogen) was added to the cells to yield final concentrations of 0.75 ng/mL and 100 nM, respectively. Afterwards, cells were cooled in ice-water, washed with ice cold PBS, fixed in 2% paraformaldehyde solution at room temperature, and mounted on polylysine-coated slides with Vectashield mounting medium (Vector Laboratories, Burlingame, CA). Cells were examined on a Deltavision SA3.1 wide-field deconvolution microscope system (Applied Precision, Issaquah, WA) using an Olympus 60 1.4 NA objective on an Olympus IX-70 inverted microscope (Olympus, Melville, NY), and images were acquired with a Photometrics CH350 cooled coupling device (CCD) camera (Photometrics, Tucson, AZ). Three-dimensional images were deconvolved using an iterative constrained algorithm (SoftWoRX software, Applied Precision).

Statistical analysis

Results from CD33 expression and internalization studies are presented as means±SEM from at least 3 independent experiments. Parametric statistical analysis was performed using repeated measures ANOVA with Tukey-Kramer Multiple Comparisons Test (InStat 3.05; GraphPad, San Diego, CA, USA); $p<0.05$ was considered significant.

III.3. Results

CD33 is a target for ITIM-dependent monoubiquitylation

In line with early studies using radio-labeled anti-CD33 antibodies,[127] Alexa Fluor 488-labeled anti-CD33 antibodies co-localized with the lysosomal marker, LysoTracker Red DND-99, in the human $CD33^+$ AML cell lines NB4 (Fig III.1) and HL-60 (not shown), indicating that the intracellular trafficking of the antibody-CD33 complex ends in the lysosomal compartment. Based on these findings, and on experiments detailed in the previous chapter demonstrating enhancement of ITIM-dependent internalization of antibody-bound CD33 by tyrosine

phosphorylation, we have focused on pathways that direct ligated cell surface receptors to lysosomes in a phosphotyrosine-dependent manner. Given the emerging importance of monoubiquitylation in internalization and lysosomal routing of activated tyrosine-motif containing cell surface receptors, including ITAM molecules and receptor tyrosine kinases,[72,120,122,128] we investigated whether CD33 could be ubiquitylated. To address this question, we performed co-transfection experiments in HEK293T and COS-7 cells, using T7-tagged CD33 constructs as well as an HA-tagged human ubiquitin expression vector; these non-myeloid cell lines seemed suitable for our purpose as we have found that various wild-type and mutant CD33 constructs showed similar endocytic properties in HEK293T and COS-7 cells as when expressed in myeloid cells (Fig III.2). Epitope-tagged ubiquitin has been widely used as a means to increase sensitivity and specificity of the detection of ubiquitylated proteins.[129] In such co-transfection assays, cell lysates were immunoprecipitated with anti-T7 antibody, and membranes probed with anti-HA antibody. As shown in Fig III.3 (Panel A), ubiquitin was readily detectable in immunoprecipitates from cells transfected with $CD33^{WT}$, and, to a lesser extent, from cells expressing $CD33^{Y358F}$. By comparison, very little ubiquitin was detected in immunoprecipitates from cells expressing $CD33^{Y340F}$ or $CD33^{Y340F/Y358F}$. Blots were then stripped and reprobed with anti-T7 antibody to detect CD33. Similar amounts of CD33 were found in cells transfected with wild-type or mutant CD33. Importantly, an overlay of the two blots showed a size-shift between the CD33 and the ubiquitin band of the expected size of the 76 amino acid protein, ubiquitin, indicating that the vast majority of CD33 was non-ubiquitylated in these assays.

These results are consistent with the hypothesis that the ITIMs mediate ubiquitylation of CD33, e.g. by offering binding sites for an E3 ligase. To study the influence of ITIM phosphorylation on ubiquitylation of CD33, we performed similar experiments in HEK293T cells as described above in the presence or absence of the co-transfected Src family kinase, Fyn, which stimulates tyrosine

phosphorylation of CD33 (see below). Ubiquitylation of $CD33^{WT}$ was greatly enhanced upon co-transfection of Fyn (Fig III.3, Panel B), indicating that ITIM phosphorylation favors ubiquitylation of CD33. Based on these findings, we hypothesized that Cbl family proteins, RING-finger containing E3 ligases that are able to bind to phosphotyrosine motifs on activated phosphotyrosine kinases via an N-terminal tyrosine-kinase binding (TKB) domain and that have been implicated in important ubiquitylation processes of immune cells,[119,120] could potentially be involved in mediating ubiquitylation of CD33. Indeed, GST fusion protein pulldown experiments showed an ITIM-dependent interaction between Cbl proteins and CD33. As shown in Fig III.4 (Panel A), a fusion protein between GST and phosphorylated tails of wild-type CD33 was able to bind to Cbl to a much higher degree than fusion proteins between GST and phosphorylated tails of either $CD33^{Y340A}$ or CD^{Y358A}. Conversely, in pulldown assays with cell lysates from pervanadate-treated HEK293T or COS-7 cells, a fusion protein between GST and the TKB domain of Cbl or Cbl-b was able to interact with $CD33^{WT}$, and, to a lesser extent, with $CD33^{Y358F}$, whereas very little interaction was found with $CD33^{Y340F}$ or $CD33^{Y340F/Y358F}$ (Fig III.4, Panel B). These binding results parallel the relative ubiquitylation of the mutants (Fig III.3, Panel A) and their relative rates of endocytosis (Fig III.2).

Enhancement of CD33 monoubiquitylation by Cbl family members

To test whether Cbl proteins can mediate ubiquitylation of CD33, we performed co-transfection experiments with T7-tagged $CD33^{WT}$ and HA-tagged ubiquitin in the presence and absence of overexpressed Cbl or Cbl-b. As shown in Fig III.5 (left panel), co-overexpression with Cbl-b resulted in a significant higher abundance of ubiquitylated $CD33^{WT}$. Additional overexpression of Fyn further increased ubiquitylation of CD33, consistent with the hypothesis that CD33 tyrosine phosphorylation favors the ubiquitylation process. To ascertain that the ubiquitin moiety indeed is bound to CD33, we took advantage of the fact that CD33 is a glycoprotein and treated parallel immunoprecipitates with the N-

glycosidase PNGase F, which resulted in a significant and parallel size shift of both the HA as well as the T7 signal, indicating that the ubiquitin signal indeed originates from CD33 rather than a co-immunoprecipitated unidentified protein (Fig III.5, right panel). To test the effect of the tyrosine phosphatase, SHP-1, on CD33 ubiquitylation, we performed similar co-transfection experiments in HEK293T cells in the presence and absence of wild-type or phosphatase-dead SHP-1 (C453S). Expression of SHP-1^{WT}, but not SHP-1^{C453S}, decreased Fyn-induced tyrosine phosphorylation of CD33. Furthermore, SHP-1^{WT}, but not SHP-1^{C453S}, decreased Fyn-enhanced ubiquitylation of CD33, both in the presence and absence of Cbl family proteins (all data not shown).

Identification of lysine residues critical for CD33 ubiquitylation

The cytoplasmic tail of CD33 contains a total of 7 lysine residues, two of which (at positions 283 and 288) are located very close to the transmembrane domain, 4 of which are clustered (at positions 309, 312, 313, and 315), and one of which is found between the ITIM and the ITIM-like motif (at position 352). In a next series of experiments, we used several lysine-to-arginine mutants of CD33 to explore which lysine residues are target for ubiquitylation (Table III.1). As indicated by the results obtained in HEK293T and COS-7 transfected with the K4R and K5R mutants depicted in Fig III.6, ubiquitylation was promiscuous and mostly involved the C-terminal 5 lysine residues, whereas the first two lysine residues contributed very little, if at all, to the maximal amount of ubiquitylated CD33. While mutation of the lysine residues abrogated the ability of CD33 to become ubiquitylated, it did not interfere with the ability of CD33 to become phosphorylated. In fact, the K7R mutant could be phosphorylated to the same degree as $CD33^{WT}$ by co-expression of Fyn or treatment with pervanadate, whereas phosphorylation was reduced with $CD33^{Y358F}$ and was abrogated with $CD33^{Y340F}$ or $CD^{Y340F/Y358F}$ (Fig III.7), consistent with findings presented in chapter II.

Ubiquitylation is central for internalization of antibody-bound CD33 in HEK293T cells

To assess the functional consequences of the inability of CD33 to become ubiquitylated, we expressed wild-type and several lysine-to-arginine mutants of CD33 in HEK293T cells, and studied internalization of antibody-bound CD33 by confocal microscopy. As shown in Fig III.8, internalization of $CD33^{WT}$ was readily detectable after 2 hours. Internalization was detected to the same degree in cells expressing the K2R mutant. By comparison, very little to absent internalization was found in cells expressing either the K5R or K7R mutant of CD33. To further ascertain that this effect was due to the lacking ability of CD33 to become ubiquitinated, we generated CD33 rescue constructs with a single ubiquitin fused in-frame to the C-terminus of either wild-type CD33 or the K7R mutant of CD33. As shown in Fig III.8 (left panel), cell surface display of these ubiquitin fusion proteins was reduced compared to cells expressing corresponding CD33 constructs without fused ubiquitin. Furthermore, anti-CD33 antibody was internalized not only in cells expressing $CD33^{WT}$, but also in cells expressing the K7R mutant of CD33 when fused to ubiquitin (Fig III.8, right panel).

Effect of lysine-to-arginine mutants of CD33 on cell surface abundance of CD33 and internalization of ligated CD33 in transduced myeloid and lymphoid cells

Since CD33 is physiologically expressed mainly on maturing myeloid cells, and possibly subsets of B and activated T and natural killer (NK) cells,[15-22] we also studied the effect of lysine-to-arginine mutants of CD33 in the mouse myeloid 32D cell line, using lentivirus-mediated gene transfer. This $CD33^-$ cell line was chosen because all human AML cell lines tested expressed endogenous CD33 to some degree, potentially interfering with transduced mutant CD33. As shown in Fig III.9 (Panel A), cell surface display of CD33 was higher on cells expressing either the K5R or K7R mutant of CD33 than on cells expressing $CD33^{WT}$ when cells were transduced with the same MOI; even higher MOIs (up to MOI of 25) with $CD33^{WT}$ did not generate cell lines with comparable surface display of CD33.

By comparison, cell surface display of CD33 on cells expressing fusion proteins between ubiquitin and either wild-type or mutant (K5R and K7R, respectively) CD33 was lower compared to cells expressing $CD33^{WT}$ only; the amount of cell surface CD33 was relatively similar in all sublines expressing CD33/ubiquitin fusion proteins, independent of whether wild-type of mutant CD33 was fused to ubiquitin (Fig III.9; Panel A). To quantify internalization of antibody-bound CD33 in transduced 32D sublines, we employed a flow cytometry-based assay.[92] As shown in Fig III.9 (Panel B), the rate of CD33 internalization was slightly, but statistically significantly diminished in cells expressing either the K5R or the K7R mutant of CD33 compared to cells expressing $CD33^{WT}$. We also tested the internalization of anti-CD33 antibody in 32D cells expressing CD33-ubiquitin fusion proteins. In this cell line with relatively rapid rate of internalization of antibody-bound CD33, in-frame fusion of ubiquitin did not result in enhancement of antibody uptake, as shown in Fig III.9 (Panel C).

Finally, we studied wild-type and mutant CD33 constructs in infected Jurkat cells, a human T cell line. These cells have previously been shown to internalize ligated CD33 very slowly (see chapter II). Similar to the findings obtained in 32D cells, cell surface display of CD33 was higher on cells expressing either the K5R or K7R mutant of CD33 than on cells expressing $CD33^{WT}$, while in-frame fusion of ubiquitin resulted in lower cell surface levels of both wild-type and mutant CD33 (Fig III.10; Panel A). Consistent with previous studies (see chapter II), transduced Jurkat cells only minimally internalized CD33 during the first 4 hours following CD33 ligation (Fig III.10; Panel B). By comparison, in-frame fusion of ubiquitin to either wild-type or mutant CD33 resulted in internalization of antibody-bound CD33 at a greatly increased rate compared to CD33 without ubiquitin fused to its C-terminus (Fig III.10; Panel C).

III.4. Discussion

The data presented in this chapter support three main conclusions. First, anti-CD33 antibodies are trafficked to lysosomes, implicating the vesicular transport to the lysosome as pathway used for degradation of CD33. Second, CD33 is target for tyrosine phosphorylation-dependent and ITIM-dependent monoubiquitylation, suggesting that ubiquitylation and signaling of CD33 are intertwined. And third, ubiquitylation of CD33 has cell type specific effects that include regulation of the rate of CD33 internalization after ligation by anti-CD33 antibodies and regulation of cell surface CD33 abundance. Together, these findings are the first to demonstrate monoubiquitylation of an ITIM-bearing immunoreceptor, and suggest the importance of this post-translational modification for the function of CD33, and, by extrapolation, possibly similar ITIM-containing cell surface receptors.

It has long been recognized that binding of bi- and multivalent anti-CD33 antibodies results in CD33 internalization in both $CD33^+$ hematopoietic cell lines and primary AML blast cells.[61-64] Subsequent studies, using radio-labeled anti-CD33 antibodies, have indicated that the CD33 cargo is trafficked to the lysosomal compartment.[127] In fact, the endocytic property of CD33 when ligated with antibody, and intracellular trafficking of anti-CD33 antibodies, has led to the development and clinical use of gemtuzumab ozogamicin (GO), an immunoconjugate consisting of a humanized IgG_4 anti-CD33 monoclonal antibody (hP67.6) joined to a derivative of the cytotoxic drug calicheamicin-γ_1, N-acetyl-γ-calicheamicin dimethyl hydrazide, via a pH labile linker.[73-75,77] It is thought that hP67.6 primarily facilitates uptake of the toxic moiety, which is then intracellularly cleaved in a compartment with low pH, and the released calicheamicin-γ_1 subsequently induces DNA damage.[77,78] Consistent with this notion, our present confocal microscopy studies demonstrate co-localization between directly labeled anti-CD33 antibodies and Lysotracker, providing further

evidence that CD33 ligated with antibody is trafficked to the lysosome. While we have shown in chapter I that the ITIMs of CD33 control the initial internalization process,[92] the mechanistic principles involved in intracellular trafficking have not been elucidated so far.

Research performed over the last 25 years has provided unequivocal evidence for the importance of certain endosomes, in particular a subset of late endosomes with multivesicular appearance termed multivesicular bodies (MVB) or multivesicular endosomes (MVE), for the vesicular transport between the *trans*-Golgi network, plasma membrane, and lysosomes.[130,131] Results emerging from recent studies have advanced our understanding of molecular mechanisms involved in this pathway that is essential for a multitude of cellular processes, including downregulation and degradation of many activated cell surface receptors and plasma membrane proteins, and have revealed a pivotal role of monoubiquitylation as a sorting signal within the MVB route.[130,131] However, even though the importance of monoubiquitylation in this transport pathway is firmly established, its exact role remains to be defined, and the available data suggest that ubiquitin might have several distinct roles. For example, monoubiquitylation has been shown to facilitate both endocytosis and post-internalization sorting into MVBs of some cell surface proteins, whereas for others, the main function of ubiquitin appears to be in MVB sorting. In some cases, such as the growth hormone receptor (GHR), the correct functioning of the cellular ubiquitin ligase machinery is required, whereas ubiquitylation of the receptor itself is dispensable.[130,131] Finally, whereas studies in mammalian cells have indicated that ubiquitin has a role in response to ligand binding, studies with the yeast a-factor receptor Ste3p have demonstrated that ubiquitin is required for constitutive ligand-independent uptake and vacuolar degradation but not for ligand-dependent internalization and recycling.[132] Thus, downregulation of cell surface proteins may be affected by ubiquitin in a ligand-dependent or independent manner at the level of receptor internalization and/or postinternalization sorting

and lysosomal degradation, highly dependent on the protein that is targeted.[130,131]

Using HEK293T and COS-7 cells transfected with epitope-tagged CD33 and ubiquitin, we now find that CD33 is a target for monoubiquitylation. With this approach, ubiquitylation of CD33 was readily observed in the absence of exogenously added ubiquitin ligases in both cell types, indicating that these cells endogenously express an E3 ligase capable of ubiquitylating CD33. Our experiments with PNGase F, in which we observed one marked and one additional faint ubiquitin band that had appropriate size shifts relative to deglycosylated CD33, indicate that ubiquitin on CD33 is mostly present in its monoform, but may be present as more than one molecule of ubiquitin per CD33 molecule in a minor fraction, either as multi-monoubiquitin or short ubiquitin chain, consistent with the notion that cell surface proteins are often monoubiquitylated rather than polyubiquitylated.[119] However, even in these co-transfection experiments, the majority of CD33 was found to be free of ubiquitin, suggesting that either CD33 becomes very short lived once ubiquitin is attached, or that the ubiquitylation reaction of CD33 is not very efficient under our *in vitro* conditions.

Monoubiquitylation has previously been implicated in the biology of activating immunoreceptors, such as the ITAM-containing ζ chain of the T cell receptor and FcγRIIA receptor,[121,122] To the best of our knowledge, however, this is the first report demonstrating ubiquitylation of an inhibitory immunoreceptor. Importantly, experiments with mutant CD33 constructs provide clear evidence that the tyrosine motifs of CD33, in particular the proximal ITIM but to a lesser degree also the distal ITIM-like motif, direct its monoubiquitylation. Furthermore, ubiquitylation is enhanced by Src family kinase activity and decreased by SHP-1 activity, indicating that tyrosine phosphorylation of the ITIMs favor the ubiquitylation reaction. Thus, our data indicate that CD33 signaling and

ubiquitylation might be intertwined: signaling through inhibitory immunoreceptors is thought to occur through Src family kinase-mediated tyrosine phosphorylation of ITIMs, which offers docking sites for the recruitment and activation of SH2 domain-containing proteins such as SHP-1 and SHP-2;[118] at the same time, tyrosine phosphorylation allows for ubiquitylation to occur, presumably by offering a docking site for an E3 ligase. As a member of the sialic acid-binding immunoglobulin-like lectins (Siglecs), CD33 recognizes sialic acid-containing molecules; however, physiological ligands of CD33 are unknown, and it has been speculated that CD33 might be engaged in sialic acid-dependent *cis*-interactions with sialylated counterparts.[30,31] Nevertheless, it is interesting to speculate that ligand binding may induce ubiquitylation of CD33. More importantly, since many inhibitory immunoreceptors contain ITIMs with very similar amino acid sequences, it could further be speculated that ubiquitylation may not be limited to CD33 but may in fact be a more general property of ITIM-bearing molecules. This may be particularly true in the case of other members of the CD33-related subgroup of Siglecs, which currently comprises 8 human proteins that are highly related to CD33 and to each other and are differentially expressed on cells of the innate immune system.[30,31]

The important role of ubiquitin in regulation of activating immunoreceptor signaling, e.g. by targeting activating non-receptor tyrosine kinases for proteosomal degradation through polyubiquitylation or by downmodulation of ITAM containing proteins through monoubiquitylation, is now firmly established; ubiquitin may thus serve as a means to switch off and limit cellular activation through such receptors.[119-122] The data from the present study indicate that ubiquitin might have a more complex role in the regulation of immunoreceptor signaling, not just by limiting activating signals but also by limiting inhibitory immunoreceptor signaling. Experiments in both HEK293T cells as well as myeloid cells suggest a role of ubiquitylation for regulation of cell surface display and/or internalization of CD33. It is currently unclear why the effect of lysine-to-

arginine mutations on CD33, i.e. rendering CD33 unable to become ubiquitylated, differs between different cell types. In HEK293T cells, such CD33 mutants fail to internalize after ligation with anti-CD33 antibody to a degree that is measurable by confocal microscopy. However, internalization can be restored after in-frame fusion of ubiquitin, providing evidence of an important role of ubiquitylation in internalization of (ligated) CD33. By comparison, internalization of CD33 constructs with identical mutations was only slightly, albeit statistically significantly, reduced in murine myeloid cells. The reason for this difference needs further investigation. However, elucidation of the role of ubiquitin in other receptor systems has demonstrated that, although monoubiquitylation serves as an internalization signal, redundant internalization pathways that are independent of ubiquitin may exist in parallel,[72] which may mask a more pronounced effect of lysine-to-arginine mutation on internalization of antibody-bound CD33 in myeloid cells. Nevertheless, cell surface abundance of such CD33 mutants is significantly increased in resting myeloid cells compared to cells expressing wild-type CD33, providing evidence for a role of ubiquitin in the regulation of CD33 abundance in the absence of CD33 ligation. One has to bear in mind that, in the absence of identified CD33 ligand(s), it is unclear whether or not CD33 is activated in resting cells. Thus, it is unclear whether ubiquitylation of CD33 is constitutive or a result of physiological receptor activation. Our experiments demonstrating increased ubiquitylation upon tyrosine phosphorylation of the ITIMs would favor a model where activation of CD33 increases its ubiquitylation. In the absence of identified bona fide ligands of CD33 and a better understanding of the signaling properties of CD33, experiments with CD33 constructs bearing mutations in the extracellular domains that mediate sialic acid binding may be necessary to investigate whether ubiquitylation of CD33 is a constitutive process or requires receptor activation. The exact reason for the lower cell surface abundance of CD33-ubiquitin fusion proteins relative to CD33 alone remains to be elucidated. Although it is conceivable to assume that ubiquitylation might result in a higher constitutive internalization from the cell surface which results in a lower steady-

state abundance at the cell surface, it is alternatively possible that a fraction of the ubiquitin fusion proteins is directly trafficked from the trans Golgi network to the lysosome and never reaches the cell surface.

A similar effect on cell surface abundance was found when wild-type and lysine-to-arginine mutant CD33 was expressed in the human Jurkat T-cell line. Experiments in this cell line are illustrative for two reasons: first, internalization of antibody-bound wild-type CD33 in Jukat cells proceeds at a much slower rate compared to the murine myeloid 32D cells, demonstrating significant differences in the uptake process of ligated CD33 between different cell lines. This confirms earlier observations (chapter I and ref[92]) and suggests that the internalization machinery involved in uptake of ligated CD33 might differ from cell type to cell type. Second, in-frame fusion of ubiquitin to wild-type or mutant CD33 results in greatly enhanced uptake of ligated CD33 in Jurkat cells, indicating that the ubiquitin moiety itself is a powerful internalization signal even in cells that otherwise show a slow uptake of ligated CD33. Thus, it appears as if ligation by anti-CD33 antibody does not result in a high degree of CD33 ubiquitylation, at least in Jurkat cells. The molecular mechanism underlying the ubiquitin-induced increased internalization remains to be investigated in more detail. Of particular note, the current studies have not addressed the possibility of receptor recycling from an early endocytic compartment back to the cell surface, and whether ubiquitin could be interfering with a recycling process. While for another Siglec, CD22, previous studies have indicated that recycling of the receptor does not occur to a detectable degree,[66] it is unknown whether CD33 undergoes recycling either under constitutive conditions or when ligated.

The endogenous E3 ligase involved in the ubiquitylation of CD33 and possibly other ITIM-bearing proteins remains to be determined. For the ITAM-dependent ubiquitylation of the ζ chain of the T cell receptor, previous studies have convincingly demonstrated a role of the E3 ligase activity of Cbl family

proteins.[121] Likewise, our co-transfection experiments indicate that Cbl family proteins are able to mediate ubiquitylation of CD33 in both HEK293T and COS-7 cells in an ITIM-dependent manner and may thus function as E3 ligase in this process. Furthermore, CD33 interacts with both Cbl and Cbl-b in an ITIM-dependent manner, as evidenced by GST-fusion protein pull-down assays. These results are consistent with a previous report demonstrating that cross-linking of CD33 induced tyrosine phosphorylation of the protooncogenes Cbl in monocytes of blood normal donors, and that Cbl could be co-immunoprecipitated with phosphorylated CD33 upon treatment with pervanadate.[49] Nevertheless, it is unclear whether the interaction between CD33 and Cbl family proteins is direct or requires additional proteins. In fact, the recognition sequences in proteins such as receptor tyrosine kinases by the TKB domain of Cbl has been extensively studied, and the consensus sequence [NXpY(S/T)XXP] was proposed.[133] The amino acid sequence around both Y340, which seems to mediate a stronger binding to Cbl and Cbl-b than Y358, as well as Y358 are quite distinct from this proposed consensus sequence ([LHYASL] and [TEYSEVR], respectively). However, the TKB-domain binding sequence of the Met receptor, which is known to directly interact with Cbl proteins, has no similarity to this consensus sequence.[133] Likewise, the TKB-domain binding sequence of APS (adaptor molecule containing pleckstrin homology and Src homology 2 domains) is quite diverse, findings suggesting that the TKB has unusual binding versatility.[133] A possible role of Cbl family proteins in the regulation of cell surface abundance of CD33 and upake of ligated CD33 is currently under investigation.

In summary, the data presented in this chapter indicate an important role of ubiquitylation for the function of CD33. The dependency of ubiquitylation on the integrity of well conserved amino acid sequences (ITIM) and Src family kinase activity not only suggest that signaling and ubiquitylation of CD33 are intertwined, but also that ubiquitylation might be a more general post-translational modification of ITIM-bearing receptors. Thus, ubiquitin appears to have a

complex dual role in regulating immunoreceptor signaling by interfering with both activating and inhibitory receptors.

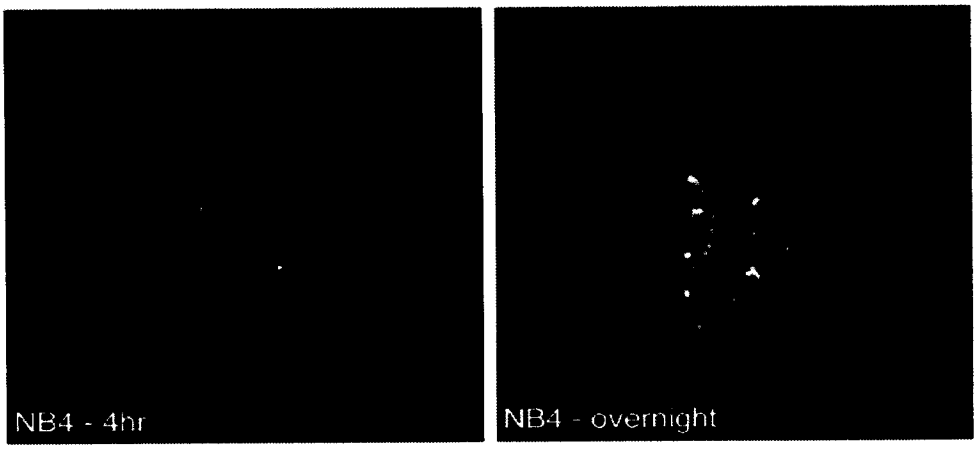

Figure III.1. Co-localization of anti-CD33 antibody with a lysosomal marker. NB4 cells were incubated for 4 hours or overnight with anti-CD33 antibody (hP67.6) that was directly labeled with Alexa Fluor 488. Cells were then incubated with LysoTracker Red DND-99 (red fluorescence) to mark lysosomes and DAPI (blue fluorescence) to mark nuclei, and examined on a Deltavision SA3.1 wide-field deconvolution microscope system. A significant portion of internalized hP67.6 co-localizes with LysoTracker Red DND-99, indicating that the intracellular trafficking of the antibody-CD33 complex ends in the lysosomal compartment. Shown is one representative experiment; similar findings were obtained with HL-60 cells.

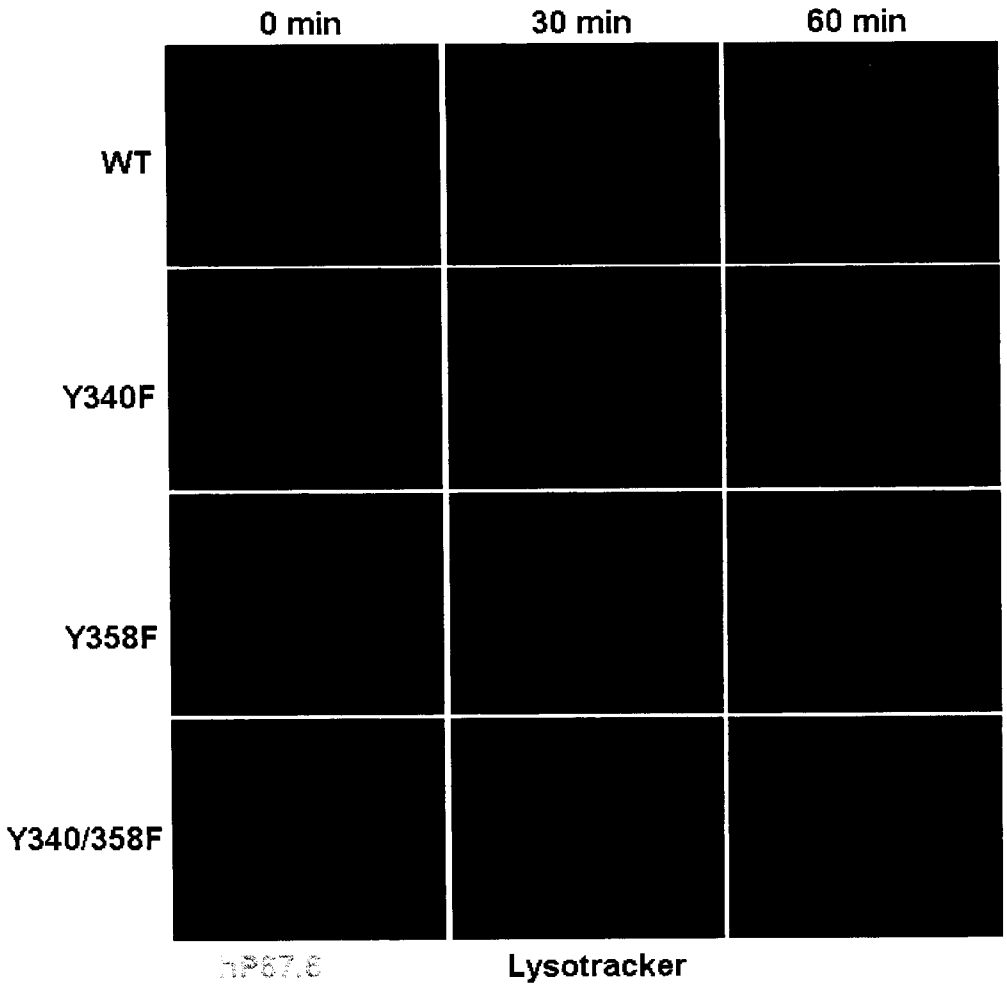

Figure III.2. Confocal microscopy study of ITIM-dependent internalization of antibody-bound CD33 in transfected HEK293T cells. HEK293T cells transfected with either wild-type or mutant CD33 were incubated with Alexa Fluor 488-labeled hP67.6 (green fluorescence) on ice-water before the cells were transferred to antibody-free medium and either kept in ice-water (left panel) or incubated in 37° C to allow internalization of antibody-bound CD33 for 30 or 60 minutes (middle and right panel, respectively). Cells were then fixed, stained with DAPI (blue fluorescence) to mark nuclei and LysoTracker Red DND-99 (red fluorescence) to mark lysosomes, and visualized by confocal microscopy. Shown is one representative experiment. Disruption of the ITIMs, mainly the proximal ITIM, by introduction of point mutations significantly reduces internalization of anti-CD33 antibody in HEK293T cells, indicating a central role of these motifs in CD33 internalization; these findings are similar to those obtained with myeloid cell lines transduced with wild-type or mutant CD33 (see chapter I and ref[92]).

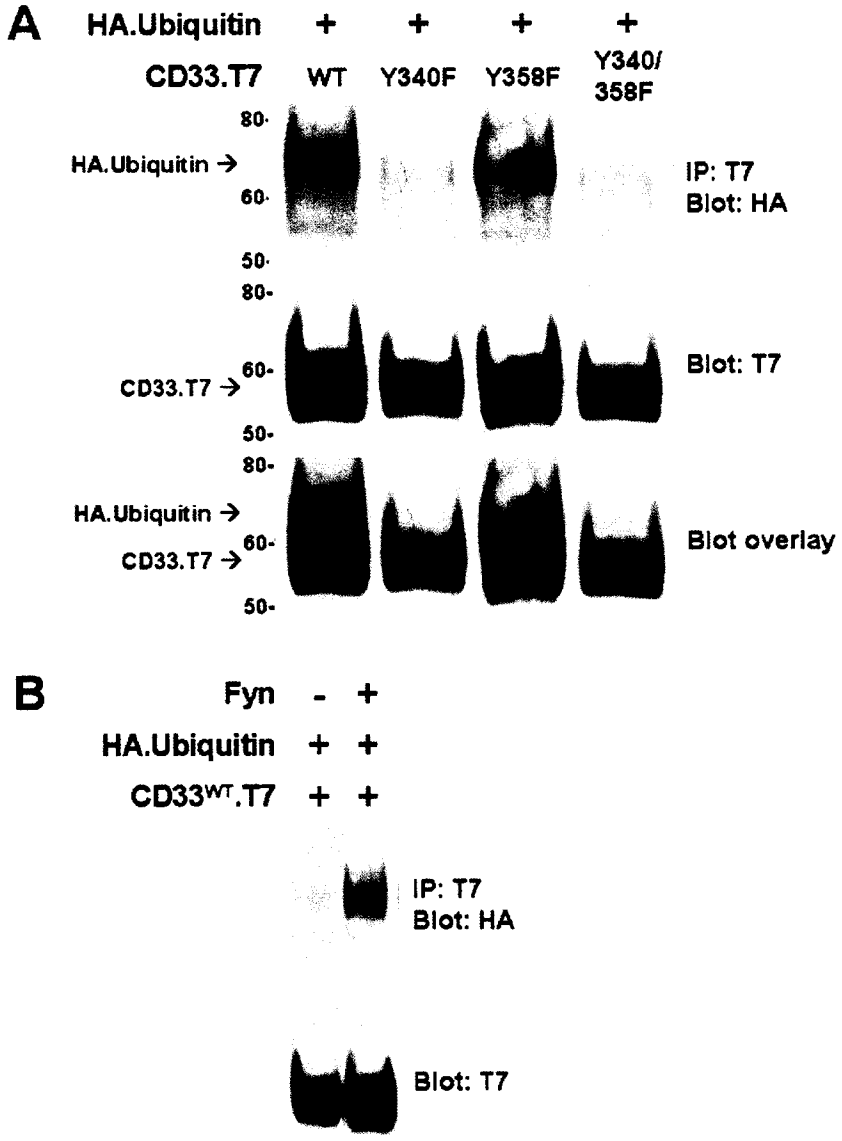

Figure III.3. CD33 is a target for ITIM- and Src-family kinase-dependent monoubiquitylation. (A) HEK293T cells were co-transfected with T7-tagged wild-type or mutant CD33 as well as HA-tagged ubiquitin as indicated. Cell lysates were immunoprecipitated with anti-T7 antibody. Blots were then probed for HA to visualize ubiquitin (upper panel), stripped, and reprobed for T7 to visualize CD33 (middle panel). Molecular weight markers were used to overlay blots (bottom panel). Presented is one representative experiment obtained with HEK293T cells; experiments with COS-7 cells showed similar findings. (B) HEK293T cells were co-transfected with T7-tagged wild-type CD33, HA-tagged ubiquitin, and wild-type Fyn as indicated. Cell lysates were immunoprecipitated with anti-T7 antibody. Blots were then probed for HA to visualize ubiquitin (upper panel), stripped, and reprobed for T7 to visualize CD33 (bottom panel). Presented is one representative experiment.

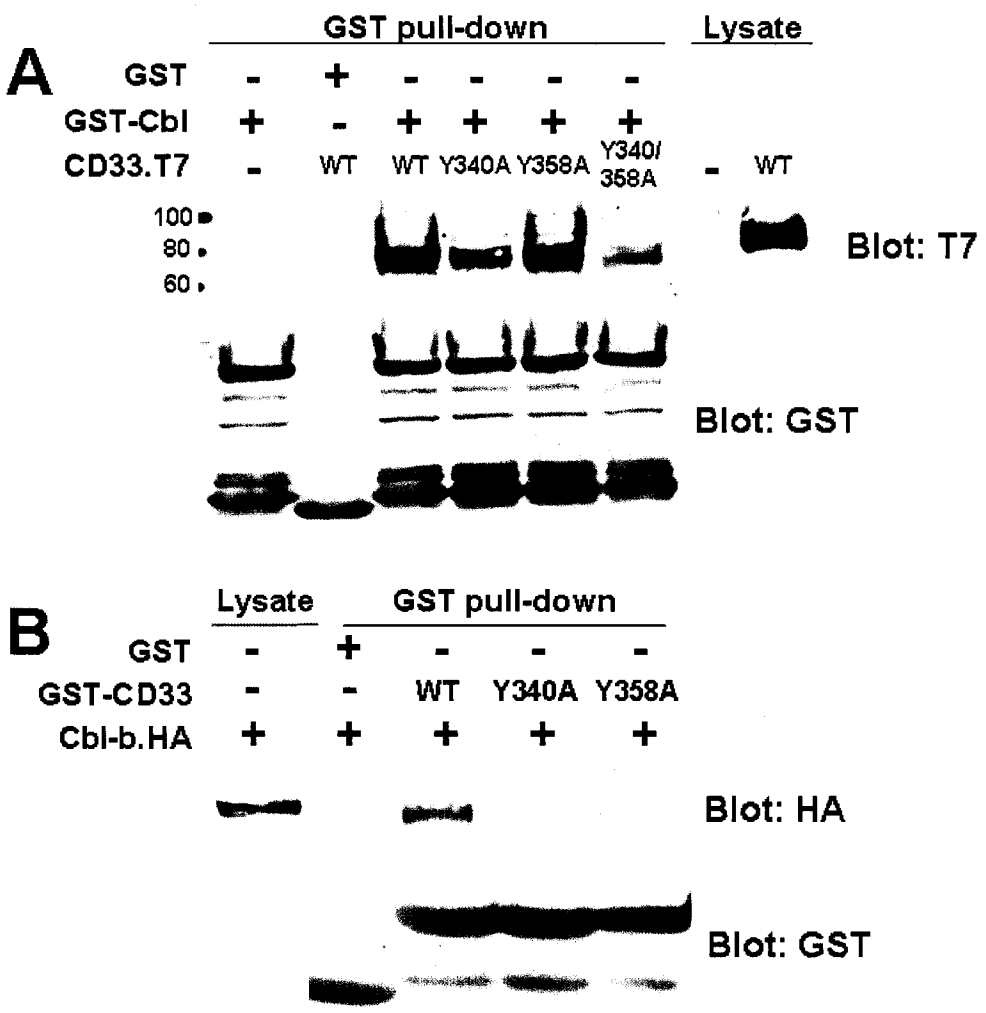

Figure III.4. Interaction of CD33 with Cbl family proteins. (A) Pull-down experiments were performed with either GST alone or GST fused to the TKB-domain of Cbl, using COS-7 cells transfected with empty vector or T7-tagged CD33 constructs as indicated. Blots were probed with anti-HA or anti-T7 antibody as appropriate, stripped, and reprobed with anti-GST antibody. (B) Reverse pull-down experiments were performed with either GST alone or GST fused to cytoplasmic tails of wild-type and mutant CD33, using pervanadate-treated cell lysates of COS-7 cells transfected with Cbl-b. Presented is one representative experiment each; similar results were obtained with GST fused to the TKB-domain of Cbl-b (for Panel B).

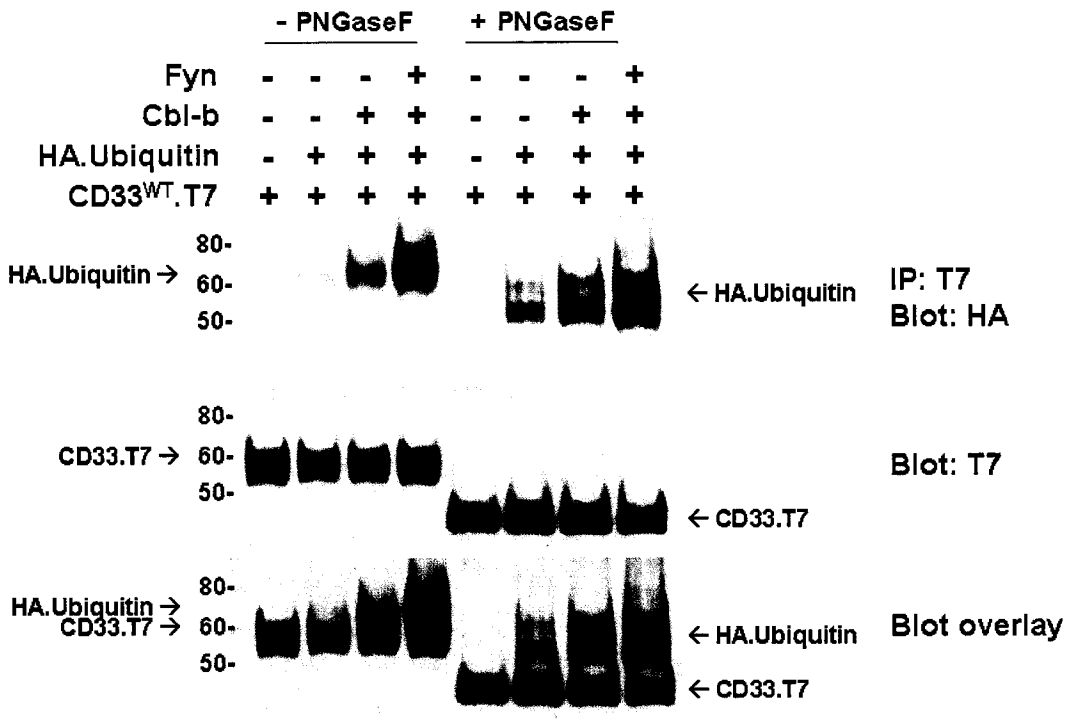

Figure III.5. Enhancement of CD33 ubiquitylation by overexpression of Cbl family proteins and Src family kinase activity. HEK293T cells were co-transfected with T7-tagged $CD33^{WT}$, HA-tagged ubiquitin, Cbl-b, as well as Fyn as indicated. Cell lysates were immunoprecipitated with anti-T7 antibody. Parallel samples were then either treated with PNGase F to remove saccharide side chains, or left untreated. Blots were probed for HA to visualize ubiquitin, stripped, and reprobed for T7 to visualize CD33. Presented is one representative experiment obtained with HEK293T cells; experiments with COS-7 cells showed similar findings.

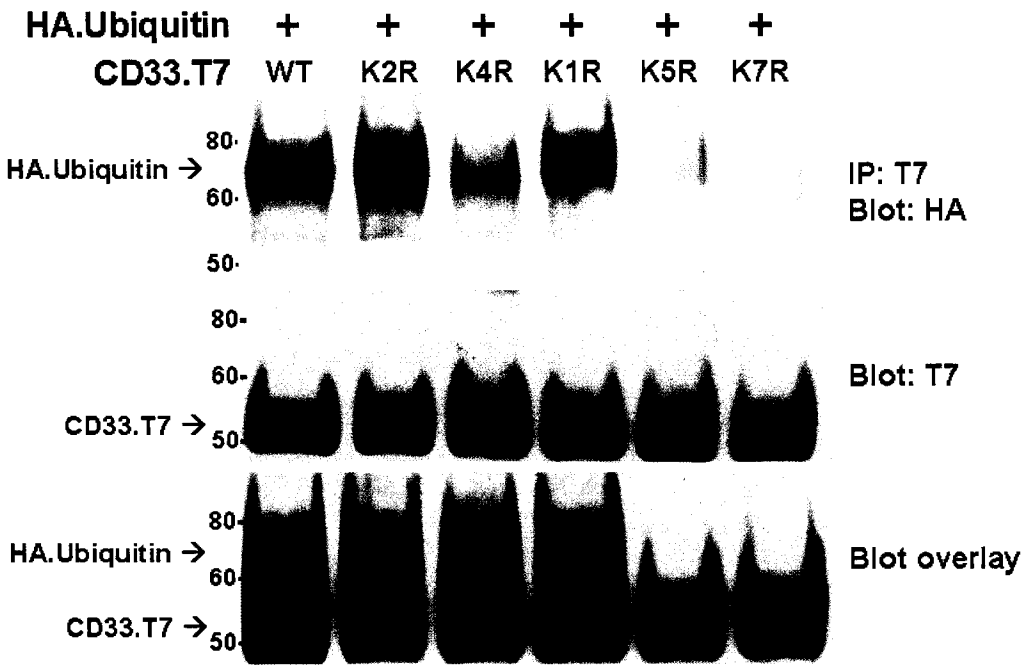

Figure III.6. CD33 is ubiquitinated between lysine residues 309 and 352. HEK293T cells were co-transfected with T7-tagged wild-type or mutant CD33, HA-tagged ubiquitin, Cbl-b, as well as Fyn as indicated. Cell lysates were immunoprecipitated with anti-T7 antibody. Blots were then probed for HA to visualize ubiquitin, stripped, and reprobed for T7 to visualize CD33. Presented is one representative experiment obtained with HEK293T cells; experiments with COS-7 cells showed similar findings.

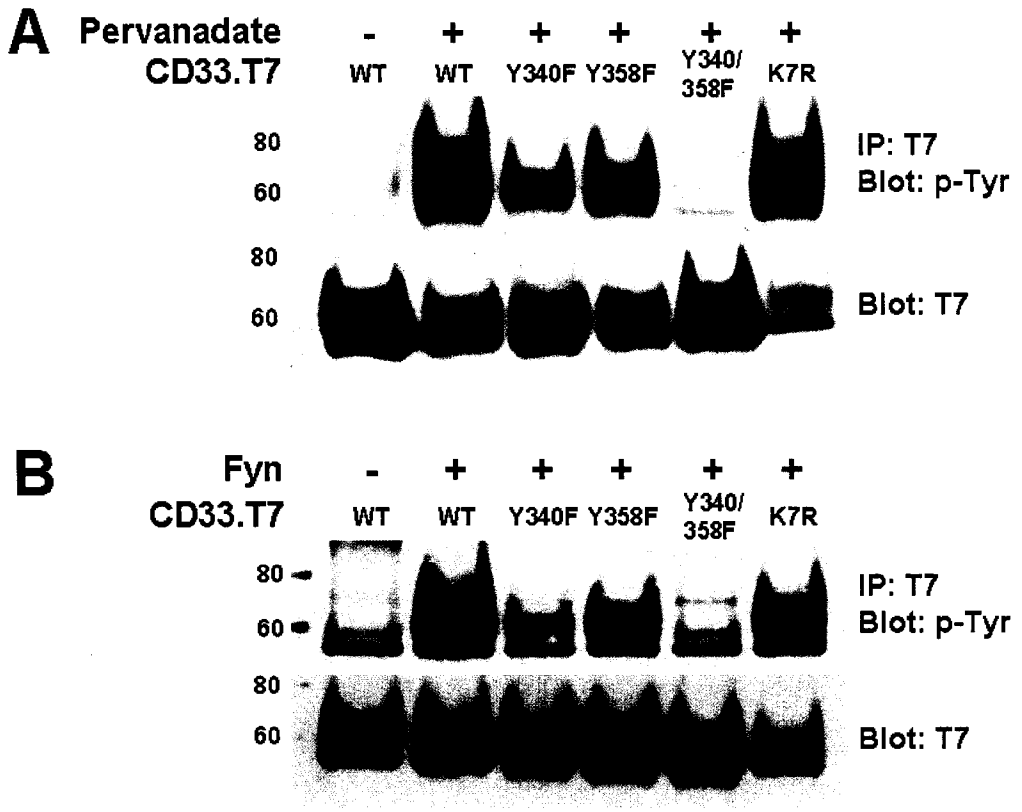

Figure III.7. Phosphorylation of wild-type and mutant CD33 by pervanadate and Fyn. (A) COS-7 cells were transfected with T7-tagged wild-type or mutant CD33 as indicated, and stimulated with pervanadate for 15 min at 37° C prior to lysis. (B) COS-7 cells were co-transfected with Fyn and either T7-tagged wild-type or mutant CD33 as indicated. Cell lysates were immunoprecipitated with anti-T7 antibody. Blots were then probed with 4G10 to assess tyrosine phosphorylation (upper panel), stripped, and reprobed for T7 to visualize CD33 (lower panel). Presented is one representative experiment each; similar findings were obtained with transfected HEK293T cells.

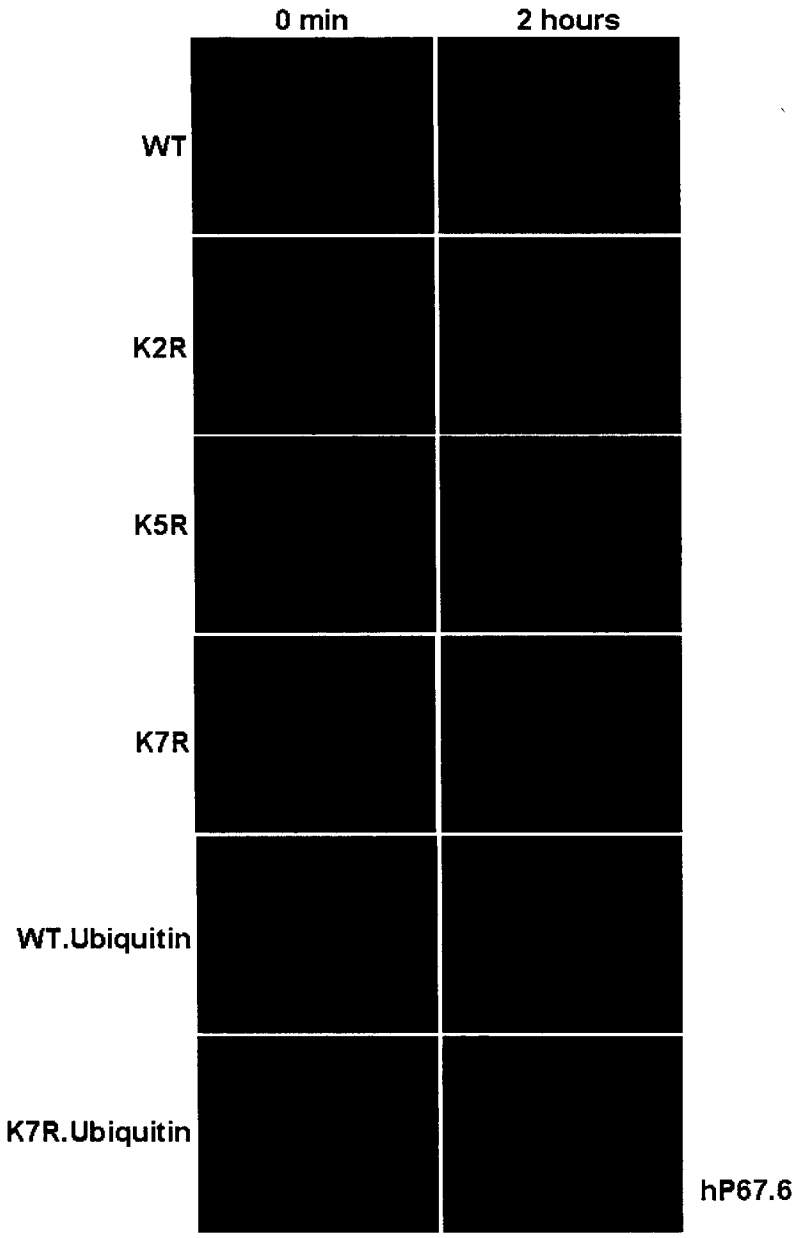

Figure III.8. Confocal microscopy study of effects of lysine-to-arginine mutants of CD33 and CD33-ubiquitin fusion proteins on internalization of anti-CD33 antibody in HEK293T cells. HEK293T cells were transfected with either wild-type CD33, lysine-to-arginine mutants of CD33, or fusion proteins between human ubiquitin and wild-type or mutant CD33 as indicated, and incubated with Alexa Fluor 594-labeled hP67.6 on ice-water before the cells were transferred to antibody-free medium and either kept in ice-water (left panel) or incubated in 37° C (right panel) to allow antibody internalization for 2 hours. Cells were then fixed, stained with DAPI, and visualized by confocal microscopy.

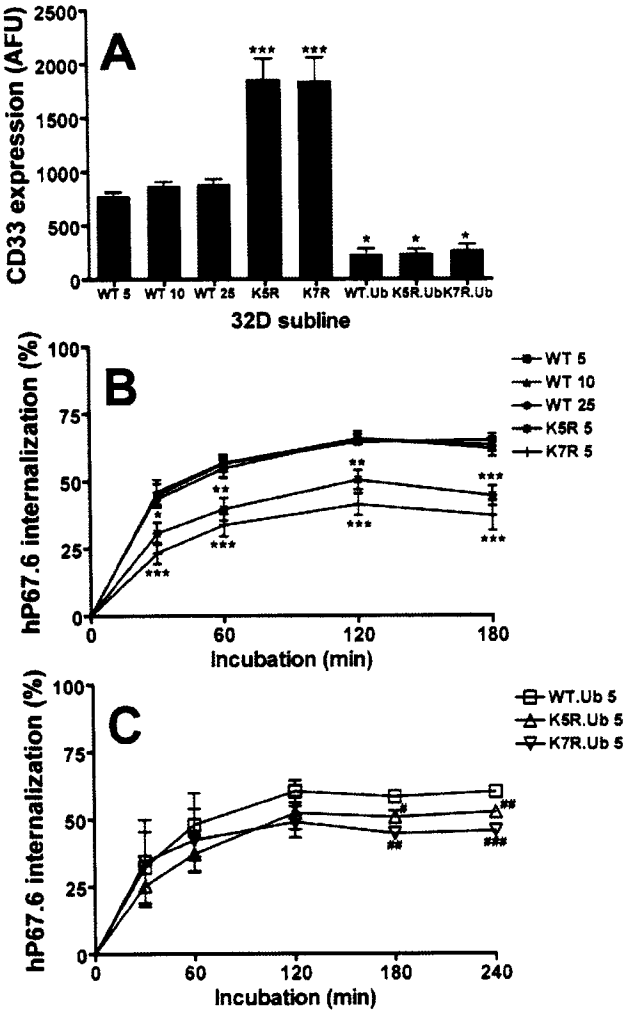

Figure III.9. Effects of lysine-to-arginine mutants of CD33 and CD33-ubiquitin fusion proteins in murine AML 32D cells. 32D cell sublines were infected with $CD33^{WT}$ at an MOI of 5-25, as well as the K5R or K7R mutants of CD33 at a MOI of 5. Additional sublines were transduced with fusion proteins between human ubiquitin and either wild-type CD33 or the K5R or K7R mutant of CD33 at a MOI of 5. (A) Cell surface CD33 display was determined using a 3-step assay with hP67.6, biotin-conjugated mouse anti-human IgG_4, and streptavidin-PE, and expressed as arbitrary fluorescence units (n=3). (B,C) Internalization of hP67.6 in sublines expressing wild-type or mutant CD33 (B; n=7), or sublines expressing wild-type or mutant CD33 fused to ubiquitin (C; n=3). Cells were labeled with unconjugated hP67.6 on ice-water before incubation at 37° C in antibody-free medium to allow internalization of antibody-bound CD33 up to 4 hours as indicated. Remaining cell surface associated hP67.6 was subsequently detected with biotin-conjugated mouse anti-human IgG_4 and streptavidin-PE. The percentage of internalized hP67.6 is expressed relative to cells kept at 0° C. Results are shown as mean±SEM. *p<0.05, **p<0.01, ***p<0.001 compared to wild-type CD33; $^{\#}$p<0.05, $^{\#\#}$p<0.01, $^{\#\#\#}$p<0.001 compared to wild-type CD33 fused to ubiquitin. AFU, arbitrary fluorescence units.

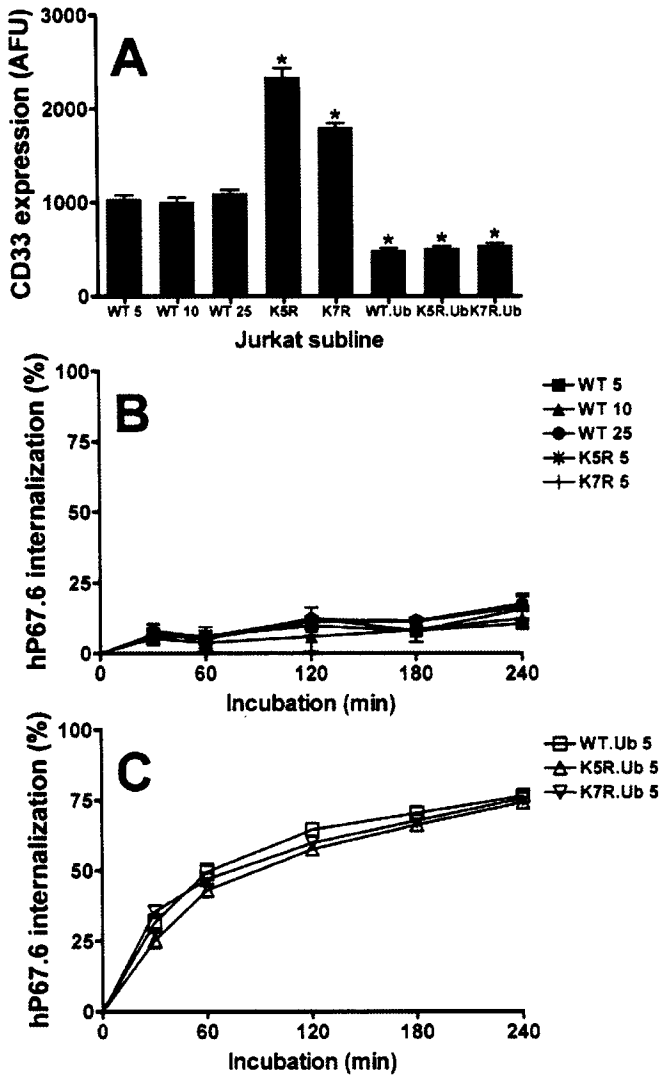

Figure III.10. Effects of lysine-to-arginine mutants of CD33 and CD33-ubiquitin fusion proteins in human Jurkat T cells. Jurkat cells were transduced with $CD33^{WT}$ at an MOI of 5-25, as well as the K5R or K7R mutants of CD33 at a MOI of 5. Additional sublines were transduced with fusion proteins between human ubiquitin and either wild-type CD33 or the K5R or K7R mutant of CD33 at a MOI of 5. (A) Cell surface CD33 display was determined using a 3-step assay with hP67.6, biotin-conjugated mouse anti-human IgG_4, and streptavidin-PE, and expressed as arbitrary fluorescence units. (B) Internalization of hP67.6 in sublines expressing wild-type or mutant CD33 (B), or sublines expressing wild-type or mutant CD33 fused to ubiquitin (C). Cells were labeled with unconjugated hP67.6 on ice-water before incubation at 37° C in antibody-free medium to allow internalization of antibody-bound CD33 up to 4 hours as indicated. Remaining cell surface associated hP67.6 was subsequently detected with biotin-conjugated mouse anti-human IgG_4 and streptavidin-PE. The percentage of internalized hP67.6 is expressed relative to cells kept at 0° C. Results are shown as mean±SEM from 3 independent experiments. *$p<0.001$ compared to wild-type CD33 (any MOI). AFU, arbitrary fluorescence units.

Table III.1. Schematic representation of lysine-to-arginine mutants of CD33. Single-letter amino acid code is used. Wild-type lysine residues are shown in bold. Lysine-to-arginine mutations are shown in bold and underlined. Tyrosine residues are shown in italic. Number in brackets denotes spacing between amino acids. Abbreviations of CD33 mutants: K2R, K283/288R; K4R, K309/312/313/315R; K1R, K352R; K5R, K309/312/313/315/352R; K7R, K283/288/309/312/313/315/352R

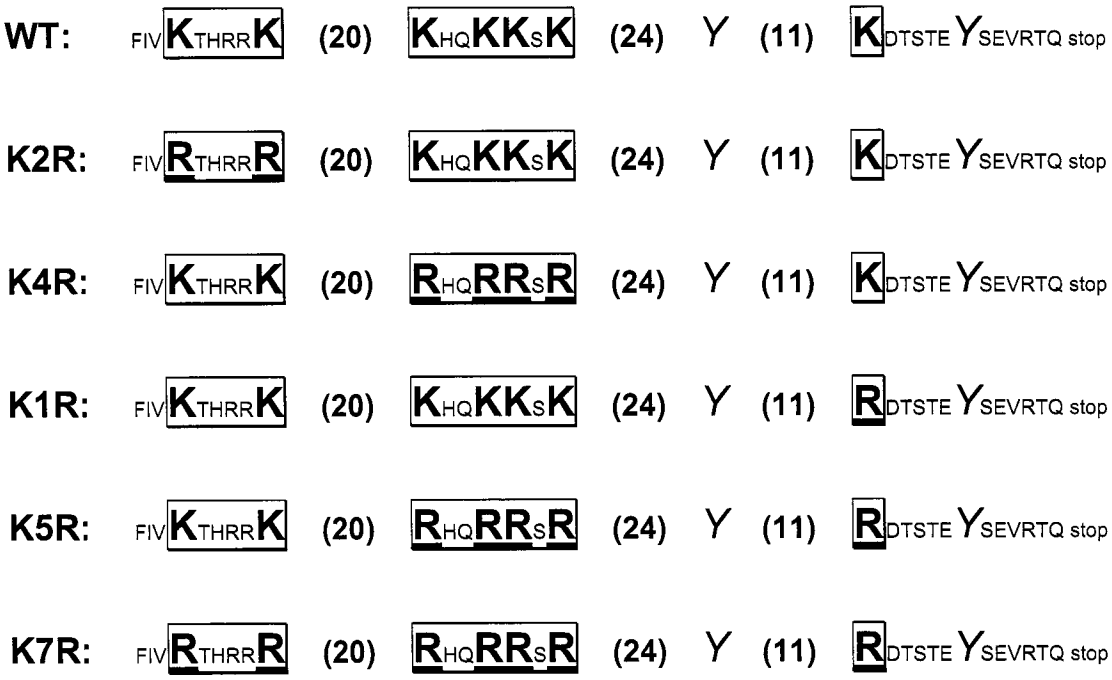

Concluding remarks

Intense research performed over the last decade has unraveled important properties of the Siglec family of proteins, both with regard to functional aspects as well as biomedical significance.[31,32] Nevertheless, the exact function of many Siglecs, and in particular the subgroup of CD33-related Siglecs, remains currently unknown, and eludication of the precise function of these proteins in the immune system will be a major focus of future research in this field.[31] Likewise, even though the presence of ITIM and ITIM-like motifs on the cytoplasmic tails of all CD33-related Siglecs implies overall inhibitory function, only very limited information is available on intracellular signaling pathways that are relevant after engagement of such receptors. Furthermore, mechanisms regulating cell surface abundance and internalization, key factors influencing the total amount of signal that is transmitted through these receptors, were hitherto completely unexplored. Elucidation of mechanisms underlying these processes will contribute to a better understanding of the biology of these elusive proteins; equally important, however, they might provide insight into how a clinically used immunoconjugate drug targeting CD33 works, and might lead to novel approaches to enhance its clinical efficacy. Research presented in this thesis has now shed some light on the mechanisms regulating cell surface expression and internalization of CD33. Specifically, this thesis describes the identification of 2 novel functions of the ITIMs of CD33, namely ITIM-dependent internalization and ITIM-dependent monoubiquitylation. These findings thus significantly expand our current understanding of the functionality of ITIM sequences contained in CD33. Clearly, as long as the physiological function of CD33 remains elusive, the exact biological significance of our findings remains uncertain. Nevertheless, it is tempting to speculate that these ITIM-dependent functions may be involved in the process of CD33 downregulation from the cell surface, either in the resting state and/or after ligand engagement, and therefore appear to have a role in the

balance of activating and inhibitory signals in the immune cell response. Once the physiological functions of CD33 become better defined, this hypothesis can be experimentally tested, and the effect of perturbations of this system studied. Importantly, however, our findings describing novel ITIM-dependent functions of CD33 may have implications that go beyond the biology of CD33. As discussed in the introduction in more detail, CD33 is founding member of the subgroup of CD33-related Siglecs.[31,32] This subgroup currently comprises 8 human Siglecs, which are highly related to each other. Of particular note in the context of our findings is the presence of conserved proximal ITIM and distal ITIM-like motifs on their cytoplasmic tails. It is thus conceivable to hypothesize that ITIM-dependent internalization and monoubiquitylation may be features that are shared among several other or all members of this Siglec subgroup. In support of this hypothesis, Biedermann et al. have very recently provided evidence that Siglec-9, another member of the CD33/Siglec-3-related subgroup of Siglecs that is found on normal monocytic precursors and a subset of acute myeloid leukemia cells, shows ITIM-dependent endocytic properties with kinetics that are very similar to those observed in our studies when targeted with anti-Siglec-9 antibodies.[59] Therefore, our findings obtained on CD33 may possibly be extrapolated to the entire class of CD33-related Siglecs. Somewhat more speculative, it is possible that ITIM-bearing receptors that belong to classes other than CD33-related Siglecs might be subject to similar regulatory mechanisms.

One important aspects of our studies was to elucidate mechanisms underlying the cytotoxic action of the anti-CD33 immunoconjugate, gemtuzumab ozogamicin (GO, Mylotarg™). We have identified three important principles that might spawn additional studies aiming to improve the cytotoxic response to GO, and, ultimately, clinical outcome of patients with acute myeloid leukemia undergoing treatment with a GO-containing or, more generally, anti-CD33 antibody-containing regimen. First, we provide direct experimental evidence that GO-induced cytotoxicity is directly correlated to the cell surface display of CD33,[92]

offering the rationale for manipulation of CD33 abundance as means to increase GO efficacy. Currently, the regulation of CD33 expression on either normal or malignant cells is not understood, but preliminary *in vitro* studies suggested that cytokines, some of which could be envisoned to be used in the clinical setting, might play a role.[91] Second, our studies demonstrate that tyrosine phosphorylation by Src family kinases increases uptake of anti-CD33 antibodies and that uptake of anti-CD33 antibodies correlates with GO-induced cytotoxicity. In line with the notion of the importance of CD33 tyrosine phosphorylation for antibody uptake, activity of the tyrosine phosphatases, SHP-1 and SHP-2, can decrease antibody uptake. Together, these findings suggests that manipulation of the phosphorylation state of the cell through activation of tyrosine kinases, e.g. by use of growth factors or cytokines, or interference with tyrosine phosphatases, might lead to increased drug uptake and cytotoxicity. And finally, our studies show that the antibody itself, in particular the Fc-part, has a significant influence on the cellular uptake, a finding that might be important for future generations of antibodies targeting CD33 or similar cell surface antigens.

REFERENCES

1. Jemal, A. et al. Cancer statistics, 2006. *CA Cancer J Clin* **56**, 106-30 (2006).

2. SEER Cancer Statistics Review, 1975-2002, National Cancer Institute. Bethesda, MD, http://seer.cancer.gov/csr/1975_2002/, based on November 2004 SEER data submission, posted to the SEER web site 2005. (eds Ries, L.A.G. et al.).

3. Liesveld, J.L. & Lichtman, M.A. Acute myelogenous leukemia. in *Williams Hematology* (eds. Lichtman, M.A. et al.) 1183-1236 (McGraw-Hill, New York, 2006).

4. Scheinberg, D.A., Maslak, P.G. & Weiss, M.A. Management of acute leukemias. in *Cancer: Principles & Practive of Oncology* (eds. DeVita Jr., V.T., Hellman, S. & Rosenberg, S.A.) 2088-2120 (Lippincott Williams & Wilkins, Philadelphia, 2005).

5. Löwenberg, B., Downing, J.R. & Burnett, A. Acute myeloid leukemia. *N Engl J Med* **341**, 1051-62 (1999).

6. Tallman, M.S., Gilliland, D.G. & Rowe, J.M. Drug therapy for acute myeloid leukemia. *Blood* **106**, 1154-63 (2005).

7. Dillman, R.O. The history and rationale for monoclonal antibodies in the treatment of hematologic malignancy. *Curr Pharm Biotechnol* **2**, 293-300 (2001).

8. Dillman, R.O. Monoclonal antibodies in the treatment of malignancy: basic concepts and recent developments. *Cancer Invest* **19**, 833-41 (2001).

9. Cheng, J.D., Adams, G.P., Robinson, M.K. & Weiner, L.M. Monoclonal antibodies. in *Cancer: Principles & Practice of Oncology* (eds. DeVita Jr., V.T., Hellman, S. & Rosenberg, S.A.) 445-456 (Lippincott Williams & Wilkins, Philadelphia, 2005).

10. Tanner, J.E. Designing antibodies for oncology. *Cancer Metastasis Rev* **24**, 585-98 (2005).

11. Polakis, P. Arming antibodies for cancer therapy. *Curr Opin Pharmacol* **5**, 382-7 (2005).

12. Andrews, R.G., Torok-Storb, B. & Bernstein, I.D. Myeloid-associated differentiation antigens on stem cells and their progeny identified by monoclonal antibodies. *Blood* **62**, 124-132 (1983).

13. Andrews, R.G. et al. The L4F3 antigen is expressed by unipotent and multipotent colony-forming cells but not by their precursors. *Blood* **68**, 1030-5 (1986).

14. Griffin, J.D., Linch, D., Sabbath, K., Larcom, P. & Schlossman, S.F. A monoclonal antibody reactive with normal and leukemic human myeloid progenitor cells. *Leuk Res* **8**, 521-534 (1984).

15. Handgretinger, R. et al. Expression of an early myelopoietic antigen (CD33) on a subset of human umbilical cord blood-derived natural killer cells. *Immunol Lett* **37**, 223-8 (1993).

16. Nakamura, Y. et al. Expression of CD33 antigen on normal human activated T lymphocytes. *Blood* **83**, 1442-3 (1994).

17. Schmidt-Wolf, I.G. et al. Propagation of large numbers of cells of a human mixed-lineage T-lymphoid/myeloid. *Br J Haematol* **90**, 512-7 (1995).

18. Márquez, C. et al. Identification of a common developmental pathway for thymic natural killer cells and dendritic cells. *Blood* **91**, 2760-71 (1998).

19. Dworzak, M.N., Fritsch, G., Froschl, G., Printz, D. & Gadner, H. Four-color flow cytometric investigation of terminal deoxynucleotidyl transferase-positive lymphoid precursors in pediatric bone marrow: CD79a expression precedes CD19 in early B-cell ontogeny. *Blood* **92**, 3203-9 (1998).

20. Tricarico, M. et al. In vitro infection of CD4+ T lymphocytes with HTLV-I generates immortalized cell lines coexpressing lymphoid and myeloid cell markers. *Leukemia* **13**, 222-9 (1999).

21. Eksioglu-Demiralp, E. et al. Phenotypic characteristics of B cells in Behcet's disease: increased activity in B cell subsets. *J Rheumatol* **26**, 826-32 (1999).

22. Hernández-Caselles, T. et al. A study of CD33 (SIGLEC-3) antigen expression and function on activated human T and NK cells: two isoforms of CD33 are generated by alternative splicing. *J Leukoc Biol* **79**, 46-58 (2006).

23. Dinndorf, P.A. et al. Expression of normal myeloid-associated antigens by acute leukemia cells. *Blood* **67**, 1048-1053 (1986).

24. Jennings, C.D. & Foon, K.A. Recent advances in flow cytometry: application to the diagnosis of hematologic malignancy. *Blood* **90**, 2863-2892 (1997).

25. Appelbaum, F.R. Antibody-targeted therapy for myeloid leukemia. *Semin Hematol* **36**, 2-8 (1999).

26. Ravandi, F., Kantarjian, H., Giles, F. & Cortes, J. New agents in acute myeloid leukemia and other myeloid disorders. *Cancer* **100**, 441-54 (2004).

27. Jilani, I. et al. Differences in CD33 intensity between various myeloid neoplasms. *Am J Clin Pathol* **118**, 560-6 (2002).

28. Simmons, D. & Seed, B. Isolation of a cDNA encoding CD33, a differentiation antigen of myeloid progenitor cells. *J Immunol* **141**, 2797-800 (1988).

29. Freeman, S.D., Kelm, S., Barber, E.K. & Crocker, P.R. Characterization of CD33 as a new member of the sialoadhesin family of cellular interaction molecules. *Blood* **85**, 2005-2012 (1995).

30. Crocker, P.R. Siglecs: sialic-acid-binding immunoglobulin-like lectins in cell-cell interactions and signalling. *Curr Opin Struct Biol* **12**, 609-15 (2002).

31. Crocker, P.R. Siglecs in innate immunity. *Curr Opin Pharmacol* **5**, 431-7 (2005).

32. Varki, A. & Angata, T. Siglecs--the major subfamily of I-type lectins. *Glycobiology* **16**, 1R-27R (2006).

33. Crocker, P.R. & Varki, A. Siglecs, sialic acids and innate immunity. *Trends Immunol* **22**, 337-42 (2001).

34. Angata, T., Margulies, E.H., Green, E.D. & Varki, A. Large-scale sequencing of the CD33-related Siglec gene cluster in five mammalian species reveals rapid evolution by multiple mechanisms. *Proc Natl Acad Sci U S A* **101**, 13251-6 (2004).

35. Initial sequence of the chimpanzee genome and comparison with the human genome. *Nature* **437**, 69-87 (2005).

36. Altheide, T.K. et al. Systemwide genomic and biochemical comparisons of sialic acid biology amongst primates and rodents - evidence for two modes of rapid evolution. *J Biol Chem* **281**, 25689-702 (2006).

37. Jones, C., Virji, M. & Crocker, P.R. Recognition of sialylated meningococcal lipopolysaccharide by siglecs expressed on myeloid cells leads to enhanced bacterial uptake. *Mol Microbiol* **49**, 1213-25 (2003).

38. Avril, T., Wagner, E.R., Willison, H.J. & Crocker, P.R. Sialic acid-binding immunoglobulin-like lectin 7 mediates selective recognition of sialylated glycans expressed on Campylobacter jejuni lipooligosaccharides. *Infect Immun* **74**, 4133-41 (2006).

39. Brinkman-Van der Linden, E.C.M. & Varki, A. New aspects of siglec binding specificities, including the significane of fucosylation and of the sialyl-Tn epitope. *J Biol Chem* **275**, 8625-8632 (2000).

40. Nakamura, M. et al. Total metabolic flow of glycosphingolipid biosynthesis is regulated by UDP-GlcNAc:lactosylceramide beta 1-->3N-acetylglucosaminyltransferase and CMP-NeuAc:lactosylceramide alpha 2->3 sialyltransferase in human hematopoietic cell line HL-60 during differentiation. *J Biol Chem* **267**, 23507-14 (1992).

41. Sasaki, K. et al. Expression cloning of a novel alpha 1,3-fucosyltransferase that is involved in biosynthesis of the sialyl Lewis x carbohydrate determinants in leukocytes. *J Biol Chem* **269**, 14730-7 (1994).

42. Sgroi, D., Nocks, A. & Stamenkovic, I. A single N-linkes glycosylation site is implicated in the regulation of ligand recognition by the I-type lectins CD22 and CD33. *J Biol Chem* **271**, 18803-18809 (1996).

43. Scharenberg, A.M. & Kinet, J.-P. The emerging field of receptor-mediated inhibitory signaling: SHP or SHIP? *Cell* **87**, 961-964 (1996).

44. Taylor, V.C. et al. The myeloid-specific sialic acid-binding receptor, CD33, associates with the protein-tyrosine phosphatases, SHP-1 and SHP-2. *J Biol Chem* **274**, 11505-11512 (1999).

45. Ulyanova, T., Blasioli, J., Woodford-Thomas, T.A. & Thomas, M.L. The sialoadhesin CD33 is a myeloid-specific inhibitory receptor. *Eur J Immunol* **29**, 3440-3449 (1999).

46. Paul, S.P., Taylor, L.S., Stansbury, E.K. & McVicar, D.W. Myeloid specific human CD33 is an inhibitory receptor with differential ITIM function in recruiting the phosphatases SHP-1 and SHP-2. *Blood* **96**, 483-490 (2000).

47. Yi, T.L., Cleveland, J.L. & Ihle, J.N. Protein tyrosine phosphatase containing SH2 domains: characterization, preferential expression in

hematopoietic cells, and localization to human chromosome 12p12-p13. *Mol Cell Biol* **12**, 836-846 (1992).

48. Grobe, K. & Powell, L.D. Role of protein kinase C in the phosphorylation of CD33 (Siglec-3) and its effect on lectin activity. *Blood* **99**, 3188-3196 (2002).

49. Balaian, L. & Ball, E.D. Direct effect of bispecific anti-CD33 x anti-CD64 antibody on proliferation and signaling in myeloid cells. *Leuk Res* **25**, 1115-1125 (2001).

50. Vitale, C. et al. Engagement of p75/AIRM1 or CD33 inhibits the proliferation of normal or leukemic myeloid cells. *Proc Natl Acad Sci U S A* **96**, 15091-6 (1999).

51. Vitale, C. et al. Surface expression and function of p75/AIRM-1 or CD33 in acute myeloid leukemias: engagement of CD33 induces apoptosis of leukemic cells. *Proc Natl Acad Sci U S A* **98**, 5764-9 (2001).

52. Mingari, M.C., Vitale, C., Romagnani, C., Falco, M. & Moretta, L. p75/AIRM1 and CD33, two sialoadhesin receptors that regulate the proliferation or the survival of normal and leukemic myeloid cells. *Immunol Rev* **181**, 260-8 (2001).

53. Balaian, L., Zhong, R.-k. & Ball, E.D. The inhibitory effect of anti-CD33 monoclonal antibodies on AML cell growth correlates with the Syk and/or ZAP-70 expression. *Exp Hematol* **31**, 363-371 (2003).

54. Lajaunias, F., Dayer, J.M. & Chizzolini, C. Constitutive repressor activity of CD33 on human monocytes requires sialic acid recognition and phosphoinositide 3-kinase-mediated intracellular signaling. *Eur J Immunol* **35**, 243-51 (2005).

55. Vanderheijden, N. et al. Involvement of sialoadhesin in entry of porcine reproductive and respiratory syndrome virus into porcine alveolar macrophages. *J Virol* **77**, 8207-15 (2003).

56. Delputte, P.L. & Nauwynck, H.J. Porcine arterivirus infection of alveolar macrophages is mediated by sialic acid on the virus. *J Virol* **78**, 8094-101 (2004).

57. Bö, L. et al. Endocytic depletion of L-MAG from CNS myelin in quaking mice. *J Cell Biol* **131**(1995).

58. Lock, K., Zhang, J., Lu, J., Lee, S.H. & Crocker, P.R. Expression of CD33-related siglecs on human mononuclear phagocytes, monocyte-derived

dendritic cells and plasmacytoid dendritic cells. *Immunobiology* **209**, 199-207 (2004).

59. Biedermann, B., Gil, D., Bowen, D.T. & Crocker, P.R. Analysis of the CD33-related siglec family reveals that Siglec-9 is an endocytic receptor expressed on subsets of acute myeloid leukemia cells and absent from normal hematopoietic progenitors. *Leuk Res* **Jul 7; [Epub ahead of print]**(2006).

60. Zhang, J. et al. Characterization of Siglec-H as a novel endocytic receptor expressed on murine plasmacytoid dendritic cell precursors. *Blood* **107**, 3600-8 (2006).

61. Scheinberg, D.A. et al. A phase I trial of monoclonal antibody M195 in acute myelogenous leukemia: specific bone marrow targeting and internalization of radionuclide. *J Clin Oncol* **9**, 478-490 (1991).

62. van der Jagt, R.H.C. et al. Localization of radiolabeled antimyeloid antibodies in a human acute leukemia xenograft tumor model. *Cancer Res* **52**, 89-94 (1992).

63. Audran, R. et al. Internalization of human macrophage surface antigens induced by monoclonal antibodies. *J Immunol Methods* **188**, 147-154 (1995).

64. van der Velden, V.H.J. et al. Targeting of the CD33-calicheamicin immunoconjugate Mylotarg (CMA-676) in acute myeloid leukemia: in vivo and in vitro saturation and internalization by leukemic and normal myeloid cells. *Blood* **97**, 3197-3204 (2001).

65. Press, O.W., Farr, A.G., Borroz, K.I., Anderson, S.K. & Martin, P.J. Endocytosis and degradation of monoclonal antibodies targeting human B-cell malignancies. *Cancer Res* **49**, 4906-12 (1989).

66. Shan, D. & Press, O.W. Constitutive endocytosis and degradation of CD22 by human B cells. *J Immunol* **154**, 4466-4475 (1995).

67. Chan, C.H.T., Wang, J., French, R.R. & Glennie, M.J. Internalization of the lymphocytic surface protein CD22 is controlled by a novel membrane proximal cytoplasmic motif. *J Biol Chem* **273**, 27809-27815 (1998).

68. Mukherjee, S., Ghosh, R.N. & Maxfield, F.R. Endocytosis. *Physiol Rev* **77**, 759-803 (1997).

69. Bonifacino, J.S. & Traub, L.M. Signals for sorting of transmembrane proteins to endosomes and lysosomes. *Annu Rev Biochem* **72**, 395-447 (2003).

70. John, B. et al. The B cell coreceptor CD22 associates with AP50, a clathrin-coated pit adapter protein, via tyrosine-dependent interaction. *J Immunol* **170**, 3534-43 (2003).

71. Traub, L.M. Sorting it out: AP-2 and alternate clathrin adaptors in endocytic cargo selection. *J Cell Biol* **163**, 203-208 (2003).

72. Marmor, M.D. & Yarden, Y. Role of protein ubiquitylation in regulating endocytosis of receptor tyrosine kinases. *Oncogene* **23**, 2057-2070 (2004).

73. Giles, F., Estey, E. & O'Brien, S. Gemtuzumab ozogamicin in the treatment of acute myeloid leukemia. *Cancer* **98**, 2095-104 (2003).

74. Sievers, E.L. et al. Efficacy and safety of gemtuzumab ozogamicin in patients with CD33-positive acute myeloid leukemia in first relapse. *J Clin Oncol* **19**, 3244-3254 (2001).

75. Larson, R.A. et al. Antibody-targeted chemotherapy of older patients with acute myeloid leukemia in first relapse using Mylotarg (gemtuzumab ozogamicin). *Leukemia* **16**, 1627-36 (2002).

76. Bross, P.F. et al. Approval summary: gemtuzumab ozogamicin in relapsed acute myeloid leukemia. *Clin Cancer Res* **7**, 1490-6 (2001).

77. Linenberger, M.L. CD33-directed therapy with gemtuzumab ozogamicin in acute myeloid leukemia: progress in understanding cytotoxicity and potential mechanisms of drug resistance. *Leukemia* **19**, 176-82 (2005).

78. Damle, N.K. & Frost, P. Antibody-targeted chemotherapy with immunoconjugates of calicheamicin. *Curr Opin Pharmacol* **3**, 386-90 (2003).

79. Linenberger, M.L. et al. Multidrug-resistance phenotype and clinical responses to gemtuzumab ozogamicin. *Blood* **98**, 988-94 (2001).

80. Walter, R.B. et al. Multidrug resistance protein attenuates gemtuzumab ozogamicin-induced cytotoxicity in acute myeloid leukemia cells. *Blood* **102**, 1466-73 (2003).

81. Walter, R.B. et al. The peripheral benzodiazepine receptor ligand PK11195 overcomes different resistance mechanisms to sensitize AML cells to gemtuzumab ozogamicin. *Blood* **103**, 4276-4284 (2004).

82. Walter, R.B. et al. Breast cancer resistance protein (BCRP/ABCG2) does not confer resistance to gemtuzumab ozogamicin and calicheamicin-g1 in acute myeloid leukemia cell lines. *Leukemia* **18**, 1914-1917 (2004).

83. Caron, P.C., Dumont, L. & Scheinberg, D.A. Supersaturating infusional humanized anti-CD33 monoclonal antibody HuM195 in myelogenous leukemia. *Clin Cancer Res* **4**, 1421-8 (1998).

84. Feldman, E. et al. Treatment of relapsed or refractory acute myeloid leukemia with humanized anti-CD33 monoclonal antibody HuM195. *Leukemia* **17**, 314-8 (2003).

85. Jedema, I. et al. Internalization and cell cycle-dependent killing of leukemic cells by gemtuzumab ozogamicin: rationale for efficacy in CD33-negative malignancies with endocytic capacity. *Leukemia* **18**, 316-25 (2004).

86. Pagliaro, L.C. et al. Humanized M195 monoclonal antibody conjugated to recombinant gelonin: an anti-CD33 immunotoxin with antileukemic activity. *Clin Cancer Res* **4**, 1971-6 (1998).

87. Naito, K. et al. Calicheamicin-conjugated humanized anti-CD33 monoclonal antibody (gemtuzumab zogamicin, CMA-676) shows cytocidal effect on CD33-positive leukemia cell lines, but is inactive on P-glycoprotein-expressing sublines. *Leukemia* **14**, 1436-43 (2000).

88. Matsui, H. et al. Reduced effect of gemtuzumab ozogamicin (CMA-676) on P-glycoprotein and/or CD34-positive leukemia cells and its restoration by multidrug resistance modifiers. *Leukemia* **16**, 813-9 (2002).

89. Hamann, P.R. et al. Gemtuzumab ozogamicin, a potent and selective anti-CD33 antibody-calicheamicin conjugate for treatment of acute myeloid leukemia. *Bioconjug Chem* **13**, 47-58 (2002).

90. Dowell, J.A., Korth-Bradley, J., Liu, H., King, S.P. & Berger, M.S. Pharmacokinetics of gemtuzumab ozogamicin, an antibody-targeted chemotherapy agent for the treatment of patients with acute myeloid leukemia in first relapse. *J Clin Pharmacol* **41**, 1206-14 (2001).

91. Sivaraman, S. et al. G-CSF and other cytokines modulated expression of CD33 antigen on the surface of myeloid cells [abstract]. *Blood* **100**, 554a (2002).

92. Walter, R.B., Raden, B.W., Kamikura, D.M., Cooper, J.A. & Bernstein, I.D. Influence of CD33 expression levels and ITIM-dependent internalization on gemtuzumab ozogamicin-induced cytotoxicity. *Blood* **105**, 1295-1302 (2005).

93. Greenberg, S. Modular components of phagocytosis. *J Leukoc Biol* **66**, 712-7 (1999).

94. Vervoordeldonk, S.F. et al. Fcgamma receptor II (CD32) on malignant B cells influences modulation induced by anti-CD19 monoclonal antibody. *Blood* **83**, 1632-1639 (1994).

95. van Oosterhout, Y.V.J.M. et al. Effect of isotype on internalization and cytotoxicity of CD19-ricin A immunotoxins. *Cancer Res* **54**, 3527-32 (1994).

96. Posada, J. & Cooper, J.A. Requirements for phosphorylation of MAP kinase during meiosis in Xenopus oocytes. *Science* **255**, 212-5 (1992).

97. Denkers, E.Y., Badger, C.C., Ledbetter, J.A. & Bernstein, I.D. Influence of antibody isotype on passive serotherapy of lymphoma. *J Immunol* **135**, 2183-6 (1985).

98. Rubinson, D.A. et al. A lentivirus-based system to functionally silence genes in primary mammalian cells, stem cells and transgenic mice by RNA interference. *Nat Genet* **33**, 401-6 (2003).

99. Yi, T. & Ihle, J.N. Association of hematopoietic cell phosphatase with c-Kit after stimulation with c-Kit ligand. *Mol Cell Biol* **13**, 3350-3358 (1993).

100. Yeung, Y.G., Berg, K.L., Pixley, F.J., Angeletti, R.H. & Stanley, E.R. Protein tyrosine phosphatase-1C is rapidly phosphorylated in tyrosine in macrophages in response to colony stimulating factor-1. *J Biol Chem* **267**, 23447-23450 (1992).

101. Bouchard, P. et al. Phosphorylation and identification of a major tyrosine phosphorylation site in protein tyrosine phosphatase 1C. *J Biol Chem* **269**, 19585-19589 (1994).

102. Uchida, T. et al. Insulin stimulates the phosphorylation of Tyr538 and the catalytic activity of PTP1C, a protein tyrosine phosphatase with Src homology-2 domains. *J Biol Chem* **269**, 12220-12228 (1994).

103. Kon-Kozlowski, M., Pani, G., Pawson, T. & Siminovitch, K.A. The tyrosine phosphatase PTP1C associates with Vav, Grb2, and mSos1 in hematopoietic cells. *J Biol Chem* **271**, 3856-3862 (1996).

104. Vogel, W. & Ullrich, A. Multiple in vivo phosphorylated tyrosine phosphatase SHP-2 engages binding to Grb2 via tyrosine 584. *Cell Growth Differ* **7**, 1589-97 (1996).

105. Solomaha, E., Szeto, F.L., Yousef, M.A. & Palfrey, H.C. Kinetics of Src homology 3 domain association with the proline-rich domain of dynamins: specificity, occlusion, and the effects of phosphorylation. *J Biol Chem* **280**, 23147-56 (2005).

106. Vidal, M. et al. Molecular and cellular analysis of Grb2 SH3 domain mutants: interaction with Sos and dynamin. *J Mol Biol* **290**, 717-30 (1999).

107. Huang, F. & Sorkin, A. Growth factor receptor binding protein 2-mediated recruitment of the RING domain of Cbl to the epidermal growth factor receptor is essential and sufficient to support receptor endocytosis. *Mol Biol Cell* **16**, 1268-81 (2005).

108. Strzelecka-Kiliszek, A., Kwiatkowska, K. & Sobota, A. Lyn and Syk kinases are sequentially engaged in phagocytosis mediated by Fc gamma R. *J Immunol* **169**, 6787-94 (2002).

109. Kant, A.M. et al. SHP-1 regulates Fcgamma receptor-mediated phagocytosis and the activation of RAC. *Blood* **100**, 1852-9 (2002).

110. Choi, J.H. et al. Phospholipase C-gamma1 is a guanine nucleotide exchange factor for dynamin-1 and enhances dynamin-1-dependent epidermal growth factor receptor endocytosis. *J Cell Sci* **117**, 3785-95 (2004).

111. Duchene, J. et al. Direct protein-protein interaction between PLCgamma1 and the bradykinin B2 receptor--importance of growth conditions. *Biochem Biophys Res Commun* **326**, 894-900 (2005).

112. Unkeless, J.C. & Jin, J. Inhibitory receptors, ITIM sequences and phosphatases. *Curr Opin Immunol* **9**, 338-43 (1997).

113. Yanagi, S., Inatome, R., Takano, T. & Yamamura, H. Syk expression and novel function in a wide variety of tissues. *Biochem Biophys Res Commun* **288**, 495-8 (2001).

114. Turner, M., Schweighoffer, E., Colucci, F., Di Santo, J.P. & Tybulewicz, V.L. Tyrosine kinase SYK: essential functions for immunoreceptor signalling. *Immunol Today* **21**, 148-54 (2000).

115. Billadeau, D.D. & Leibson, P.J. ITAMs versus ITIMs: striking a balance during cell regulation. *J Clin Invest* **109**, 161-8 (2002).

116. Isakov, N. ITAMs: immunoregulatory scaffolds that link immunoreceptors to their intracellular signaling pathways. *Receptors Channels* **5**, 243-53 (1998).

117. Veillette, A., Latour, S. & Davidson, D. Negative regulation of immunoreceptor signaling. *Annu Rev Immunol* **20**, 669-707 (2002).

118. Ravetch, J.V. & Lanier, L.L. Immune inhibitory receptors. *Science* **290**, 84-89 (2000).

119. Liu, Y.C. Ubiquitin ligases and the immune response. *Annu Rev Immunol* **22**, 81-127 (2004).

120. Rao, N., Dodge, I. & Band, H. The Cbl family of ubiquitin ligases: critical negative regulators of tyrosine kinase signaling in the immune system. *J Leukoc Biol* **71**, 753-63 (2002).

121. Wang, H.Y. et al. Cbl promotes ubiquitination of the T cell receptor zeta through an adaptor function of Zap-70. *J Biol Chem* **276**, 26004-11 (2001).

122. Booth, J.W., Kim, M.K., Jankowski, A., Schreiber, A.D. & Grinstein, S. Contrasting requirements for ubiquitylation during Fc receptor-mediated endocytosis and phagocytosis. *EMBO J* **21**, 251-8 (2002).

123. Treier, M., Staszewski, L.M. & Bohmann, D. Ubiquitin-dependent c-Jun degradation in vivo is mediated by the delta domain. *Cell* **78**, 787-98 (1994).

124. Takeuchi, M. et al. Functional and physical interaction of protein-tyrosine kinases Fyn and Csk in the T-cell signaling system. *J Biol Chem* **268**, 27413-9 (1993).

125. Ettenberg, S.A. et al. cbl-b inhibits epidermal growth factor receptor signaling. *Oncogene* **18**, 1855-66 (1999).

126. Peschard, P., Ishiyama, N., Lin, T., Lipkowitz, S. & Park, M. A conserved DpYR motif in the juxtamembrane domain of the Met receptor family forms an atypical c-Cbl/Cbl-b tyrosine kinase binding domain binding site required for suppression of oncogenic activation. *J Biol Chem* **279**, 29565-29571 (2004).

127. Press, O.W. et al. Comparative metabolism and retention of iodine-125, yttrium-90, and indium-111 radioimmunoconjugates by cancer cells. *Cancer Res* **56**, 2123-2129 (1996).

128. Naramura, M. et al. c-Cbl and Cbl-b regulate T cell responsiveness by promoting ligand-induced TCR down-modulation. *Nat Immunol* **3**, 1192-9 (2002).

129. Mimnaugh, E.G., Bonvini, P. & Neckers, L. The measurement of ubiquitin and ubiquitinated proteins. *Electrophoresis* **20**, 418-28 (1999).

130. Katzmann, D.J., Odorizzi, G. & Emr, S.D. Receptor downregulation and multivesicular-body sorting. *Nat Rev Mol Cell Biol* **3**, 893-905 (2002).

131. Raiborg, C., Rusten, T.E. & Stenmark, H. Protein sorting into multivesicular endosomes. *Curr Opin Cell Biol* **15**, 446-55 (2003).

132. Chen, L. & Davis, N.G. Ubiquitin-independent entry into the yeast recycling pathway. *Traffic* **3**, 110-23 (2002).

133. Thien, C.B. & Langdon, W.Y. c-Cbl and Cbl-b ubiquitin ligases: substrate diversity and the negative regulation of signalling responses. *Biochem J* **391**, 153-66 (2005).

CURRICULUM VITAE

Personal data:

Name:	Roland B. Walter
Birthdate:	November 3, 1970
Place of birth:	Biel BE, Switzerland
Citizenship:	Switzerland

Education:

4/1983-9/1989	Kantonsschule Hohe Promenade, Zürich, Switzerland (Comprehensive Secondary School)
10/1990-11/1996	Medical School, Faculty of Medicine, University of Zürich, Switzerland (Diplome Federal)
11/1996	Medical Licensure (Switzerland)
1/1997	Doctor of Medicine, Faculty of Medicine, University of Zürich, Switzerland
1/2002	Board Certification in Internal Medicine, Swiss Medical Association, Switzerland
2/2004	Habilitation (venia legendi), Medical Faculty, University of Zürich, Switzerland
5/2004	Educational Commission for Foreign Medical Graduates (ECFMG) Certification, Philadelphia, PA, USA (permanent validation)
6/2004-6/2006	Graduate Program, Department of Pathology, University of Washington, Seattle, WA, USA
8/2004	United States Medical Licensing Examination Step 3

Internship/residency:

8/1997-7/1999	Department of Medicine, Rätisches Kantons- und Regionalspital, Chur, Switzerland
8/1999-1/2002	Department of Internal Medicine, University Hospital, Zürich, Switzerland

Research and clinical fellowships:

11/1996-7/1997	Department of Internal Medicine, University Hospital, Zürich, Switzerland
2/2002-12/2004 **7/2005-**	Clinical Research Division, Fred Hutchinson Cancer Research Center, Seattle, WA, USA
1/2005-	Division of Hematology, University of Washington School of Medicine, Seattle, WA, USA

Grants:

2/2002-1/2004	Swiss Foundation for Medical-Biological Grants (No. 1098)
1/2004-12/2004	Interdisciplinary Dual Mentor Fellowship, Fred Hutchinson Cancer Research Center, Seattle, WA, USA
1/2005-12/2005	Janggen-Pöhn Foundation, Switzerland
7/2005-6/2007	American Society of Hematology Clinical/Translational Research Scholar Award, Washington, DC, USA
7/2006-6/2009	The Leukemia & Lymphoma Society Special Fellow Award, White Plains, NY, USA

Awards:

2005	SIAK/ESSEX Award in Applied Cancer Research
2005	Dr. Ernst Th. Jucker Price for Cancer Research